MECHANICAL AND MICROSTRUCTURAL PROPERTIES OF GEOPOLYMERIC FLY ASH BASED MORTAR CURED IN AMBIENT CONDITIONS

Thesis

Submitted in partial fulfilment of the requirements for the degree of

DOCTOR OF PHILOSOPHY

by

PRASANNA K M

(165117CV16P02)

DEPARTMENT OF CIVIL ENGINEERING

NATIONAL INSTITUTE OF TECHNOLOGY KARNATAKA,

SURATHKAL, MANGALORE - 575025

FEBRUARY 2024

MECHANICAL AND MICROSTRUCTURAL PROPERTIES OF GEOPOLYMERIC FLY ASH BASED MORTAR CURED IN AMBIENT CONDITIONS

Thesis

Submitted in partial fulfilment of the requirements for the degree of

DOCTOR OF PHILOSOPHY

by

PRASANNA K M

(165117CV16P02)

Under the Guidance of

Dr. BIBHUTI BHUSAN DAS Professor

Dr. GANGADHAR MAHESH Professor

DEPARTMENT OF CIVIL ENGINEERING

NATIONAL INSTITUTE OF TECHNOLOGY KARNATAKA,

SURATHKAL, MANGALORE - 575025

FEBRUARY 2024

DECLARATION

I hereby declare that the Research Thesis entitled **"Mechanical and Microstructural Properties of Geopolymeric Fly ash Based Mortar Cured in Ambient Conditions"** which is being submitted to the **National Institute of Technology Karnataka, Surathkal** in partial fulfilment of the requirements for the award of the Degree of **Doctor of Philosophy** in **Civil Engineering** is a bonafide report of the research work carried out by me. The material contained in this Research Thesis has not been submitted to any University or Institution for the award of any degree.

Place: NITK, SURATHKAL

Date:

PRASANNA K M
165117CV16P02
Research Scholar
Department of Civil Engineering

CERTIFICATE

This is to certify that the Research Thesis entitled **"Mechanical and Microstructural Properties of Geopolymeric Fly ash Based Mortar Cured in Ambient Conditions"** submitted by **PRASANNA K M** (Registration number: 165117CV16P02) as the record of research work carried out by him, is accepted as Research Thesis submission in partial fulfilment of the requirements for the award of degree of **Doctor of Philosophy**.

Dr. BIBHUTI BHUSAN DAS
Department of Civil Engineering
Research Supervisor

Dr. GANGADHAR MAHESH
Department of Civil Engineering
Research Supervisor

NATIONAL INSTITUTE OF TECHNOLOGY KARNATAKA, SURATHKAL
DEPT. OF CIVIL ENGG.

Dr. SUBHASH C YARAGAL
Department of Civil Engineering
Chairman - DRPC

Chairman (DRPC)
Department of Civil Engineering
National Institute of Technology Karnataka
Surathkal, Mangalore - 575 025, Karnataka, INDIA

Dedicated to

My Beloved Parents

Late Wife

and

Teachers

ACKNOWLEDGEMENTS

I take this opportunity express my sincere gratitude and profound thanks to my guide and co-guide Dr. Bibhuti Bhusan Das, and Dr. Gangadhar Mahesh, Professors, Department of Civil Engineering for their advice, guidance and reference materials provided during the course for the preparation of my thesis work.

I wish to extend my sincere thanks to Dr. A S Balu, Associate Professor, Department of Civil Engineering, and Dr. B M Kunar, Associate Professor, Department of Mining Engineering for being the Research Progress Assessment Committee (RPAC) members and their valuable suggestions at various stages of the research.

I wish to thank Prof. Subhash C Yaragal., Head of the Department of Civil Engineering and Prof. B R Jayalekshmi, former Head of the Department of Civil Engineering, for their support and encouragement throughout the journey of my research. I am grateful to the course instructors during my course work Dr. Bibhuti Bhusan Das, Dr. Gangadhar Mahesh, Prof. Katta Venkataramana and my research supervisor Dr. Bibhuti Bhusan Das, through whom I have learnt a lot.

I would also like to thank the support and facilities extended by Dr. T Palanisamy faculty-in-charge of Structures Laboratory and Dr. Bibhuti Bhusan Das, faculty-in-charge of Materials and Testing Laboratory.

This research work would not have been possible without the support and cooperation of the Foremen of Materials and Testing Laboratory Mr. Geetesh Shetty. The help rendered by the laboratory staff Mr. Ramanath Acharaya and Mr. Ranjith is humbly acknowledged.

Without the support and help of Research Scholars Dr Shivaprasad K N, Dr Sharan Kumar Goudar, Dr Snehal K, Mr Sumukh E P, Mr Sharath B P, Mr. Shiv Sai Trivedi and Mr Sanjeet Kumar Mishra the research work would not have seen the light of the day.

I am extremely thankful to Ms. K Bhavani, Executive Vice President and Mr. Arvind Ramakrishna Nerurkar, TFL Head MAHSR C3, Larsen and Toubro Ltd. and Mr. P Niranjana, Vice President, Adani Ltd. for providing the opportunity and support for my research work.

I acknowledge the help received from the former M.Tech students of Construction Technology and Management Engineering Mr. Saif Asrab Tamboli, Mr. Irambona Theodose, Mr.

Himanshu Choukade, and Mr. Kamal Kumar Behra in the conduction of laboratory experiments.

I am thankful to my parents, children, brothers and sisters for their constant support and encouragement.

Above all I thank almighty for guiding me and showering blessings to complete this thesis successfully.

PRASANNA K M

ABSTRACT

This experimental study aims to improve the IST and FST, flowability, and compressive strength of FA-based geopolymer mix samples for pastes, mortars, and mortars with steel fibre additions by substituting GGBS with various alkaline to binder ratios. GGBS substitution in geopolymeric mixtures is essential for achieving quicker setting in the resultant geopolymeric samples and also to accomplish the practical viability without any heat curing. SEM-EDS and FTIR were used to perform microstructural characterization and chemical identification of structural growth in the resulting geopolymers.

According to the obtained findings, GGBS addition increased geopolymeric samples compressive strength while decreasing their setting time. The IST attained for geopolymeric paste samples is 20 minutes for F50:G50 samples with an alkaline to binder ratio of 0.5. However, the FST attained is 485 minutes for F100:G0 samples with an alkaline to binder ratio of 0.8. The highest 28 days compressive strength attained for geopolymeric paste samples is 85 MPa for F50:G50 samples with an alkaline to binder ratio of 0.5. Furthermore, for geopolymeric mortars, the IST attained is 22 minutes for F50:G50 samples with an alkaline to binder ratio of 0.5, whereas the FST attained is 668 minutes for F100:G0 samples with an alkaline to binder ratio of 0.8. A highest compressive strength of 56 MPa at 28 days is attained for F50:G50 geopolymeric mortar samples with an alkaline to binder ratio of 0.6. Additionally, for geopolymeric samples with steel fibres, after a curing period of 28 days, the compressive strength obtained is 69.5 MPa. This was observed in specimens containing 1% steel fibre content, an alkaline to binder ratio of 0.6, and binder proportions of 50%:50%. SEM microphotographs of geopolymeric pastes and mortar samples revealed the presence of a dense matrix with the GGBS substitution. Furthermore, the presence of rough steel fibre surfaces and hydration reaction products on the steel surface implies a rather good link between the geopolymer matrix and steel fibre, which boosts compressive strength values, as observed in SEM images of steel fibre-containing mortar samples. The FTIR analysis of geopolymeric paste samples reveals a notable downward shift in wavenumbers of distinctive bands, corresponding to varying levels of GGBS substitution. This shift signifies a heightened degree of geopolymerization within the paste samples.

CONTENTS

LIST OF TABLES

LIST OF FIGURES

NOMENCLATURE

Abbreviations

IST	:	Initial setting time
FST	:	Final setting time
FA	:	Fly ash
GGBS	:	Ground granulated blast furnace slag
SEM-EDS	:	Scanning electron microscopy-energy dispersive spectroscopy
FTIR	:	Fourier transform infrared spectroscopy
BIS	:	Bureau of Indian standards
MK	:	Metakaolin
ASTM	:	American society for testing and materials
RH	:	Relative humidity
UFA	:	Ultrafine fly ash
M	:	Molarity
C-S-H	:	Calcium silicate hydrate
XRD	:	X-ray diffraction spectroscopy
C-A-S-H	:	Calcium alumino-silicate hydrate
N-A-S-H	:	Sodium alumino-silicate hydrate
CTM	:	Compressive testing machine
EN	:	European standards

CHAPTER – 1

INTRODUCTION

1.1 GENERAL

Manufacturing of cement accounts for 8%-9% of total anthropogenic emission of CO_2 (Brinkman and Miller 2021). Direct CO_2 emission in India in the year 2017 was 588 kg CO_2 per ton of cement and 5% decrease as likened to the baseline of 2010 which is well below the target of 40% reduction to be achieved by 2050. Rapid urbanization has increased construction demand, and Indian Brand Equity Foundation's (IBEF) cement industry assessment predicts cement production would exceed 600 million tonnes per year by 2025. Therefore, the need for cement alternatives in the near future is an important matter to be considered.

Thermal power plants use coal to generate energy and waste FA. According to reports from the central electricity authority, Government of India, FA generation and utilization in 2022 was 270.82 million tons, with 95.95 percent utilization in cement, concrete, blocks, and tile production and some disposal in landfills and embankments. However, unutilized FA is environmentally detrimental. The published reports states that around the year of 2030, unutilized FA count may go up to 128 MT which will necessitate extra land of 2,300 hectares, intensifying the current glitches regarding dumping of FA.

The construction industry is widely recognized as a significant consumer of portland cement. Additionally, various grouting applications in use today continue to rely on the conventional utilization of cement for ground improvement techniques. Furthermore, previous studies revealed that over-reliance on ordinary portland cement causes a variety of environmental issues such as massive CO_2 emissions, resource depletion, and so on (Bilondi et al., 2018; Provis et al., 2010). Moreover, the utilization of cement presents several drawbacks, such as heightened bleeding, plastic shrinkage, and diminished strength, leading to water loss and incomplete hydration during the initial stages (Güllü and Agha 2021). To address these issues, several researchers have taken the significant step of substituting portland cement with different pozzolanic materials, with the goal of improving performance through the incorporation of various eco-friendly ingredients. (Islam et al., 2015; Thakur & Ghosh, 2009; Ahmed et al., 2021). A new material known as geopolymer has emerged in the last two decades

and has been popular in the construction sector. It can be used as an excellent substitute for cement in grouting-based applications. (Ahmed et al., 2021; Xu et al., 2014).

The geopolymer-based binders are made up of Al and Si-rich sources such as FA, rice husk ash, metakaolin, GGBS, and others that are activated using alkaline activators such as Na/K OH^- and Na_2SiO_3/K_2SiO_3 (Almutairi et al., 2021; Aboulayt et al., 2018; Provis et al., 2010). These are durable, resistant to chemical and alkali aggregate assault, have good mechanical performance, behave visco-elastically like Portland cement, and are environmentally friendly (Tayeh et al., 2021; Taher et al., 2021; Çevik et al., 2018; Palacios et al., 2008; Pacheco-Torgal et al., 2008). These geopolymer-based materials might offer a practical response to the problems posed by conserving and disposing these industrial wastes and byproducts (Cherki El Idrissi et al., 2018; Wang et al., 2005; Blash & Lakshmi, 2016). When compared to cement, it has been reported that these materials can cut CO_2 emissions by 80–90%, improving mechanical and chemical resilience (Abdulkareem et al., 2012, Al Bakri Abdullah et al., 2012). The geopolymeric reaction's ability can be linked to the occurrence of constitutional formation when a powdered, aluminosilicate-rich material is blended with an adequate alkaline activator (Kong et al. 2007). The aforementioned combination subsequently undergoes polycondensation in a highly alkaline milieu, resulting in the rearrangement of aluminum (Al) and silicon (Si) into a stable Si-O-Al structure. This process yields a material that exhibits favorable mechanical properties and chemical stability (Wang et al. 2005). Due to their widespread availability, the typical alkaline activator solution formulation for the synthesis of geopolymers (Bui et al., 2012; Pacheco-Torgal et al., 2008) consists of either NaOH and Na_2SiO_3 or KOH and K_2SiO_3, as described above. It is well known that the suitability of employing FA for the synthesis of geopolymers and the resulting qualities depend entirely on the material's CaO content, vitrification level, and presence of unburned coal. Despite the presence of various impurities in FA, it has a low reactivity as well as a reduced rate of dissolution (Lee and Van Deventer 2002). On the contrary, GGBS exhibits higher reactivity and is thus employed in the production of hydraulic concrete, known for its exceptional durability and strength properties. The reaction process of GGBS-based geopolymers is significantly influenced by the presence of magnesium oxide content. A reduction in this major content, on one hand helps in accelerating early reaction process and on the another hand, reduces the extent of reaction but favors the formation of calcium aluminate silicate hydrate gel (Bernal et al. 2014).

The construction industry is prone to following many standard methods, and introducing novel geopolymer-based materials as alternatives in this industry will take more time to grasp their

behavioral aspects (van Deventer et al. 2010). But there are other specialized applications wherein this geopolymer based materials finds its suitability without any inclination towards the existing standards (Van Deventer et al. 2012) and conventional construction methods. From the standpoint of workability, the dosage levels of water content in geopolymers play a vital function that is not directly involved in the geopolymerization process (Chindaprasirt et al., 2007; Sathonsaowaphak et al., 2009) as stated in past studies. In the initial stages of the reaction, it functions as a solvent, a crucial component. Moreover, it is worth noting that only a limited fraction of the water is genuinely interconnected within the geopolymer network, while the majority is predominantly confined within the pores of the material (Fang and Kayali 2013). Consequently, due to the absence of any alteration in the material structure during the expulsion of water, geopolymers exhibit enhanced resistance to fire and elevated temperatures (Bakharev, 2006; Lyon et al., 1997).

The process of producing geopolymer materials using only FA as a raw material has its own drawbacks. According to the findings of a study conducted by Hardjito et al. 2008, the presence of Ca influences the rate of setting in geopolymers, notably those produced from FA (Hardjito et al. 2008). The Class–F FA-based geopolymers were found to have longer setting times unless they were subjected to elevated temperatures for accelerating the polymerization process (Hardjito et al. 2008). A study stated that the IST and FST of geopolymers cured at a temperatures 65°C - 80°C ranged from 129 – 270 min (Mallikarjuna Rao and Gunneswara Rao 2015). Furthermore, the specimens subjected to ambient temperature conditions necessitated a minimum duration of one full day for the process of solidification. A subsequent investigation revealed that the production of adequate strength in geopolymer paste and mortar incorporating class - F FA required a duration of 21-25 hours (Elyamany et al. 2018). Furthermore, with the inclusion of Ca rich material like GGBS has drastically declined the FST from 24 hours to 100-150 min which was mainly because of an increment in Ca content (Wijaya and Hardjito 2016). According to studies, using GGBS in the binder together with FA results in a number of modifications in the geopolymer matrix, including decreased setting time and greater compressive strength due to the presence of higher Ca content in GGBS. It is understood from the available literature with the adoption of heat curing had resulted in higher values of compressive strength as it speeds up the process of geopolymerization (Garcia-Lodeiro et al. 2015). Furthermore, feasibility of adopting heat curing is not possible and impractical for in-situ applications. Several studies have been conducted to examine the influence of various types of fibers on fibre FA-based cementitious systems/geopolymer composites. These investigations have consistently demonstrated that all types of fibers enhance mechanical

properties, including flexural strength, energy absorption, and tensile strength, among others (Al-Majidi et al. 2017; Bhalchandra and Bhosle 2013; Mohod 2015; Natali et al. 2011; Plizzari 2004; Porkodi et al. 2015; Ramkumar et al. 2015). The performance of fibre-based geopolymer composites is primarily influenced by two key factors: the type of fibre and the quantity of fibre present within the system (Al-Majidi et al. 2017; Bhalchandra and Bhosle 2013; Mohod 2015; Natali et al. 2011; Plizzari 2004). The workability of fresh geopolymer composite reduced significantly by incorporating fibres, because of higher shear resistance to flow (Al-Majidi et al. 2017). Hardened properties of the geopolymer composites have improved with increase in percentage of fibre content (Lee and Lee 2013). In summary, with the use of geopolymer mix a smaller carbon footprint can be achieved by minimal usage of natural resources without comprising the desired mechanical properties.

An adequate amount of information is available on the production of FA-based geopolymeric paste and mortars with alkaline solution as the binder which requires heat/oven curing to achieve the required engineering properties, making it energy-efficient, costly, impractical, and unsustainable. This experimental study will aim in developing the FA based geopolymeric mixes that will be cured in ambient temperature conditions only. This practice will help in solving the disposal problems of growing industrial by-product as well as the environmental hazards in a more sustainable and cost-effective strategy.

1.2 NEED OF THE PRESENT RESEARCH WORK

This research work investigates the development of a geopolymer mix from industrial by-products that holds a strong potential for drawing on sustainability concepts worldwide. An excessively longer setting time is one of the obstacles that prevents the construction industry from making use of FA-based geopolymers at the present moment. Furthermore, the majority of the researchers also believed that it requires heat curing to achieve higher strength characteristics, which is practically non-viable. Hence, utilization of GGBS coupled with steel fibers is incorporated to achieve the deficient characteristics of FA-based geopolymers cured in ambient temperature conditions in this study, which is the need of the hour, thus making it a sustainable and cost-effective approach.

1.3 THESIS STRUCTURE

The present thesis is structured into seven different chapters. The chapter one discusses a generalized introduction and necessity of the present research work is presented. The chapter two discusses a complete literature review and a critical review for identification of research

gap/problem. The third chapter consists of all the source materials utilized in this experimental research, methodology adopted for the production of geopolymeric pastes, mortars and mortars with steel fibres is presented and standard testing methods applicable for testing of the resultant geopolymeric samples is presented. The chapters four, five and six presents the obtained test results and discussion on geopolymeric pastes, mortars and mortars with steel fibres addition, respectively. The seventh chapter presents the conclusions derived from the current experimental study as well as future research opportunities.

CHAPTER – 2

LITERATURE REVIEW

2.1 GENERAL

This chapter provides a detailed assessment of relevant literature on geopolymer pastes and mortars using various fibres. Further, the influence of application of heat curing on the properties of resulting geopolymer pastes and mortars is reviewed aided with the usage of advanced characterization techniques as well.

2.2 THEORY OF GEOPOLYMERIZATION

Glukhovsky first identified alkali activated aluminosilicates in the 1950s, which makes them to function as a binding agent comparable to cement-like construction material (Glukhovsky 1965). The term "geopolymer" was preferred by the vast majority of researchers to describe all alkali activated aluminosilicate binders. According to Davidovits, geopolymers novel type of binding agents that varies from alkali activated aluminosilicates (Davidovits 1999a).

2.2.1 Process of geopolymerization

The process of geopolymerization, also known as geo-synthesis, hold the involvement of the occurrence of a quick chemical reaction with the incorporation of minerals. FA, GGBS, MK, and other aluminosilicate minerals are exposed to high-alkaline environments, undergoes through geopolymerization process, resulting in the geopolymer formation. They are inorganic, with Al and Si ions serving as the backbone on which the chain structures are developed. The resulting geopolymer's chemical composition is comparable to that of natural zeolitic materials, but the microstructure is amorphous rather than crystalline. In the polymerization process, when the materials constituting with Si-Al minerals are subjected to a strong alkaline environment result in formation of a 3-D chain ring structured polymer, consisting of Si-O-Al-O bonds, as described are undergoes through a significantly quick chemical reaction under strong alkaline environment, a 3-D polymeric chain and ringed structure of Si-O-Al-O linkages results, described below (Davidovits 1999b; Nikolić et al. 2015)

$$M_n\,[-(SiO_2)_z\text{-}AlO_2]_n \,.\, wH_2O \qquad (Eq\ 2.1)$$

where, M represents alkaline element (K, Na or Ca); z can be 1, 2, or 3; n represents polycondensation/polymerisation degree. The geopolymer structure is a linear 2-D network,

and its properties rely greatly on value of z (z = 1–15, up to 300). When the value of z is low (z properties and across-linked 3-D network), the geopolymer exhibits adhesive properties. Geopolymerisation process can be better understood with the help of diagrammatic explanation presented in Figure 2.1, proposed by Duxson et al (2007).

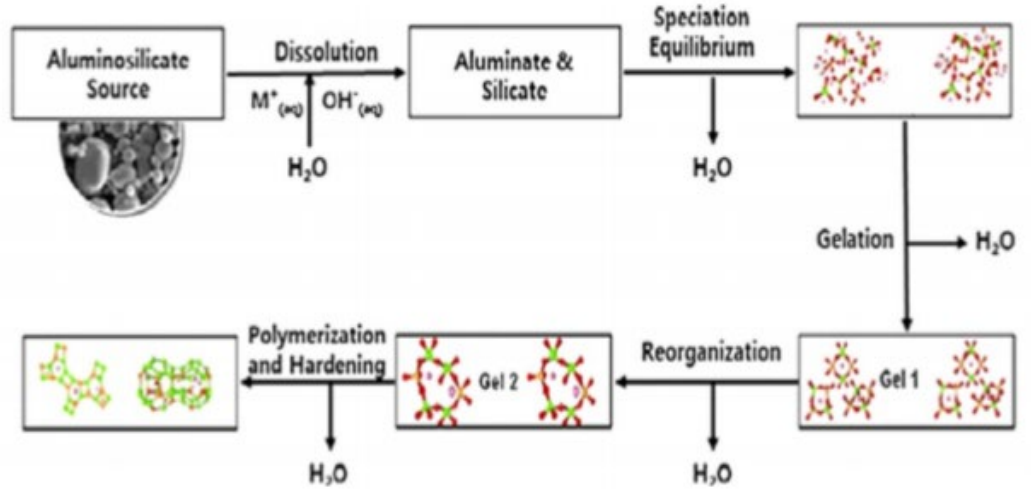

Figure 2.1: Geopolymerization theoretical model representation (Source: Duxson et al. 2007).

Geopolymerisation mechanism involves polycondensation reaction of geopolymeric precursors i.e., alumino-silicate oxide with alkali polysilicates yielding polymeric Si – O – Al – O – bond. According to researchers the hardening mechanism for geopolymerisation essentially involves the polycondensation reaction of geopolymeric precursors, usually alumino-silicate oxides, with alkali polysilicates yielding polymeric Si-O-Al-O bonds:

$$(Si_2O_5, Al_2O_2)_n + 3nH_2O \xrightarrow{NaOH/KOH} n(OH)_3 - Si - O - Al^{(-)}(OH)_3$$

$$n(OH)_3 - Si - O - Al^{(-)}(OH)_3 \xrightarrow{NaOH/KOH} (Na,K) - (-Si(O) - O - Al^{(-)}(O) -)_n + 3nH_2O$$

$$(Si_2O_5, Al_2O_2)_n + nSiO_2 + 4nH_2O \xrightarrow{NaOH/KOH} n(OH)_3 - Si - O - Al^{(-)}(OH)_2 - (OH)_3$$

$$n(OH)_3 - Si - O - Al^{(-)}(OH)_2 - (OH)_3 \xrightarrow{NaOH/KOH} (Na,K) - (-Si(O) - O - Al^{(-)}(O) - O - Si(O) - O -)_n + 4nH_2O$$

ortho(sialate-siloxo) (sodium, potassium) - poly(sialate - siloxo)

A geopolymer can take one of the three basic forms as shown in the Figure 2.2, i.e.:

- Poly (sialate), which has [-Si-O-Al-O-] as the recurring unit.
- Poly (sialate - siloxo), which has [-Si-O-Al-O-Si-O-] as the recurring unit.

- Poly (sialate - disiloxo), which has [-Si-O-Al-O-Si-O-Si-O-] as the recurring unit.

According to the molarity fraction of Si to Al, in Figure 2.2, Davidovits (1999) suggested various possibilities for geopolymer materials. Figure 2.3 briefly describes the possible applications of geopolymeric materials.

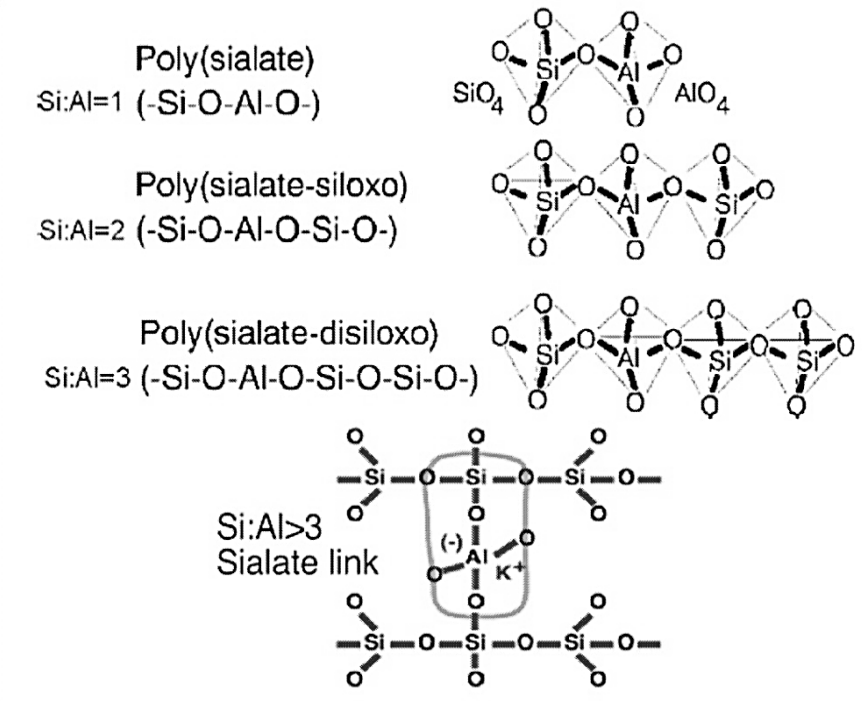

Figure 2.2: Terminologies used in geopolymerization concept (Source: Davidovits 1999)

Note: Sialate is an abbreviation of silicon-oxo-aluminate.

Siloxo is abbreviation of silicon-oxo.

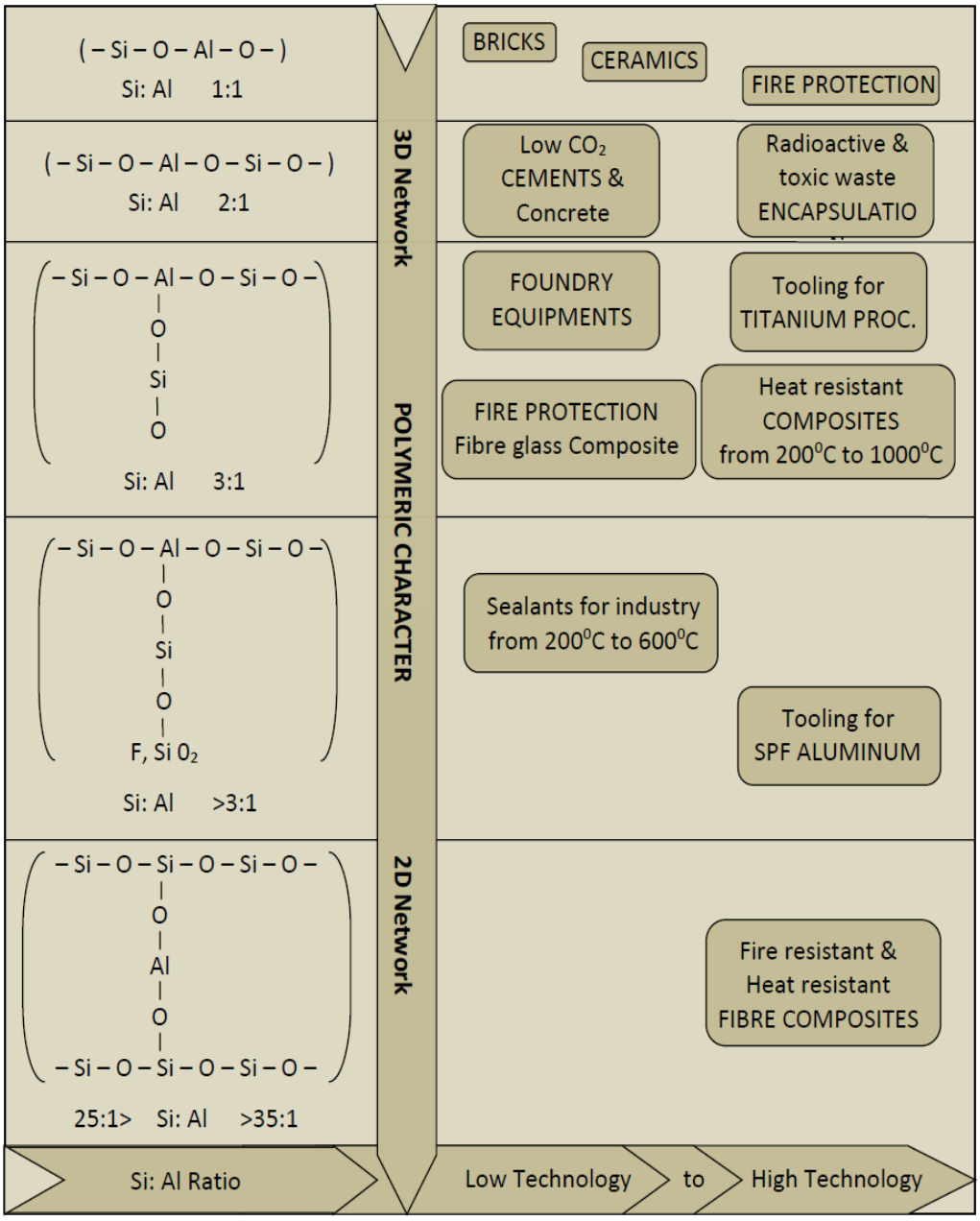

Figure 2.3: Various applications of geopolymeric materials (Source: Davidovits 1999)

2.2.2 Elements of Geopolymer

(a) Aluminosilicate materials

Materials primarily composing of amorphous Si and Al are potential sources for geopolymers (Shuaibu 2014). In comparison to products derived from non-calcined materials like kaolin clay, mine tailings, and naturally occurring minerals, demonstrated that calcined source materials such FA, GGBS and calcined kaolin displayed a greater compressive strength and reduction in reaction time.

MK, ASTM Class F FA natural Al-Si minerals, combination of calcined material and non-calcined materials, combination of FA and MK, and combination GGBS and MK were investigated as source materials in the past (Fifinatasha et al. 2013). Because of its high dissolving rate, ease of control of the Si/Al ratio, and white colour, MK is chosen by geopolymer product developers.

(b) Alkali based activators

In the process of geopolymerization, NaOH or KOH and Na_2SiO_3 or K_2SiO_3 solution are the most frequently utilised alkali based activators (Barbosa et al. 2000; Davidovits 1999b; Palomo et al. 1999). Some studies also conducted using single alkali based activator (Teixeira-Pinto et al. 2002). Type of activator plays an important role in the polymerisation process. Compared to using solely alkaline hydroxides, reactions happen much more quickly when the alkali-based activator also contains soluble silicate (either Na_2SiO_3 or K_2SiO_3). The addition of Na_2SiO_3 solution to the K_2SiO_3 as the alkali based activator enhanced the reaction of source material (Palomo et al. 1999).

2.2.3 Applications of geopolymeric materials

Geopolymeric materials find various applications in the field of civil engineering mainly for concrete repair methodologies such as grouting, shotcrete operations. It also finds applications in industries such as metallurgy, automobile and plastic industries. The type of application depends mainly on the Si/Al ratio. Table below describes the various applications of geopolymeric materials based on Si/Al ratio.

2.3 PARAMETERS AFFECTING THE PROPERTIES OF FA BASED GEOPOLYMERS

For the practical use of cementitious materials, the characteristics of fresh mixtures and hardened products are crucial. Workability and setting time are the important rheological characteristics of fresh geopolymer mixes. Compressive load carrying capacity and tensile load carrying capacities of geopolymers are important engineering characteristics. Properties of the geopolymer depends on a number of factors. Type of alkali activator, alkali binder ratio, regime, and types of source material are main factors that influence the geopolymerization. In order to comprehend the variables impacting compressive load carrying capacity of geopolymer, setting time of geopolymer, and impact of curing regime on properties of geopolymer, journals have been reviewed for the current study.

2.3.1 Parameters affecting the compressive load carrying capacity characteristics of FA based geopolymers

The alkaline based activator has a significant impact on the beginning of the surface hydrolysis of the particles, which acts as a binder in the process of geopolymerization, which uses aluminosilicate minerals as raw materials (Hardjito and Rangan 2005; Ridtirud et al. 2011). Strong alkalis like NaOH, Na_2SO_4, Na_2SiO_3, K_2CO_3, KOH, and K_2SO_4 can be employed in the geopolymerization mechanism for activating Si and Al in FA, as well as a tiny volume of cement clinker/combination of the alkali solutions (Khale and Chaudhary 2007; Komljenović et al. 2010; Leong et al. 2016; de Vargas et al. 2014). Several studies reported that concentration of alkali solution has a significant impact on how easily Si and Al species dissolve during the synthesis of geopolymer (Rattanasak and Chindaprasirt 2009; Singh et al. 2005). Figure 2.4 makes it evident that the mechanical properties of geopolymers are increased by alkali activator concentration up to a point, beyond which they tend to decrease as the concentration is increased.

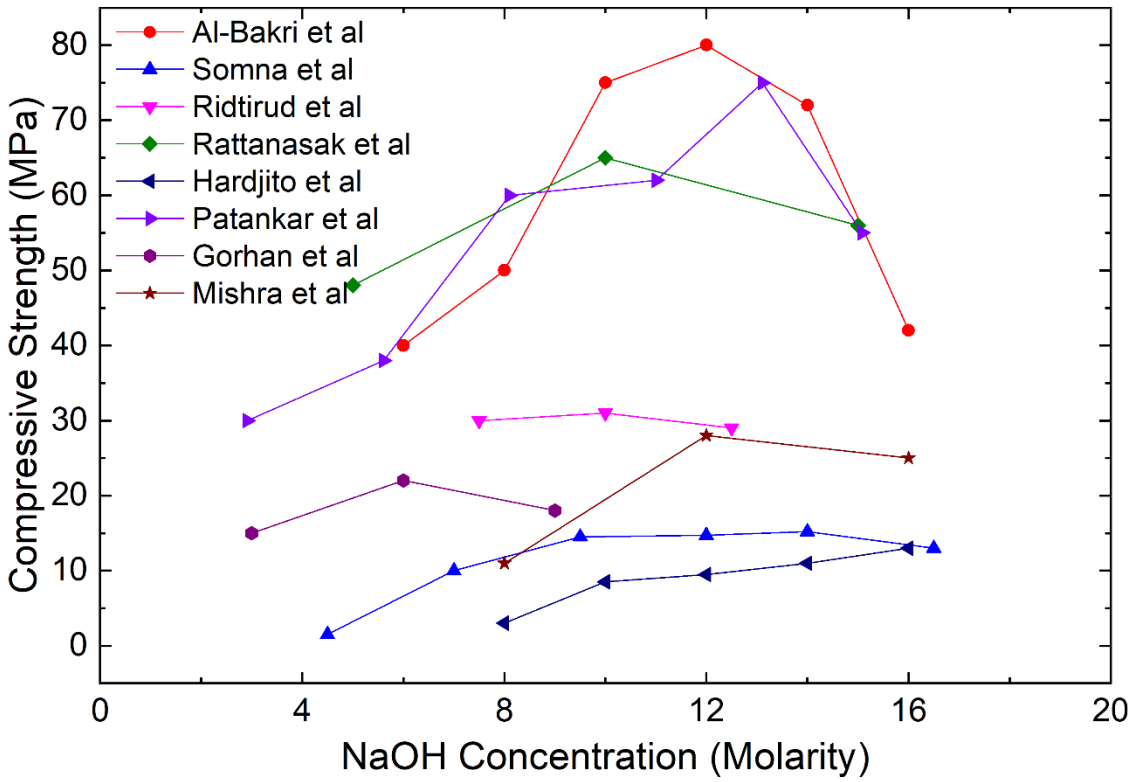

Figure 2.4: Influence of molarity of alkali on FA based geopolymers compressive load carrying capacity (compiled results from various researchers)

The use of NaOH and Na_2SiO_3 solutions in FA-based geopolymers was shown to produce crystalline structures that coexisted with amorphous gel in a similar manner. However, when Na_2SiO_3 was used solely, the majority of the results were amorphous. When cured at room temperature, either usage of NaOH or Na_2SiO_3 solution solely, resulted in acquiring lower strengths. It is clear that mixing NaOH and Na_2SiO_3 solutions will facilitate the development of strength in FA-based geopolymers (Phoo-ngernkham et al. 2015). Researchers found that varying ratios of Na_2SiO_3 to NaOH had a substantial impact on the engineering characteristics of FA-based geopolymeric binder (Hardjito et al. 2008; Morsy et al. 2014; Mustafa et al. 2012; Ridtirud et al. 2011). Figure 2.5 makes it evident that, up to a point, the alkali activator's NaOH/Na_2SiO_3 ratio boosts mechanical properties of geopolymers; nevertheless, when concentration is increased, mechanical properties drop.

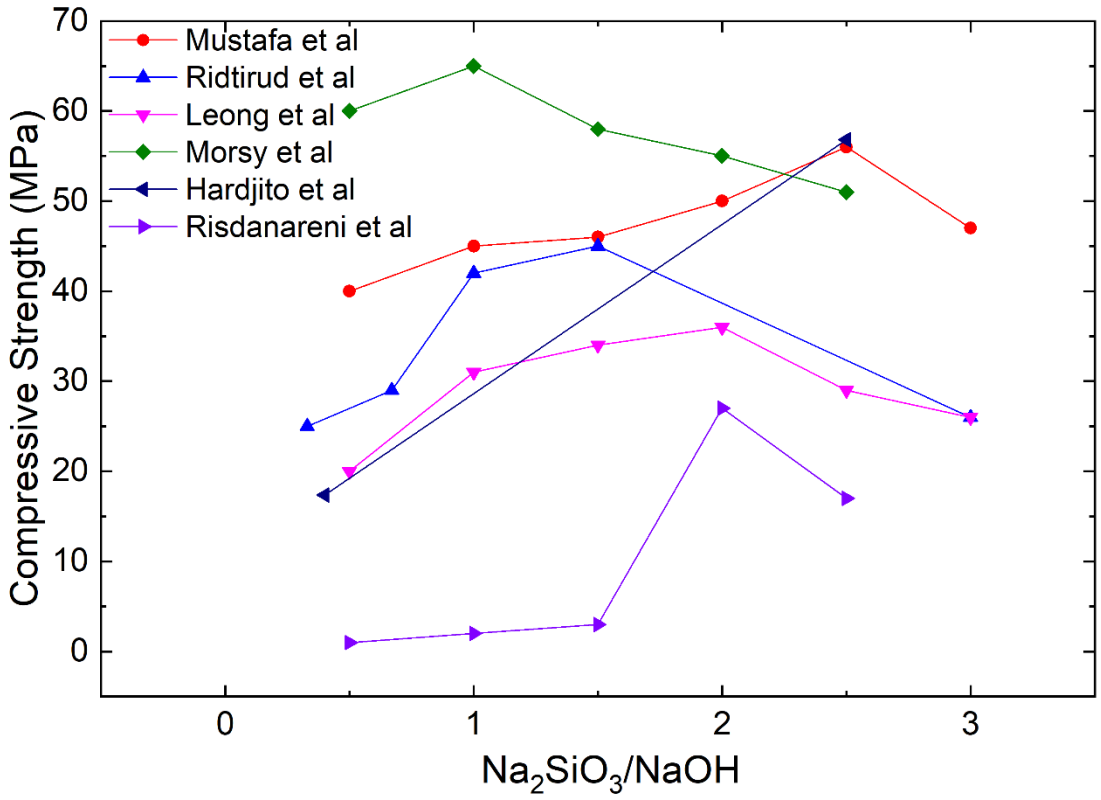

Figure 2.5: Influence of the ratio of NaOH to Na_2SiO_3 on the compressive load carrying capacity of FA based geopolymers (compilation of obtained results from various researchers)

On the other hand, alkali activator to binder ratio has a significant impact on understanding behaviour of geopolymerization process as well as the fresh and hardened properties of geopolymers. Fresh mixture characteristics, in particular their flowability or workability and setting rate, are crucial for the practical application of cement materials. Workability and setting are important rheological properties of fresh geopolymer mixtures, which are strongly influenced by amount of water added. Influence of FA to activator or solution-to-FA ratios on the geopolymeric system on workability and setting time has been found to be the most crucial aspect in the development of the geopolymer binder (Abdul Rahim et al. 2014; Kong et al. 2007; Patankar et al. 2014; Rahmiati et al. 2015; Yellaiah et al. 2014). Furthermore, it is clear from literature that heating is required for FA based geopolymers, and many researchers have reported that the optimum temperature for 24 hours is 60 to 90°C. Figure 2.6 shows effect of the water to binder/alkaline solution ratio on heat curing of geopolymers.

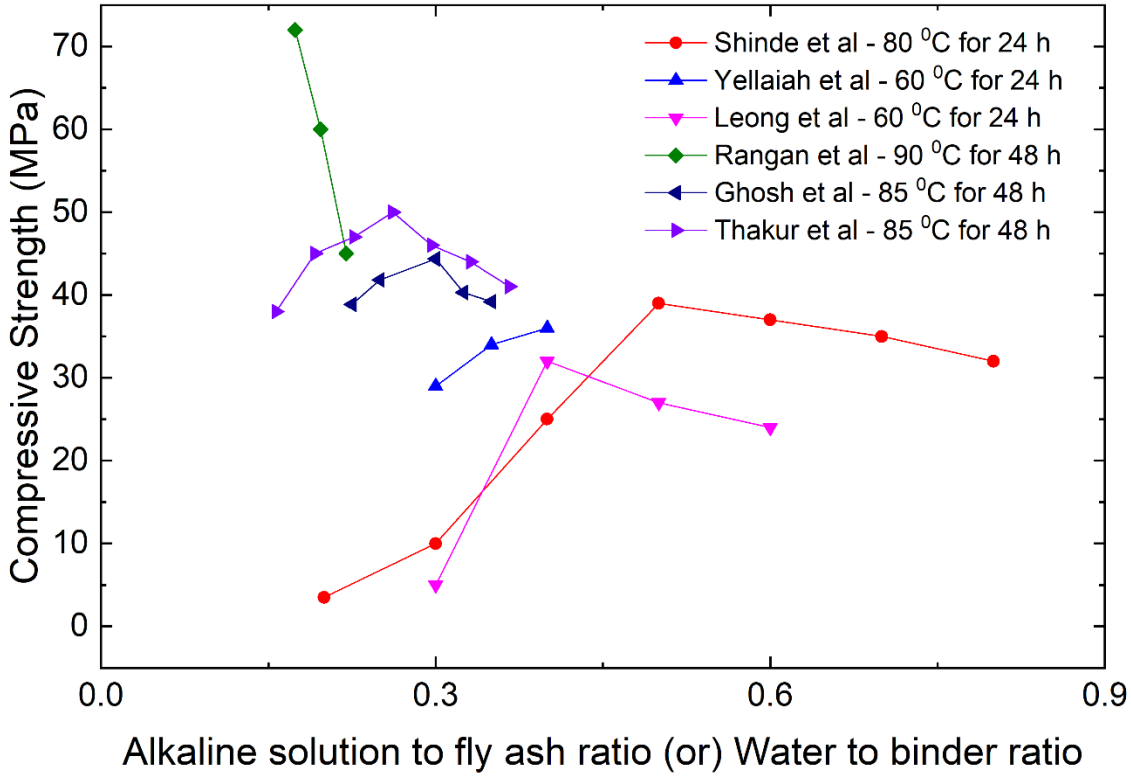

Figure 2.6: Influence of an alkaline solution to FA/water-to-binder ratio on the compressive load carrying capacity of FA-based geopolymeric samples (compilation of obtained results from various researchers)

2.4 REVIEW OF LITERATURES PERTAINING TO SETTING TIME OF GEOPOLYMERIC PASTES AND MORTARS

Mallikarjuna Rao (2015) studied about setting time of FA and GGBS based geopolymer paste and mortar. Alkaline activator in study consisted of Na_2SiO_3 and NaOH of varying molarities (8M, 12M, and 16M) and ratio of Na_2SiO_3 to NaOH was fixed as 2.5 throughout the study. Mass ratio of SiO_2 to Na_2O of Na_2SiO_3 solution was 2.61. Prepared solution was stored at room temperature of 25±2°C for 24 hours before its use. FA and GGBS were locally procured from thermal power plant and had specific gravities of 2.90 and 2.17 respectively. It was found in the study that increment in the molarity of NaOH resulted in the incremented FST, and with rise in content of GGBS as a replacement to FA FST setting decreased.

Chindaprasirt et al. (2014) investigated how characteristics of a high Ca FA geopolymer paste were affected by high speed mixing (Chindaprasirt et al. 2014). High speed mixers (1000 rpm) were used in the study, and results were compared to mixes prepared with normal mixers (140 rpm). The FA which was used was lignite high Ca FA from Mae Moh power station in northern

Thailand. The alkaline to FA ratio and $NaOH/Na_2SiO_3$ were fixed as 0.4 and 0.67, respectively. It was found that increasing the mixing time had slowed down the setting time of geopolymeric paste. Obtained results also showed that factors such as alkaline to FA ratio, the ratio of $Na_2SiO_3/NaOH$, and the concentration of NaOH affect the IST and FST of geopolymeric pastes.

Rattanasak et al. (2011) investigated how chemical admixtures affected properties of a high Ca FA-based geopolymeric paste (Rattanasak et al. 2011). Admixtures like $CaCl_2$, $CaSO_4$, Na_2SO_4 and sucrose for improvising the fast-setting characteristics of geopolymeric paste. The mass ratio of $Na_2SiO_3/NaOH$ and solid to total mixture ratio were kept constant as 1.5 and 0.6, respectively. The admixtures were added in the final step of mixing

Vicat's apparatus was used for testing the setting time of geopolymeric paste in accordance with the ASTM C125. The obtained results revealed that $CaCl_2$ significantly decreases the geopolymeric paste's IST and FST. Furthermore, sucrose also delayed the FST significantly.

Chindaprasirt et al. (2012) studied effect of Si and Al contents on setting time and other physical characteristics of high Ca FA geopolymeric pastes (Chindaprasirt et al. 2012). Nano Si and nano alumina were sources of silica and alumina apart from FA. Amounts of Si and alumina was so adjusted to keep the silica to alumina ratio between 2.87-4.79. Obtained results revealed that when compared to standard Class F geopolymer systems, impact of varying silica and alumina on setting and hardening properties in high Ca FA systems was noticeably different. In a contrary to typical geopolymer systems where increasing Al_2O_3 speeds up setting, high Ca based systems seem to set more quickly with incremented Si or Al content.

Deb and Sarker (2017) examined the influence of Si and Al concentration on setting time and other physical properties of high Ca FA geopolymeric pastes (Deb and Sarker 2017). Source materials utilized in their study were class F FA, ultrafine FA (UFA), GGBS and ordinary portland cement (OPC) along with alkali activators like NaOH and Na_2SiO_3. SiO_2/Na_2O ratio was maintained as 2.6 in this study. Geopolymeric samples were prepared in three different series (total twelve samples) which were (i) only FA, (ii) 10% OPC blended with FA and (iii) 15% GGBS blended with FA. Alkaline activator/binder and $Na_2SiO_3/NaOH$ ratios were fixed at 0.4 and 2.0, respectively. The obtained results showed a decrement in IST and FST due to the admixing of UFA. With 5% UFA, reduction in setting time was quite significant; however, as the proportion of UFA increased, the reduction in setting time decremented to relatively small amount. The study's concluding observations specified that managing the setting time characteristics of geopolymers cured under ambient temperature can be accomplished well by combining the effects of Ca and increased specific area UFA.

Al-Majidi et al. (2016) studied setting time and flowability of GGBS-FA based geopolymer mortar cured under ambient temperature (Al-Majidi et al. 2016). Combination of alkaline activators used in this study were KOH and K_2SiO_3 in 1:2.5 ratio. The study revealed that as the GGBS content increased from 15% to 25% and then to 50%, the IST reduced from 75 minutes to 45 min and then to 30 min respectively. Similarly, for FST it reduced 180 minutes to 85 minutes and then to 40 minutes respectively.

Saha and Rajasekaran (2017) studied the characteristic properties of geopolymeric paste by admixing GGBS. The setting time of the mixes with admixed GGBS (variations ranging from 0% to 50% in 10% increments) was determined. It was found that the IST and FST of geopolymeric pastes decremented by approximately 75% with the addition of GGBS from 10% to 50%. Furthermore, an analysis of micrographs concluded that as the admixing of GGBS in the mix increased, an occurrence of denser microstructure took place due to C-S-H and N-A-S-H gels formation because of the presence of Ca in GGBS.

2.5 REVIEW OF LITERATURES PERTAINING TO COMPRESSIVE STRENGTH OF GEOPOLYMER PASTE AND MORTAR

Li and Liu (2007) studied the effect of GGBS addition in FA based geopolymeric paste (Li and Liu 2007). Source materials utilized in this study consisted class F FA, MK, GGBS and Na_2SiO_3. On cast cube samples, compressive load carrying capacity was conducted (40x40x40 mm) while maintaining a loading rate of 0.375 MPa/s. By analysing obtained test results, it was found that strength in compression incremented for samples with GGBS addition (4%). The increase in strength in compression values for two sets of curing (30 and 70°C) was about 18 and 15 MPa respectively. It was deduced that co-existence of geopolymeric gel and C-S-H gel is the prime reason for the increased strength aspects.

Mallikarjuna Rao and Gunneswara Rao (2015) investigated compressive strength of FA-GGBS based geopolymeric pastes. By varying the amounts of FA and GGBS as well as the molarities of the alkaline activator, several geopolymeric pastes were produced. Compressive strength of the mix was checked at 8M, 12M and 16M concentration of alkaline activator and two types of curing conditions i.e., outdoor and oven curing were adopted for the study (Mallikarjuna Rao and Gunneswara Rao 2015). Findings gathered showed that oven curing increased the samples' 28-day compressive strength, showing that curing conditions have a significant impact on the properties of the resulting geopolymers. It was additionally found that the higher the molarity of the alkaline activator, the greater strength in compression values of paste samples.

Furthermore, increasing the GGBS proportion as a partial replacement for FA resulted in higher strength in compression values of resultant geopolymeric samples. This increase in strength can be attributed to the presence of GGBS's higher Ca level.

Saha and Rajasekaran (2017) investigated into how adding GGBS affected the characteristics of geopolymeric pastes based on FA. The GGBS addition was varied from 10% to 50% in this study. The alkaline solutions (Na_2SiO_3 and NaOH) were used in equal proportions and alkali to binder ratio was maintained as 0.4. Concentration of NaOH was varied as 6M, 8M, 10M, 12M, 14M and 16M (Saha and Rajasekaran 2017). The obtained results stated that an increase in GGBS percentage as well as concentration of NaOH resulted in an increment in strength in compression values of the paste samples.

By using Taguchi's experimental design methodology, Ramezanianpour and Alapour (2013) studied the compressive strength of FA-based geopolymeric pastes. The factors that were of prime interest in this study were curing temperature (varied in 40, 50, 60 and 70 °C) Na_2SiO_3 to NaOH ratio (varied in 0.5, 1.5, 2.5 and 3.5), molarity of NaOH (varied in 4M, 8M, 12M and 16M) (Ramezanianpour and Alapour 2013). Alkaline to binder ratio was kept as 0.4 for all samples. According to results, strength in compression values improves significantly when NaOH concentration rises from 4 to 12 M; however, strength in compression values barely changed as NaOH concentration rose from 12 to 16 M. Additionally, strength in compression values of FA-based geopolymer paste with NaOH concentrations < 8 M is not considerably increased by oven curing temperature. Additionally, it can be inferred from a comparison of FA-based geopolymer paste with that of OPC, preparations are required; (i) replace OPC paste with geopolymer, (ii) NaOH concentration should be > 8 M, (iii) Na_2SiO_3 to NaOH ratio between 0.5 and 2.5, and (iv) temperature of the curing should be > 50°C.

Islam et al. (2014) Investigated strength in compression development of GGBS-palm oil fuel oil ash (POFA)-FA geopolymer mortar (Islam et al. 2014). Eleven different mixes were prepared by using FA, POFA and GGBS. The study found that introducing GGBS in the mix increased the compressive strength, however addition of POFA decremented the strength due to coarser particles. Optimum mix was found to be 70% GGBS and 30% POFA, achieved a highest compressive strength of 66 MPa. Additional admixing of GGBS content in the mix didn’t yield the required outcomes.

Alkali activated GGBS-FA based mortar blends were explored by Wardhono et al. (2015) under conditions of ambient temperature curing (Wardhono et al. 2015). The mix proportions of GGBS: FA were 100:0%, 90:10%, 80:20%, 70:30%, 60:40%, 50:50%, respectively. The study revealed that the mix 50:50% achieved maximum compressive strength of 62MPa at 28

days. Furthermore, admixing FA to GGBS increased overall mix stability as the standard deviation with respect to compressive strength trended downwards. Higher values for early age strength was achieved for the mix 100:0%. However, this mixture showed a decline in strength with time, reaching its lowest strength value at day 28.

Effects of alkali content on production of high performance FA-GGBS blended geopolymeric composites were explored by Ghosh and Ghosh (2018) (Ghosh and Ghosh 2018). In this study, all the test samples were formulated with a FA:GGBS ratio of 70:30, water to binder ratio as 0.38, Na_2SiO_3 content as 8% (by weight), with a varying NaOH dosage (4, 6, 8, 10, 12%) relative to binder content (by weight). The obtained findings revealed that the addition of NaOH content upto 8% tended to form a dense and compact microstructure resulting in the acquiring higher values for compressive strength of resultant geopolymers. Beyond this percentage resulted in crack formation in the geopolymeric samples.

Slump loss rate and setting time of blended FA-GGBS based geopolymers activated with pentahydrate (pH) and anhydrous sodium metasilicate (AH) at room temperature were studied by Tennakoon et al. (2016). With the help of two activators indicated above (FA/GGBS%_pH and AH- 100/0%, 90/10%, 80/20%, 70/30%, 60/40%, and 50/50%), FA and GGBS were combined in a variety of ratios. Results showed that geopolymers produced with AH and pH had early endothermic reactions (heat absorption) and early exothermic reactions (heat release), respectively. Additionally, the kinetics of the reaction upon alkali activation retarded in the case of pH based geopolymers, which led to a slower reaction mechanism, tending to a lower dissolution as well as better diffusability of ions from FA and GGBS. Later on, compressive strength was achieved as a result of this delayed response mechanism.

2.6 REVIEW OF THE LITERATURE ON ALKALINE ACTIVATORS EFFECTS ON THE CHARACTERISTICS OF GEOPOLYMERIC MORTARS

Saloma et al. (2016) examined the effects of liquid activator concentration on the slump flow, setting time, density, and strength in compression for geopolymeric mortar. Concentration of NaOH was varied as 8M, 12M, 14M and 16M by keeping Na_2SiO_3/NaOH ratio as 1. The sand to binder and activator to FA ratios were taken as 2.75 and 0.8, respectively. Cubes of sizes 50 x 50 x 50 mm were casted and steam cured at a temperature of 60°C for a duration of 48 hours. Obtained results revealed that higher the concentration of NaOH, lesser value for slump flow was obtained, in turn reducing the workability of the mixture. Fast setting time and greater density of mortar samples was achieved with higher concentration of NaOH. Additionally, higher compressive strength (10.06 MPa) was achieved by using the NaOH concertation as

14M, hence concluding it as the optimum concentration for achieving the maximum strength in geopolymeric mortar samples.

Thakur and Ghosh (2009) investigated the development of compressive strength as well as microstructural characteristics by taking into consideration of main synthesizing parameters (like Na_2O/Al_2O_3 content, SiO_2/Al_2O_3 content, water to geopolymer solid ratio and sand to FA ratio) and processing parameters (like time and temperature of curing) on the compressive strength attainment of FA based geopolymeric paste and mortar (Thakur and Ghosh 2009). Obtained findings revealed that the geopolymeric mixture with an alkali content of 0.62 and silica content of 4.0 achieved a compressive strength of 48.2 MPa cured at 85°C. Mineralogical and microstructural studies on hardened geopolymers using SEM-EDS revealed formation of a new amorphous alumino-silicate phases such as hydroxysodalite and herschelite, that influenced strength in compression development in the resultant geopolymers.

2.7 REVIEW OF LITERATURE ON INFLUENCE OF TEMPERATURE OF CURING ON THE PROPERTIES OF GEOPOLYMER MORTAR

Hardjito and Tsen (2008) investigated the characteristics of FA based geopolymeric mortar activated using potassium-based activators (Hardjito and Tsen 2008). The concentration of KOH was varied in between 6 to 14M and the ratio of K_2SiO_3 to KOH ratio was varied in range of 0.4 to 2.5. Test specimens of size 50 x 50 x 50 mm were casted for nine mixtures each and were oven cured at a higher temperature of 60°C for a duration of 24 hours. Obtained results revealed that higher concentrations of KOH resulted in obtained higher values for compressive strength of FA-based geopolymers. However, the setting times of resultant geopolymers decremented with the increased molarity of KOH solution. Furthermore, there was a progressive decline in strength with rising temperature when the FA-based geopolymeric mortar samples were exposed to 400, 600, and 800°C. The highest strength in compression was yielded for samples exposed to 400°C. This points to the fact that for the continuation of geopolymerization process to take place, application of an elevated temperature becomes necessary which in turn improvises the characteristics of the resultant geopolymeric mortar samples.

2.8 REVIEW OF LITERATURES PERTAINING TO THE MICROSTRUCTURAL STUDIES CONDUCTED ON GEOPOLYMER PASTES AND MORTAR

Saha and Rajasekaran (2017) conducted morphological studies of FA-GGBS based geopolymeric pastes using SEM. In this study, the GGBS content was varied as 10, 20, 30, 40

and 50% as a replacement to FA for enhancing the characteristics of resultant geopolymers. Equal amounts of both alkaline activators (NaOH and Na2SiO3) were utilised (Saha and Rajasekaran 2017). The observations obtained by analzying the microphotographs revealed that the admixing of GGBS from 10 to 50% exhibited a denser microstructure. The formation of such denser microstructure can be attributed to more and more formation of C-S-H gel due to the incrementing percentages of GGBS in pastes.

Characteristics of alkali activated FA/GGBS geopolymeric pastes when they are new and when they have hardened have been studied by Jang et al. (2014) using plasticizers. Binders (GGBS and FA) were formulated followed by dry mixing of GGBS and FA in 0, 0.3, 0.5, 0.7 and 1 ratios. Combination of alkaline activators (NaOH and Na_2SiO_3) was used in this study. Two types of superplasticizers (polycarboxylate and naphthalene-based) were added at a variation level of 0%, 1%, 2%, 3% and 4% by mass of the binder (Jang et al. 2014). Results of analysing the microphotographs' observations showed that presence of hydration products caused a denser matrix to form when more GGBS was added to the mixture. However, inclusion of superplasticizers had no appreciable impact on production of hydration products.

Rashad (2015) investigated the influence of some additives like silica fume, FA, limestone, hydrated lime and portland cement on fresh characteristics (slump value) and hardened characteristics (compressive strength and shrinkage) of GGBS based geopolymeric pastes activated by Na_2SO_4 (Rashad 2015). The microstructural changes in the resultant geopolymeric pastes were anlayzed with the aid of SEM. Studying of crystalline phases were conducted using X-ray diffraction (XRD) and mass loss studies were conducted with the aid of thermogravimetric analysis (TGA). The observations obtained by analzying the microphotographs revealed that activated neat GGBS samples exhibited limited dispersed porosity and presence of rod-shaped crystals of ettringite and C-S-H. According to the findings from the analysis of the microphotographs, the activated neat GGBS samples had only a little amount of distributed porosity and rod-shaped crystals of ettringite and C-S-H. Because of the admixing of silica fumes in the paste samples, a higher strength was achieved, Unreacted spherical shaped particles of FA were observed for samples with 5% FA addition which could be the reason for achievement of lower compressive strength. A denser microstructure was observed for samples with 5% limestone addition compared to that of neat GGBS, which resulted in achievement of higher strength values with its addition. The samples with 5% hydrated lime addition portrayed the presence of a larger number of voids indicated a decrement in the compressive strength values with its addition. The micrograph with 5% portland cement addition showed a large number of unreacted particles which is the reason for

lower strength values with its incorporation in paste samples. According to the results of the XRD study, the activated GGBS, whether it contained additives or not, saw a diffuse hump at about 30° 2. The amorphous phases of activated GGBS combined with silica fume or FA showed no apparant modifications. Additional amount of calcite was noticed in the samples consisting of limestone and hydrated lime used as additives in the paste samples.

Alkali activated GGBS based geopolymeric paste's fresh (workability, setting time) and hardened (strength in compression) characteristics were studied by Allahverdi et al. (2010) (Allahverdi et al. 2010). SiO_2/Na_2O content was taken as 0.6 and the trial mixes were designed to in such a manner to consist varied levels of Na_2O (1, 2, 3, 4, 5 and 6%) by weight of dry GGBS. Microstructural and structural alterations in the resulting geopolymeric pastes were studied using SEM and FTIR. In order to assess influence of Na_2O concentration on morphology of GGBS samples, the 40^{th} day hardened samples were chosen for SEM analysis that contains 1 and 2% of weight % Na_2O. Obtained micrographs revealed that decrease in pore sizes when Na_2O was increased from 1 to 2%. While the GGBS particles were found to be bounded by a cementitious matrix of reaction products in the samples with 2% of Na_2O, indicating a significant effect of refinement on the microstructural characteristics of 40th day cured GGBS based paste samples, the GGBS particles maintained their distinct shape and size in the samples with 1% of Na_2O, demonstrating their non-involvement in the reactions. The observations obtained from FTIR analysis stated that for the samples with 2 to 6% of Na_2O resulted in the shifting of main band from 960 to 966 cm^{-1} that could be attributed to a higher degree of polymerization as Na_2O content is increases in GGBS. Additionally, it was stated that the creation of silico-aluminate structures and C-S-H gel have a key role in the production of greater strength values.

Saludung et al. (2018) investigated morphological and mechanical characteristics of FA-GGBS based geopolymeric paste samples through alkali activation. A total of five sets of paste samples were prepared wherein apart from the reference paste, FA was replaced by GGBS from 15 to 60% at an interval of 15% by mass. The alkaline solution to binder and Na2SiO3 to NaOH ratios were maintained as 0.45 and 2.0, respectively. The observations obtained from SEM microphotographs and XRD analysis exhibited that C-S-H gel formation becomes more significant with the increment in the GGBS. Furthermore, excess formation of C-S-H can damage the specimen structure at elevated temperatures because of its decomposition.

Effects of alkaline content on production of high performance FA-GGBS blended geopolymeric composites were explored by Ghosh and Ghosh (2018) (Ghosh and Ghosh 2018). In this study, all test samples had different amounts of NaOH (4, 6, 8, 10, 12%) in relation to

the amount of binder (by weight), an FA:GGBS ratio of 70:30, a water to binder ratio of 0.38, and a Na_2SiO_3 content of 8%. The reaction products were identified through FTIR and XRD. The observations from FTIR analysis stated that in general, as the alkali content increases, absorption values of various functional groups increase, that signifies an occurrence of complete geopolymerization reaction with increased alkali content.

Ismail et al. (2013) investigated response of alkali-silicate activated FA/GGBS geopolymeric pastes to varied forms of sulphate exposures like specifically immersing into 5 weight % $MgSO_4$ or Na_2SO_4 for a period of 3 months. Advanced characterization studies like SEM, XRD and FTIR were conducted for understanding the occurrence of changes in the microstructure of resultant geopolymeric pastes due to sulphate exposure (Ismail et al. 2013).

The observations obtained by analzying the SEM microphotographs revealed that the samples exposed to Na_2SO_4 neither represented any difference or formation of any new phase in the pastes. However, samples exposed to $MgSO_4$ showed formation of gypsum crystals. The observations obtained from energy dispersive spectroscopy (EDS) stated that Ca/Si and Mg/Si ratio after exposure confirms the decalcification of C-A-S-H due to sulphate attack in the case of $MgSO_4$ exposure, but these ratios remained unchanged in the case of Na_2SO_4 exposure, stating that there was zero occurrence of decalcification in the latter case. The observations obtained by FTIR stated that main asymmetric stretching phase located at 950-970 cm^{-1} neither represented any difference or any shift when exposed to Na_2SO_4, suggesting that Na_2SO_4 doesn't harm/change the structure of resultant geopolymeric pastes. However, in the case of $MgSO_4$ exposure, C-A-S-H phase decomposes in the microstructure of the pastes. Primary Si-O-T bands' disappearance and the emergence of additional bands (at 1115 and 1018 cm^{-1}) in geopolymeric paste samples, which are compatible with the presence of gypsum, are related to the decomposition of C-A-S-H. Formation of new bands as well as disappearance of calcite bands is consistent that was responsible to the degradation of the binders in the paste samples.

2.9 FIBRES ADMIXED GEOPOLYMERIC COMPOSITES – AN OVERVIEW

Although geopolymers have good thermal and durability properties, they are brittle and less able to withstand tensile and flexural loads, which prevents them from being used in a number of structural applications (Ranjbar et al. 2016; Ranjbar and Zhang 2020). Researchers have concentrated on strengthening geopolymers with synthetic and natural fibres to increase their flexibility and resistance to tensile strength as a means of resolving these problems. A practical strategy for preventing geopolymers' early-stage brittleness is the use of natural fibres in them.

(Silva et al. 2020). Fibres can be categorised as natural or man-made (Amor et al. 2021; Noman et al. 2022). Figure 2.7 briefs an overview of the broad classification of fibres.

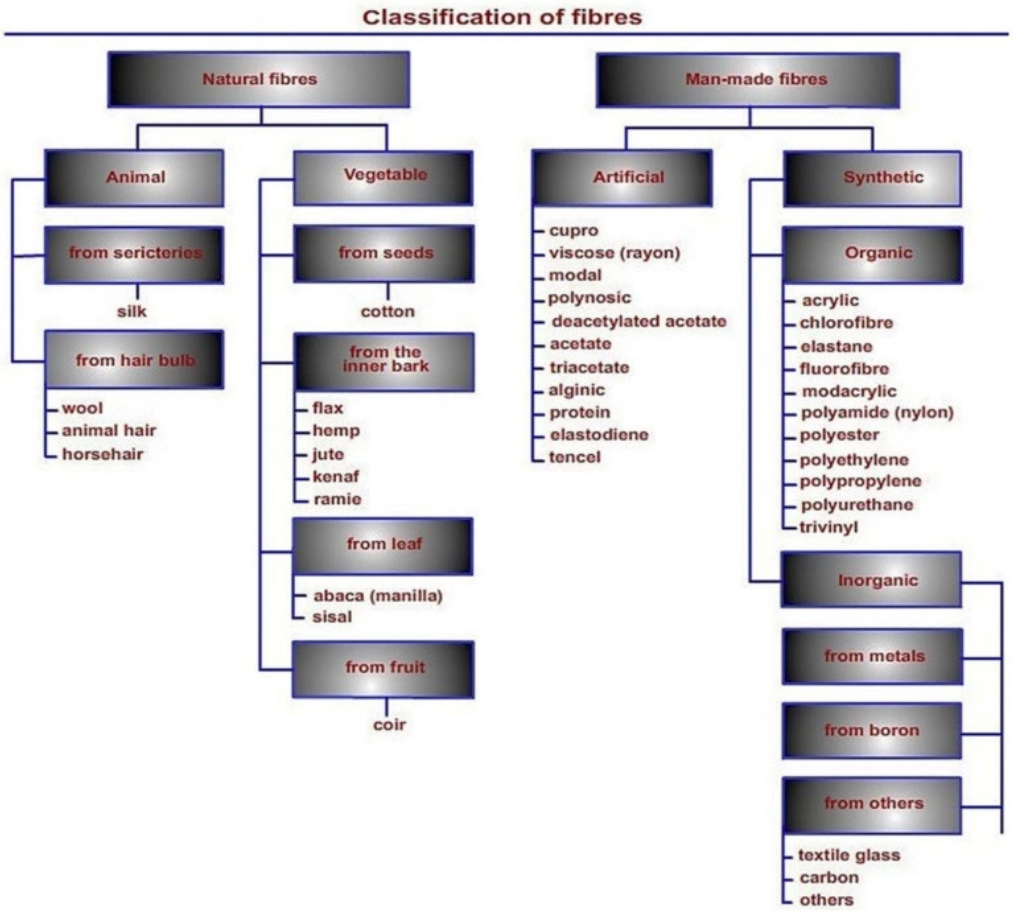

Figure 2.7: An overview of broad classification of fibres (Mahmood et al. 2021)

Fibres in the form of threads, filaments, whiskers, and nanoparticles can be employed as reinforcement in geopolymer composites for increasing flexural strength and energy absorption (Shaikh 2013). Additionally, fibres improve the geopolymer matrix's energy absorption and deformation resistance. In terms of toughness, geopolymers outperform OPC-based composites when reinforced with any type of fibre. Several factors affect fibre performance in geopolymer composites, including the fibre's inherent qualities, composition, precursors and composite age. Interface between fibre and matrix, on the other hand, plays the most essential role in overall mechanical properties, and with a strong contact interface, large loads can be easily transferred from the matrix to the fibres. The majority of fiber-reinforced geopolymer research has used steel fibres, carbon fibres, glass fibres, polypropylene fibres, polyvinyl alcohol fibres, and basalt fibres (Jamshaid et al. 2016, 2018; Shaikh 2013). Some selected literatures connected to the influence of fibres on the properties of geopolymeric pastes and mortars are presented in 2.11.

2.10 REVIEW OF LITERATURES ON INFLUENCE OF FIBRES ON THE PROPERTIES OF GEOPOLYMERIC PASTE AND MORTARS

Porkodi et al. (2015) assessed the self-compaction, strength, and mix proportions of geopolymer mortar for various fibre induced mix proportions (Porkodi et al. 2015). This study used class F FA, natural river sand, NaOH, Na_2SiO_3, commercially available superplasticizer, polypropylene fibres (PPF), Recron 3S fibres, E-glass fibres and steel fibres (SF). The alkaline solution to FA, Na_2SiO_3 to NaOH and FA to sand ratios were kept as 0.45, 1:1 and 1:1, respectively. Standard sized mortar specimens were casted and were kept in an oven for a duration of 24 hours. V-funnel test (at T5 minutes as per European Federation of National Associations Representing for Concrete - EFNARC regulations), U-box test, and J-ring test were performed to assess the workability of fresh mortar slump flow test. Obtained results revealed that geopolymeric mortar samples admixed with polypropylene fibres exhibited more compressive strength than cement mortar samples. Furthermore, self-compacted geopolymeric mortar samples admixed with polypropylene fibres with a solution/binder ratio of 0.45 exhibited higher strength in compression values than cement mortar samples, meeting the EFNARC guidelines for workability characteristics of self-compacting mortar.

Different characteristics of geopolymeric pastes like setting time and slump were tested for evaluating its properties at fresh state. However, characteristics like strength in compression, strength in flexure and shrinkage were tested for evaluation of hardened properties of geopolymeric paste samples. The admixing content of PPF in geopolymeric pastes samples was varied in 0.5%, 1%, 2%, 3%, 4%, and 5%. The obtained results revealed the workability of the pastes decremented significantly with the incrementing percentages of fibres, as it tended to higher resistance to flow. Furthermore, it was found that 3% was the optimal dose of fibre content addition for controlling shrinkage of geopolymeric pastes. However, it was also observed that the hardened characteristics of geopolymeric paste samples (compressive and flexural strength) without PPF content incremented with the progression in time. However, the paste samples with admixed PPF content nullified their strengthening parameter because of poor bonding between fibre-paste matrix and breakage of geopolymeric bonds.

Guo and Pan (2018) developed a FA-steel GGBS based geopolymeric mortar that aimed to recycle solid wastes so as to stick to the idea of developing a sustainable substitute to the portland cement (Guo and Pan 2018). The researchers investigated at how different types of fibres, such as polypropylene fibres (PPF), steel fibres (SF), and basalt fibres (BF), affected the mechanical properties of FA-steel sla based geopolymeric mortar samples. The water to binder and binder to sand ratios used were 0.4 and 1:2.5, correspondingly. PPF were varied in 0.1%,

0.2%, 0.3% and 0.4% whereas SF and BF were varied in 0.1%, 0.2%, 0.3%, 0.4% and 0.5%. All the characteristics of three fibre admixed mixes (compressive strength) were compared with control mix. Results showed that strength in compression values and strength in flexure values of PPF and BF mixes increased after 28 days, with the optimum dosages being 0.2 and 0.3-0.4%, correspondingly. However, strength in compression and flexure values of SF admixed mixes incremented obviously wherein optimum dosage stood at 0.4-0.5%. Overall comparison of mixes with the three types of fibres (PPF, SF and BF), it was concluded that the FA-steel GGBS based geopolymeric mortar sample with 0.4% of SF achieved the highest strength characteristics at the age of 28 days. Microstructural studies revealed that admixing of fibres can relieve the concentration of stress within the matrix so that spreading of cracks and matrix cracking can be prevented. Also, a homogenous densely packed pore structure suggested the advantageous usage of fibres in mortars for improving their mechanical characteristics.

2.11 CRITICAL REVIEW

Geopolymer is an environment friendly material and there is a need to understand and develop the geopolymeric binder, which would furnish the same characteristics of a cementitious binder. It is found that researchers on the FA based geopolymer binders have done abundant research, however, it is reported that heat curing is essential in such cases. According to additional research, the setting time in a FA-based geopolymeric binder is too long, and the strength in compression obtained is likewise insufficient for structural work.

Researchers used GGBS to increase compressive strength while decreasing setting time. It is reported that strength in compression of the FA and GGBS mix increased with the increase of GGBS proportion, but up to a certain limit only. It is observed from literature review that several parameters on which the setting time and strength in compression of geopolymeric binder depend are constituent mix proportion, physical and chemical properties of source material, concentration and amount of alkaline activators, curing conditions and alkali binder ratios. Furthermore, it was also understood from the past literature that among the parameters influencing the characteristics of resultant geopolymers as discussed previously, the alkali binder ratio was found to have a dramatic effect on the strength characteristics of geopolymers wherein an increase in its content parallelly escalated the strength characteristics up to a certain level and beyond which it was found to be decreased. Additionally, a usage of the balanced proportion of FA to GGBS in the resultant geopolymers coupled with the correct combination of influential parameters will tend to attain a denser and crack-free microstructural characteristics which can be related to the strength gaining mechanism in the geopolymers.

A thorough analysis of the literature on influence of various fibres on geopolymeric pastes and mortars indicated that steel and polypropylene fibres are the most commonly employed reinforcing materials, followed by glass and a few other fibre types. It was also shown that precursor blending and proportioning had a similar effect on the mechanical properties of fibre-induced geopolymeric samples. It has been reported that partially replacing FA with GGBS or increasing GGBS content to an optimum level in blended geopolymers improves strength in compression and modulus of elasticity. However, most of reported studies used method of curing either as heat or oven curing, which is in one way advantageous for achieving the required characteristics of resultant geopolymers, but on the other way it is energy conducive, cost additive, impractical as well as non-sustainable method.

As a result, the goal of this research is potentially producing geopolymeric mixes (of pastes and mortars) by combining abundant industrial by-products like GGBS and FA with alkaline solution as a binder. From the sustainability and cost-effective point of view, all the geopolymeric mixtures developed will be cured in ambient temperature conditions only. This practice will help in solving the disposal problems of growing industrial by-product as well as the environmental hazards in a more sustainable and cost-effective strategy.

2.12 OBJECTIVES OF THIS EXPERIMENTAL RESEARCH WORK

The objectives of this experimental research are

- To investigate effect of variation of binder proportions (FA and GGBS) on the setting time (initial and final), flow and microstructural properties of geopolymeric paste with different alkali to binder ratios.
- To investigate the effect of variation of binder proportions (FA and GGBS) on the setting time (initial and final), flow and microstructural properties of geopolymeric mortar with different alkali to binder ratios.
- To investigate the effect of steel fibres content on the setting time (initial and final) and flow properties of FA and GGBS based geopolymeric mortar.
- To examine the compressive strength and microstructural behavior of incorporation of steel fibres in FA and GGBS based geopolymeric mortar cured under ambient temperature with different alkali to binder ratios.

CHAPTER – 3

MATERIALS AND METHODS

3.1 GENERAL

This section discusses numerous materials that were used, tests conducted on them and pertaining results are shown. Additionally, sequential processes adopted for producing geopolymeric pastes, mortars and mortars with steel fibres is presented, along with standard testing procedures adopted to examine their engineering properties.

3.2 SOURCE MATERIALS FOR GEOPOLYMER PASTES, MORTARS AND MORTARS WITH STEEL FIBRES

3.2.1 FA

The utilized FA in this experimental research was acquired from Udupi Power Corporation Limited, Udupi Dist., Karnataka. Physical characteristics and chemical compositions of Based on the obtained chemical compositions, it is categorised as class F type under IS 3812 (Part-1) - 2013. The fineness of FA was analyzed with the aid of Blaine's air permeability apparatus. The microphotograph obtained from SEM is depicted in Figure 3.1 from which it can be stated that FA particles are found to have a spherical and smooth surface.

Table 3.1: Physical characteristics and chemical compositions of FA

Physical characteristics	
Characteristic property	**Obtained value**
Blaine fineness (m^2/kg)	260
Specific gravity	2.28
Chemical compositions (%)	
Element	**Oxide percentage**
Silicon dioxide	60.6
Aluminium oxide	28.6
Ferric oxide	3.9
Calcium oxide	1.7
Magnesium oxide	1.8
Sulfur trioxide	1.2
Sodium oxide	0.4
Loss on ignition	1.6

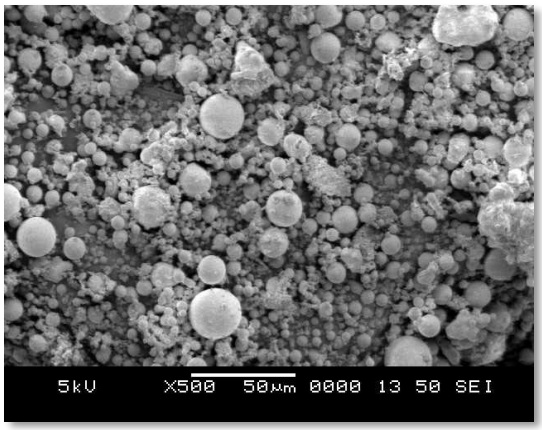

Figure 3.1: Microphotograph of FA obtained from SEM

3.2.2 GGBS

The GGBS was procured from Jindal Steels, Karnataka. Physical properties and chemical compositions of GGBS were analyzed, and the corresponding findings have been organized in Table 3.2. Obtained microphotograph from SEM is illustrated in Figure 3.2 from which it can be stated that the GGBS particles are found to have straight and flaky (elongated) shape with a rough texture.

Table 3.2: Physical characteristics and chemical compositions of GGBS

Physical characteristics	
Characteristic property	**Obtained value**
Blaine fineness (m^2/kg)	350
Specific gravity	2.85
Chemical compositions (%)	
Element	**Oxide percentage**
Silicon dioxide	34.4
Aluminium oxide	9.0
Ferric oxide	2.58
Calcium oxide	44.8
Magnesium oxide	4.43
Sulfur trioxide	2.26
Sodium oxide	-
Loss on ignition	1.32

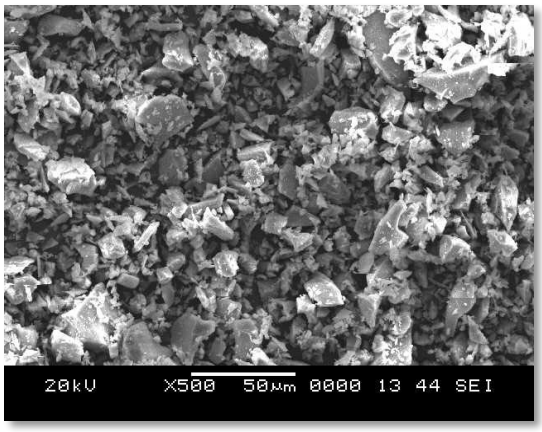

Figure 3.2: Microphotograph of GGBS obtained from SEM

3.2.3 Alkaline solution

The alkaline solution was prepared using laboratory-grade NaOH pellets and Na_2SiO_3 solution (constituents: 7.5 to 8.5%: Na_2O; 25-28%: SiO_2; 65.5% H_2O by mass). To prepare a 10 M NaOH solution, NaOH pellets were dissolved in distilled water. Subsequently, the NaOH solution that had been prepared was combined with Na_2SiO_3 in order to obtain the alkaline solution. This alkaline solution is left for cooling at room temperature for 24 hours before its usage in trial mixes.

3.2.4 Fine aggregates

The fine aggregates, specifically river sand, were obtained from a local source and were found to meet the specifications outlined in zone - I according to the IS 383:2016 standards. The analysis of the physical properties of fine aggregates was conducted, and the corresponding findings are shown in Table 3.2. Gradation of fine aggregates is depicted in Figure 3.3.

Table 3.3: Physical characteristics of fine aggregates

Properties		Fine Aggregates
Specific gravity		2.63
Bulk density (kg/m^3)	Loose state	1520
	Compacted state	1760
Water absorption		1%

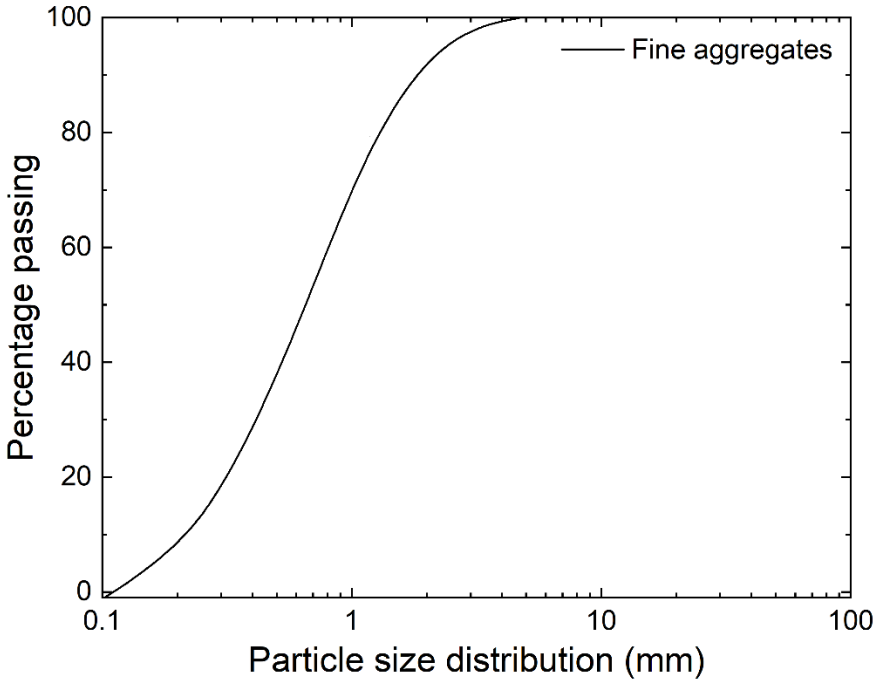

Figure 3.3: Gradation of fine aggregates

3.2.5 Steel fibres

In this experimental study, steel fibers consisting of a diameter = 0.45 mm and a length = 12.5 mm were utilized, as depicted in Figure 3.4. These fibers had an aspect ratio of 27.77.

Figure 3.4: Steel fibres

3.2.6 Water

For the production of geopolymeric pastes, mortar and mortar with steel fibres, all used potable tap water.

3.3 PRODUCTION OF FA-GGBS BASED GEOPOLYMERIC PASTE, MORTAR AND MORTAR WITH STEEL FIBRES

3.3.1 Mix proportioning for geopolymeric pastes

A. Based on alkaline liquid to binder ratio and partial replacement of FA with GGBS

Mix proportioning for geopolymeric paste samples was designed for obtaining a comparative assessment of variation in mainly two sets of parameters which are as follows.

(i) Alkaline to binder ratio, varied as 0.5, 0.6, 0.7 and 0.8 and

(ii) Partial replacement of FA with GGBS, varied in amounts 0%, 10%, 20%, 30%, 40% and 50% by weight of the binder (FA+GGBS).

Hence, a total of 24 trial mixes were formulated by considering both sets of parameters, as mentioned above. The trial mixes details are presented in Table 3.4, along with their respective mix designations. In each of the mixes shown in Table 3.4, a constant NaOH content of 10 M and a $NaOH/Na_2SiO_3$ ratio of 1:2.5 were maintained.

Table 3.4: Mix proportions for geopolymeric pastes

FA: GGBS (F:G)	Alkaline to binder ratio			
	0.5	**0.6**	**0.7**	**0.8**
F100:G0	A0	B0	C0	D0
F90:G10	A10	B10	C10	D10
F80:G20	A20	B20	C20	D20
F70:G30	A30	B30	C30	D30
F60:G40	A40	B40	C40	D40
F50:G50	A50	B50	C50	D50

B. Based on solid to liquid ratio

The mix proportioning for geopolymeric paste samples was again designed for obtaining another comparative assessment of variation in solid to liquid ratios, varied as 1:2.5, 1:2, 1:1.5 and 1:1 in conjunction with varied alkaline to binder ratios (as explained under 'A'). This variation of solid to liquid ratio was limited for samples A0, B0, C0 and D0 i.e., for samples with 100% FA

3.3.2 Mix proportioning for geopolymeric mortars and mortars with steel fibres

A. For geopolymeric mortars

Mix proportioning for geopolymeric mortars was designed by taking into consideration of variation in alkaline to binder ratio (0.5, 0.6, 0.7 and 0.8), partial replacement of FA with GGBS (0% to 50% by weight of the binder at an interval of 10%) with maintaining a constant binder to sand ratio was 1:3 in all the trial mixes. Hence, a total of 24 geopolymeric mortar samples were formulated by considering both the sets of parameters. The details of formulated trial mixes are presented in Table 3.5, along with their respective mix designations. Each of the mixtures presented in Table 3.5 maintained a constant molarity of NaOH as 10 M; $NaOH/Na_2SiO_3$ as 1:2.5.

Table 3.5: Mix proportions of geopolymeric mortars

FA: GGBS (F:G)	Binder to sand ratio	Alkaline to binder ratio			
		0.5	**0.6**	**0.7**	**0.8**
F100:G0	1:3	A0	B0	C0	D0
F90:G10	1:3	A10	B10	C10	D10
F80:G20	1:3	A20	B20	C20	D20
F70:G30	1:3	A30	B30	C30	D30
F60:G40	1:3	A40	B40	C40	D40
F50:G50	1:3	A50	B50	C50	D50

B. For geopolymeric mortars with steel fibres

The mix proportioning for geopolymeric mortars with steel fibre addition was designed by taking into consideration of as usual ongoing parameters like variation in alkaline to binder ratio (0.5, 0.6, 0.7 and 0.8), replacement of FA with GGBS (0%-50% by weight of the binder at an interval of 10%), constant binder to sand ratio (1:3), along with the addition of steel fibre content (0.5%, 1% and 1.5% by weight of the mortar). Hence, a total of 72 mixes geopolymeric mortar samples with admixed steel fires were formulated by considering all the parameters, as described previously. Table 3.6 contains information on the formulated trial mixes, as well as their mix designations. Each of the mixtures presented in Table 3.6 maintained a constant concentration of NaOH at 10 M and a $NaOH/Na_2SiO_3$ ratio of 1:2.5.

Table 3.6: Mix proportions for geopolymeric mortars with steel fibres

Alkaline to binder ratio	FA: GGBS	Binder to sand ratio	Steel fibre content (%)		
			0.5 (S_1)	1 (S_2)	1.5 (S_3)
0.5 **(A Mixes)**	100:0	1:3	A0 S_1	A0 S_2	A0 S_3
	90:10	1:3	A10 S_1	A10 S_2	A10 S_3
	80:20	1:3	A20 S_1	A20 S_2	A20 S_3
	70:30	1:3	A30 S_1	A30 S_2	A30 S_3
	60:40	1:3	A40 S_1	A40 S_2	A40 S_3
	50:50	1:3	A50 S_1	A50 S_2	A50 S_3
0.6 **(B Mixes)**	100:0	1:3	B0 S_1	B0 S_2	B0 S_3
	90:10	1:3	B10 S_1	B10 S_2	B10 S_3
	80:20	1:3	B20 S_1	B20 S_2	B20 S_3
	70:30	1:3	B30 S_1	B30 S_2	B30 S_3
	60:40	1:3	B40 S_1	B40 S_2	B40 S_3
	50:50	1:3	B50 S_1	B50 S_2	B50 S_3
0.7 **(C Mixes)**	100:0	1:3	C0 S_1	C0 S_2	C0 S_3
	90:10	1:3	C10 S_1	C10 S_2	C10 S_3
	80:20	1:3	C20 S_1	C20 S_2	C20 S_3
	70:30	1:3	C30 S_1	C30 S_2	C30 S_3
	60:40	1:3	C40 S_1	C40 S_2	C40 S_3
	50:50	1:3	C50 S_1	C50 S_2	C50 S_3
0.8 **(D Mixes)**	100:0	1:3	D0 S_1	D0 S_2	D0 S_3
	90:10	1:3	D10 S_1	D10 S_2	D10 S_3
	80:20	1:3	D20 S_1	D20 S_2	D20 S_3
	70:30	1:3	D30 S_1	D30 S_2	D30 S_3
	60:40	1:3	D40 S_1	D40 S_2	D40 S_3
	50:50	1:3	D50 S_1	D50 S_2	D50 S_3

3.4 PREPARATON OF TEST SAMPLES AND APPLICABLE TESTING METHDOLOGIES

3.4.1 Preparation of geopolymeric paste samples

The mixing of geopolymeric pastes was performed with the aid of an automatic mixer that complies to EN 196-3. Cubical moulds of size 50 x 50 x 50 mm were utilized for casting of geopolymeric pastes, with the purpose of conducting tests to determine their setting time and compressive strength. Additionally, the compressed cubic samples were subjected to curing at room temperature. (27 ± 2 °C with a RH of 95%) After a period of 24 hrs, the samples were removed from the moulds. Subsequently, paste samples were stored in a safe designated place till the day of testing. For conducting the microstructural characterization studies, the chucks

obtained after performing the compressive strength test were collected and stored safely till testing day

3.4.2 Preparation of geopolymeric mortars and mortars with steel fibres

The mixing of geopolymer mortars was performed with the aid of an automatic mortar mixer that complies to EN 196-3. The steel fibres were just spread on the blended geopolymer mortar mixture for about 3 to 4 minutes and it was again thoroughly mixed in the mortar mixture for obtaining a homogeneous steel fibre admixed geopolymeric mortar. Cubical specimens measuring each side as 70.6 mm were used to conduct compressive load carrying capacity tests on a combination of blended geopolymeric mortars and geopolymeric mortar admixed with steel fibers. Cube samples measuring each side as 150 mm were made for purpose of evaluating the properties of geopolymeric mortars and mortars containing steel fibres. Additionally, the compressed cubes of both dimensions were subjected to curing at room temperature (27 ± 2 °C After a period of 24 hrs, cubes were removed from moulds. Subsequently, mortar samples were stored in a safe designated place till the day of testing. For conducting the microstructural characterization studies, the chucks obtained after performing the compressive strength test were collected and stored safely till the testing day.

3.4.3 Test methods for geopolymeric samples

The experimental methodologies employed for the evaluation of geopolymeric pastes, geopolymeric mortars, and mortars containing steel fibers are outlined in Tables 3.7 and 3.8, correspondingly.

Table 3.7: Test methods for geopolymeric pastes

Tests	In accordance with	Particulars
Setting time	IS 4031-Part 5:1988	Using Vicat apparatus
Workability	IS 4031-Part 7:1988	Mini flow table (15 strokes)
Compressive strength	IS 4031-Part 6:1988	Using CTM Cured at 7, 14 and 28 days
SEM-EDS	-	Using SEM (measured at 28 days) Model no: JSM-638OLA associated with EDS analyzer.
FTIR	-	Using FTIR (measured at 28 days) Model no: Bruker Alpha (KBr)

Table 3.8: Test methods for geopolymeric mortars and mortars with steel fibres

Tests	In accordance with	Particulars
Setting time	IS 8142:1976	Using Penetrometer
Workability	IS 4031-Part 7:1988	Mini flow table (15 strokes)
Compressive strength	IS 4031-Part 6:1988	Using CTM Cured at 3, 7 and 28 days
SEM-EDS	-	Using scanning electron microscope (measured at 28 days) Model no: JSM-638OLA associated with EDS analyzer.

3.4.3.1 Setting time for geopolymeric pastes, geopolymeric mortars and mortars with steel fibres

The IST and FST for all the geopolymeric paste mixes were conducted as per IS 4031-Part 5:1988. The IST and FST for all geopolymeric mortars and mortars with steel fibres was conducted as per IS 8142:1976.

3.4.3.2 Flowability

The flow table test was conducted for measuring the flowability of geopolymeric paste, mortar and mortar with steel fibres in accordance to IS 4031-Part 7:1988 with 15 strokes. The mean flow diameter was measured and flow value was calculated using equation 3.1 shown below.

$$Flow = \frac{D_{average} - D_o}{D_o} * 100 \quad (3.1)$$

where, $D_{average}$ = Average base diameter and D_o = Original base diameter

3.4.3.3 Compressive load carrying capacity

The determination of the strength in compression values of geopolymeric pastes, mortars, and mortars containing steel fibers was conducted using a loading rate of 35 N/mm^2, following the guidelines outlined in IS 4031-Part 6: 1988. For assessing strength in compression of each mix, three test specimens were selected for analysis across all curing ages. The average value obtained from these specimens was then reported as the strength in compression for the respective mix.

3.4.3.4 SEM-EDS analysis

A total of 15 samples were collected from the core of geopolymeric pastes, mortars, and mortars with steel fibres (5 samples each from geopolymeric paste, mortar and mortar with

steel fibres), as defined in sections 3.4.1 and 3.4.2. These samples were then subjected to gold sputtering for microstructural analysis SEM. The SEM images were taken using a scanning electron microscope (JEOL, JSM-638OLA make) in secondary electron mode. The elemental analysis was carried out using and EDS analyzer for analysing the changes in elemental compositions within the boundary of the image.

3.4.3.5 FTIR analysis

Stored samples, as indicated in section 3.4.1, were crushed, and pieces from the core of the geopolymeric pastes were sieved through a 75 mm IS sieve to produce fine typed samples for minimising the reflectance in the instrument. An insight about the formation of heterogenous aluminosilicates was obtained with the aid of FTIR.

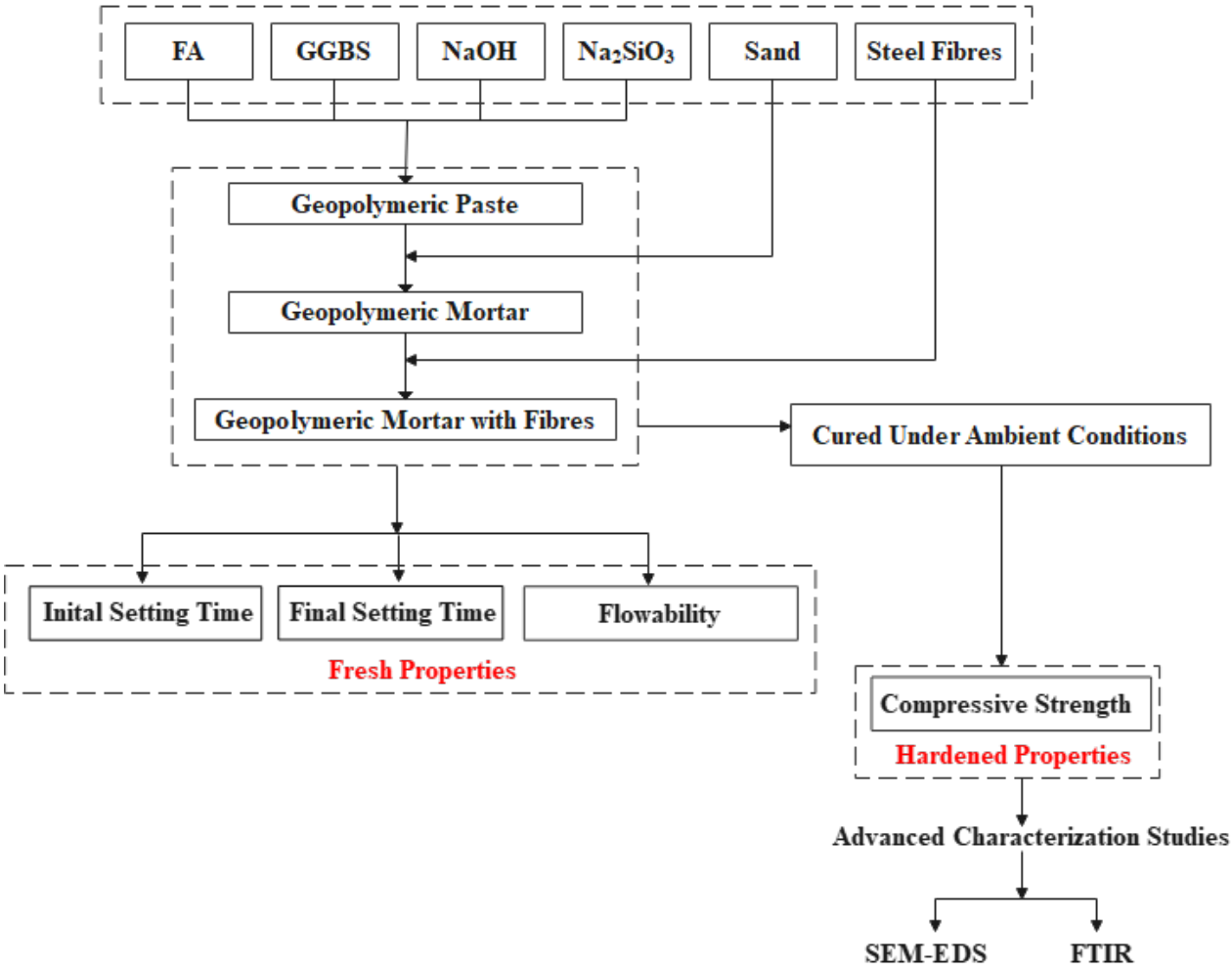

Figure 3.5: Flowchart representing the materials and experimental methodology

CHAPTER – 4

RESULTS AND DISCUSSION ON GEOPOLYMERIC PASTES

4.1 GENERAL

The findings of the tests performed on FA-based geopolymeric pastes that were cured at room temperature are presented in this chapter. Engineering properties of geopolymeric pastes were evaluated following the testing specifications outlined by the BIS. Advanced characterization techniques like SEM-EDS and FTIR were incorporated for characterizing the geopolymeric paste samples.

4.2 ENGINEERING PROPERTIES OF FA BASED GEOPOLYMERIC PASTES

4.2.1 Setting time and flow table test

Setting time and flow table test are the prominent benchmarks for measuring the performance of geopolymer mix samples. The obtained results for setting time for geopolymer mix samples with the variation in (i) alkaline to binder ratio and partial replacement of FA with GGBS and (ii) solid to liquid ratio in conjunction with varied alkaline to binder ratios for samples A0, B0, C0 and D0 (samples with 100% FA) is presented in subsequent sections, respectively.

4.2.1.1 Setting time and mini flow table test results for geopolymeric paste samples with the variation in alkaline to binder ratio and partial replacement of FA with GGBS

The IST and FST of geopolymeric mix samples with variation in alkaline to binder ratio and partial replacement of FA with GGBS are depicted in Figure 4.1, wherein it can be noticed that the lowest IST and FST is 20 and 58 minutes, respectively for F50G50 composition with alkaline to binder ratio of 0.5. The highest IST and FST is 305 and 485 minutes, correspondingly for F100G0 composition with alkaline to binder ratio of 0.8. The setting time of geopolymer mixes is susceptible to the addition of GGBS content and alkaline binder ratios, as evidenced by the findings that the setting time of geopolymeric mixes decreases as the GGBS% in the mixes increases. From Figure 4.1 (a) and 4.1 (b), a decrement of about 77-86% and 78-80% in IST and FST can be observed as GGBS content varies from 0% to 50%, by weight of binder, respectively. This could be related to faster hydration and a lower degree of

GGBS polymerization, which reduces setting time as GGBS content in geopolymer mix samples increases (Xu et al. 2021).

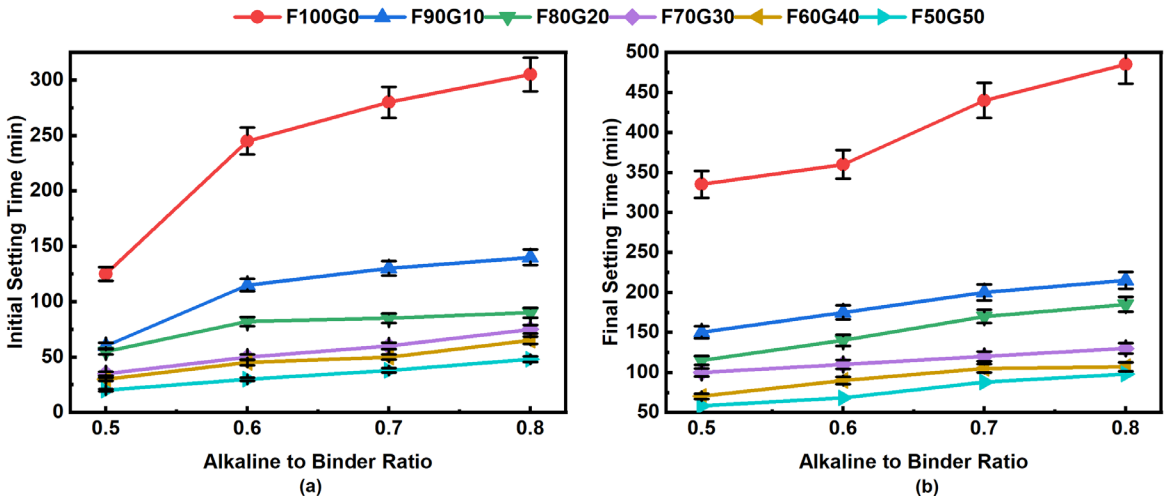

Figure 4.1: Effect of alkaline to binder ratio on setting time (a) Initial setting time, (b) Final setting time of geopolymeric pastes

Table 4.1 summarizes results of the mini flow table, which show that all of the geopolymer mix samples (group B, C, and D mixes) with alkaline to binder ratios of 0.6, 0.7, and 0.8 were overflown from the base of the table due to the combined effect of GGBS addition as well as alkaline binder ratio in all of the paste samples. Whereas, all the samples of 0.5 ratio (group A mix) have resulted in some extended diameter which could be attributed to the two reasons. One is FA possess a greater specific surface area compared to that of GGBS and second one is this particular mix group comprises higher fraction of FA for which alkaline binder ratio of 0.5 has lubricated the particle surface owing to overflow in this mix as represented in Figure 4.2. Furthermore, a same trend was noticed in the reported results by Rao and Rao (Mallikarjuna Rao and Gunneswara Rao 2015).

Table 4.1: Results of mini flow table test

Sample Name	Alkaline to Binder Ratio	Trial 1					Trial 2				
		D1	D2	D3	D4	$D_{average}$	D1	D2	D3	D4	$D_{average}$
Group A	0.5	-	-	-	-	Overflow	190	180	190	180	185
Group B	0.6	-	-	-	-	Overflow	-	-	-	-	Overflow
Group C	0.7	-	-	-	-	Overflow	-	-	-	-	Overflow
Group D	0.8	-	-	-	-	Overflow	-	-	-	-	Overflow

Figure 4.2: Sample A (alkaline to binder ratio-0.5)

4.2.1.2 Setting time results for geopolymeric paste samples with the variation in solid to liquid ratio in conjunction with varied alkaline to binder ratios

Figure 4.3 depicts the IST and FST of geopolymeric mixes for geopolymeric paste samples with varying solid to liquid ratios in conjunction with varying alkaline to binder ratios. Table 4.2 shows the percentage Na_2O and SiO_2 content of geopolymeric mixes with various solid-to-liquid ratios and alkaline-to-binder ratios, where the ratio of NaOH and Na_2SiO_3 varies in solution.

Table 4.2: Details of Na_2O and SiO_2 content

NaOH/Na_2SiO_3	**% Na_2O in solution**	**% SiO_2 in solution**	**Na_2O/SiO_2**
1:2.5	58.42	18.92	3.08
1:2	59.61	17.75	3.35
1:1.5	61.48	15.9	3.86
1:1	64.15	13.25	4.84

(Note: The variation in NaOH/Na_2SiO_3 was carried out only on A0 to D0)

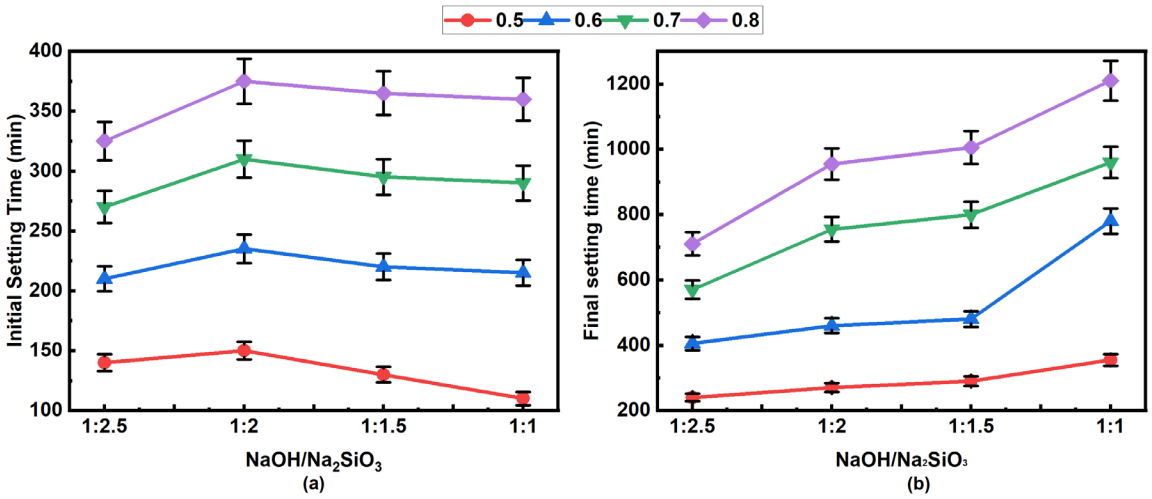

Figure 4.3: Effect of solid to liquid ratio on setting time (a) Initial setting time, (b) Final setting time

From Figure 4.3 (a), it can be noticed that the IST gradually increases (140-150 minutes: for 0.5; 210-235 minutes: for 0.6; 270-310 minutes: for 0.7; 325-375 minutes: for 0.8) with an increase in solid to liquid ratio from 1:2.5 to 1:2 which henceforth decreases as the ratio progresses from 1:2 to 1:1 (150-110 minutes: for 0.5; 235-215 minutes: for 0.6; 310-290 minutes: for 0.7; 375-360 minutes: for 0.8). But in the case of FST (Figure 4.3 (b)), a reverse trend can be observed wherein it increases (240-355 minutes: for 0.5; 405-780: for 0.6; 570-960: for 0.7; 710-1210: for 0.8) continuously with respect to an increment in solid to liquid ratios (1:2.5 to 1:1). The reduction in IST could be attributed to an increment in Na_2O content percentage and a decrement in SiO_2 content percentage in the solution. An increase in FST, on the other hand, could be attributable to the fact that in later phases of the geopolymerization reaction, SiO_2 is involved in substitution, and the only factor affecting setting time is an increment in Na_2O%.

4.2.2 Compressive load carrying capacities of geopolymeric pastes with variation in alkaline to binder ratio and partial replacement of FA with GGBS

Figure 4.4 (a), (b), (c), and (d) show the compressive load carrying capacity of geopolymeric pastes with varied GGBS % and alkaline to binder ratio at curing ages 7, 14, and 28.

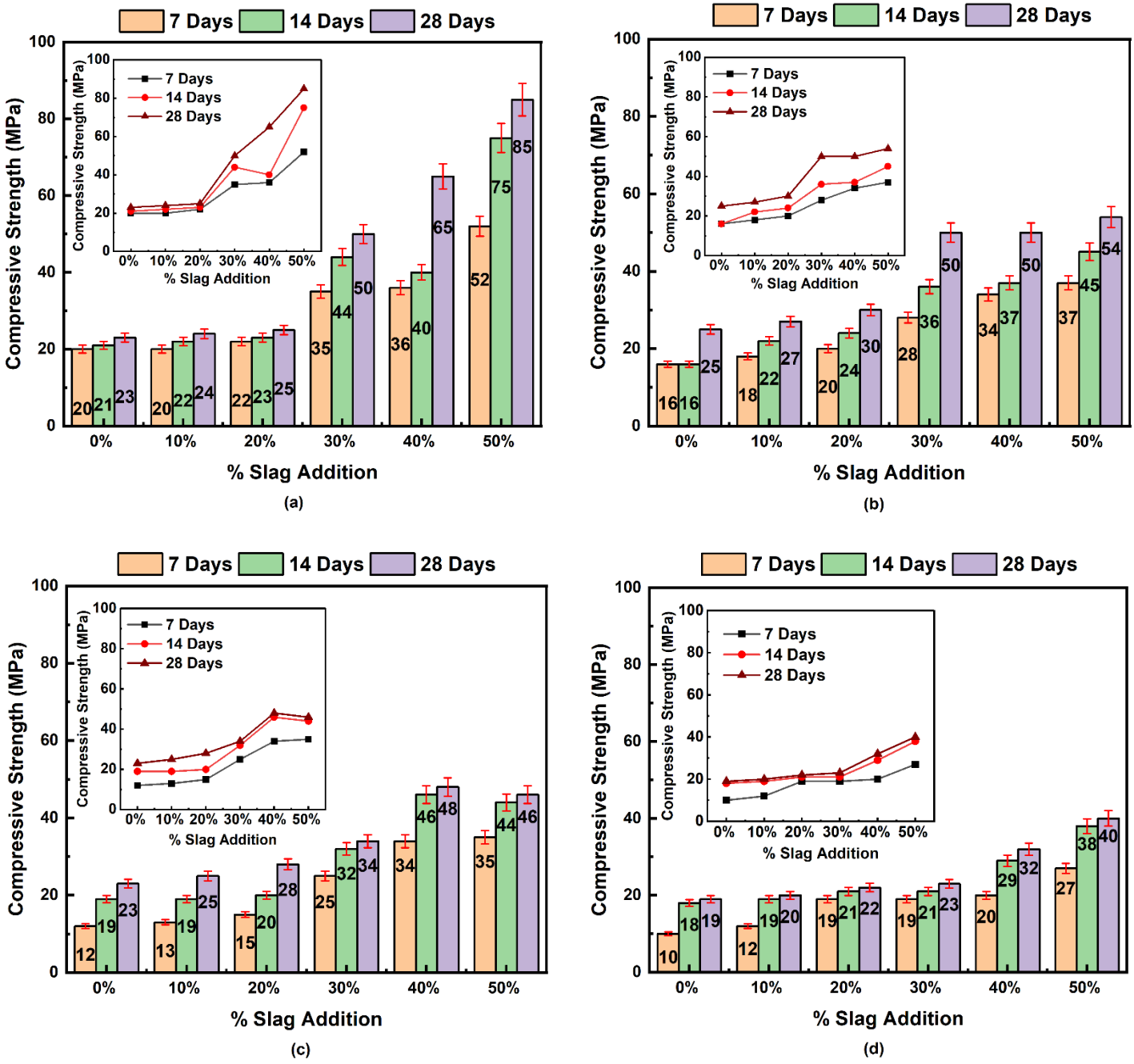

Figure 4.4: Compressive load carrying capacities of geopolymeric pastes at curing ages 7, 14 and 28 days at alkaline to binder ratio (a) 0.5 (b) 0.6 (c) 0.7 and (d) 0.8

As the GGBS substitution in FA rises, the compressive load carrying capacity of geopolymeric samples increments. The strength in compression of geopolymeric mix samples at 28 days is 85 MPa for 50% GGBS substitution with an alkaline to binder ratio of 0.5 and 40 MPa for 50% GGBS substitution with an alkaline to binder ratio of 0.8, correspondingly. Probable reasons for this strength development with age for GGBS rich specimens compared to only FA ones is that the latter ones leaches slowly under ambient curing conditions (Li et al. 2013). Furthermore, since GGBS comprises good amount of Ca, this factor has an optimistic influence

on the strength characteristics (Samantasinghar and Singh 2019). Furthermore, it is clear that alkaline to binder ratio is a key factor in strength development of geopolymeric mixtures. Since a high alkaline to binder ratio indicates that there is substantial porosity present in hardened geopolymer samples, the strength decreases as the alkaline to binder ratio rises above 0.5. (Bakharev 2006; Kong et al. 2007). The presence of excess water due to increased activator content has resulted in geopolymer mix samples with lower strength, as shown in Figure 4.4.

4.3 ADVANCED CHARACRTERIZATION STUDIES ON GEOPOLYMERIC PASTES

4.3.1 SEM with EDS analysis

Geopolymeric paste samples from group A (A0-A50) that had higher compressive load carrying capacity values at 28 days curing age as compared to other group were chosen for SEM investigation, and microphotographs of those samples are shown in Figure 4.5. Reaction products/elemental compositions were obatined using EDS analysis which gives an inference about the presence of type of gel within the paste samples.

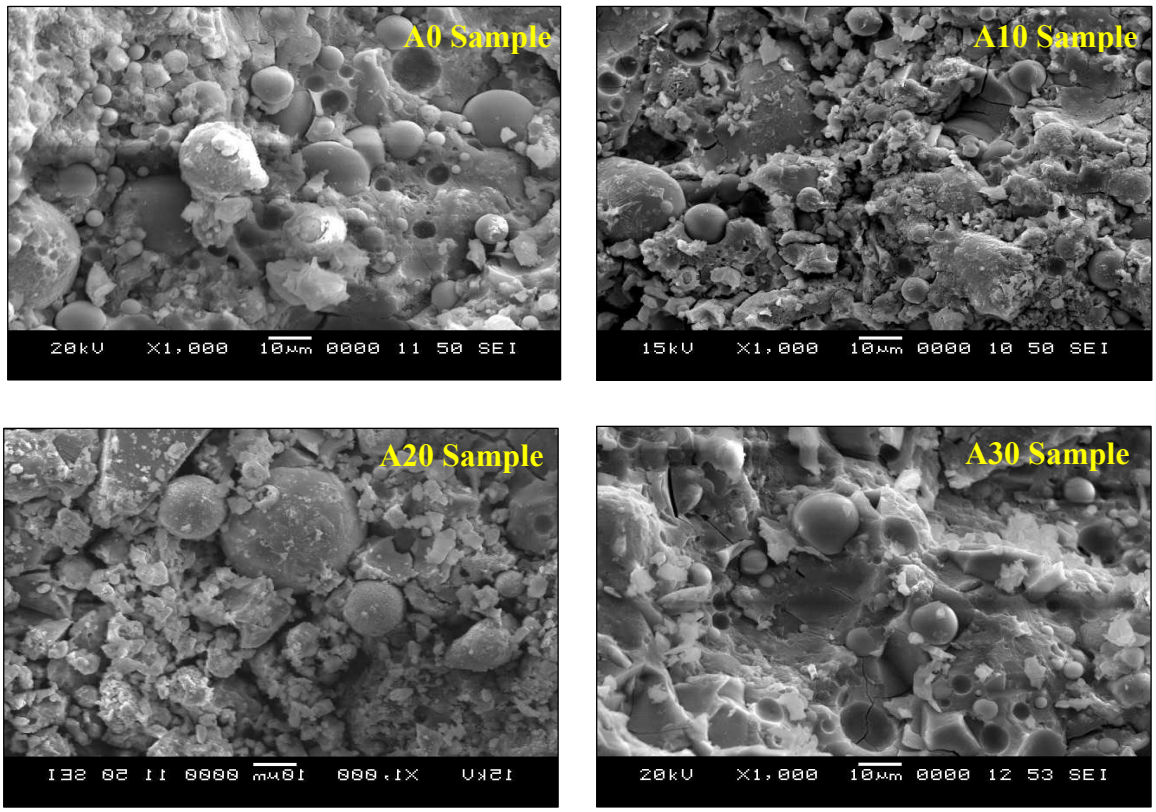

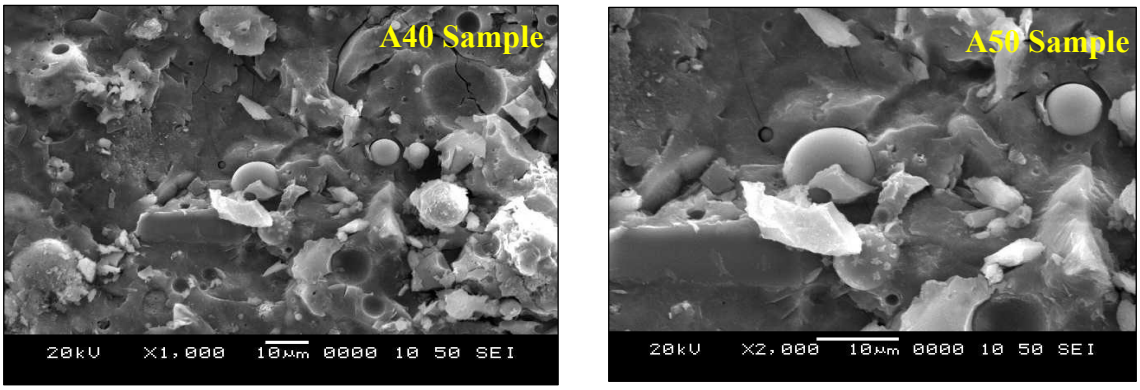

Figure 4.5: SEM microphotographs of group A mixes with alkaline to binder ratio of 0.5

Images show that microstructure of geopolymer mix samples develops more compact and denser as quantity of C-A-S-H (calcium alumino-silicate hydrate) gel increases with an increment in GGBS substitution (A0-A50) in the precursor, FA. C-A-S-H gel produced throughout the reaction acts as a microaggregate, improving the microstructure of the geopolymer mix samples (Xu et al. 2021). This phenomenon can be corresponded with the increased compressive strength in geopolymer mix samples for alkaline to binder ratio of 0.5 as represented in Figure 4.4 (a).

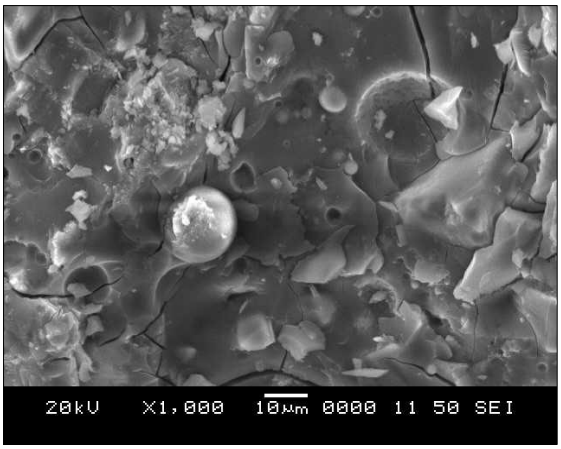

Figure 4.6: SEM microphotograph of geopolymer mix sample with alkaline to binder ratio as 0.8

Figure 4.6 represents the SEM microphotograph of a selected geopolymer mix sample with alkaline to binder ratio of 0.8. From figure, it can be noticed that with an increased alkaline to binder ratio has resulted in the development of significant cracks in the microstructure of the specimen which supports the lowering of strength with higher alkaline to binder ratios.

By overlooking all the above represented SEM microphotographs of geopolymer samples, it can be generalized that there is a presence of varying amounts of unreacted FA particles in

almost all the samples. However, it can also be noticed from the figures (Fig. 4.6) that there is a propagation of cracks towards the outside from the centre of unreacted FA globules, especially in geopolymer mix samples with an alkali binder ratio of 0.8. This unreacted FA particles are weak points in the microstructure of geopolymer mix samples (Xu et al. 2021). Engineering characteristics of the resulting samples were influenced by the appropriate GGBS substitution levels in FA, alkaline to binder ratio, and reaction method.

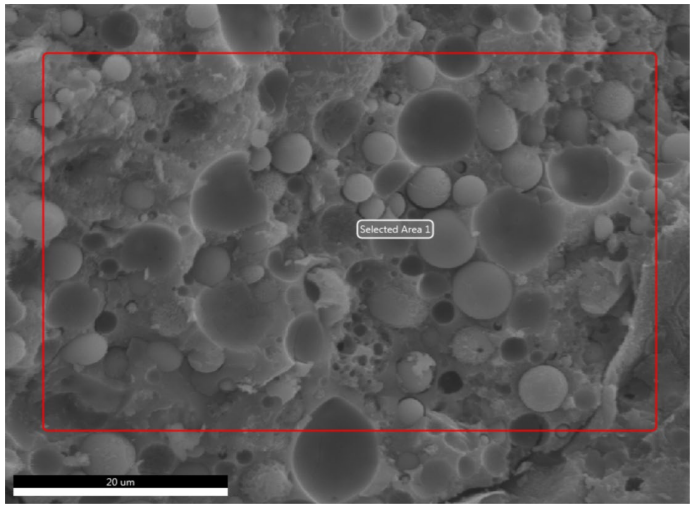
Selected Area 1
20 um

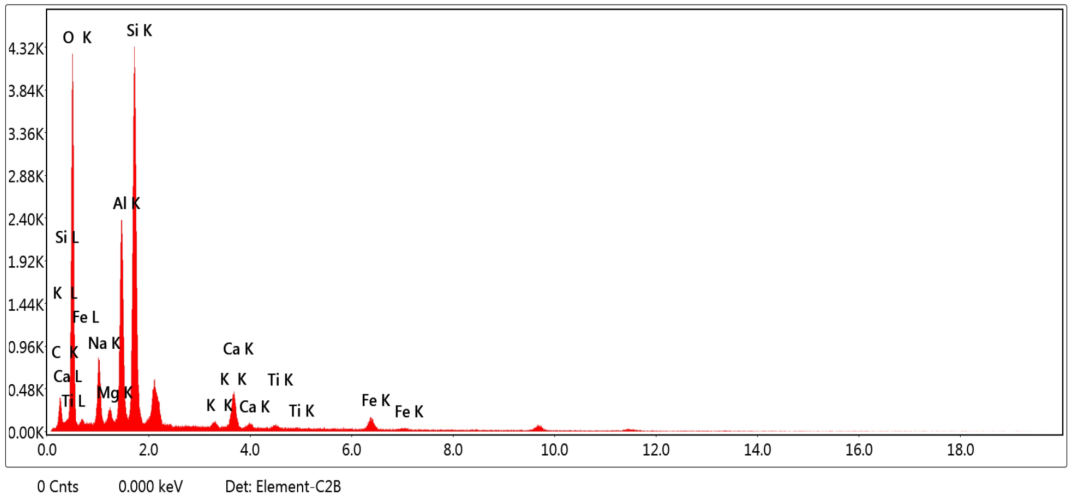
O K
Si K
Al K
Si L
K L
Fe L
Na K
C K
Ca L
Ti L
Mg K
Ca K
K K
Ti K
Fe K
4.32K
3.84K
3.36K
2.88K
2.40K
1.92K
1.44K
0.96K
0.48K
0.00K
0.0
2.0
4.0
6.0
8.0
10.0
12.0
14.0
16.0
18.0
0 Cnts
0.000 keV
Det: Element-C2B

(a)

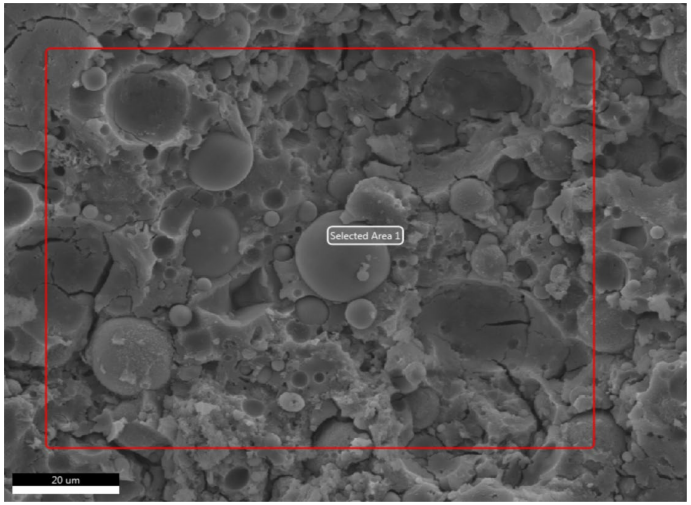
Selected Area 1
20 um

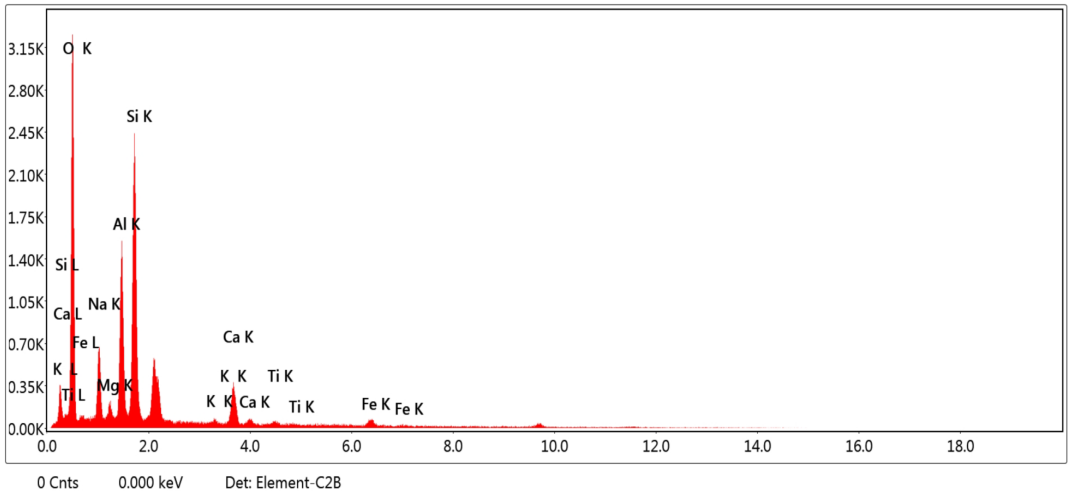
O K
Si K
Al K
Si L
Ca L
Na K
Fe L
K L
Ti L
Mg K
Ca K
K K
Ti K
Fe K
3.15K
2.80K
2.45K
2.10K
1.75K
1.40K
1.05K
0.70K
0.35K
0.00K
0.0
2.0
4.0
6.0
8.0
10.0
12.0
14.0
16.0
18.0
0 Cnts
0.000 keV
Det: Element-C2B

(b)

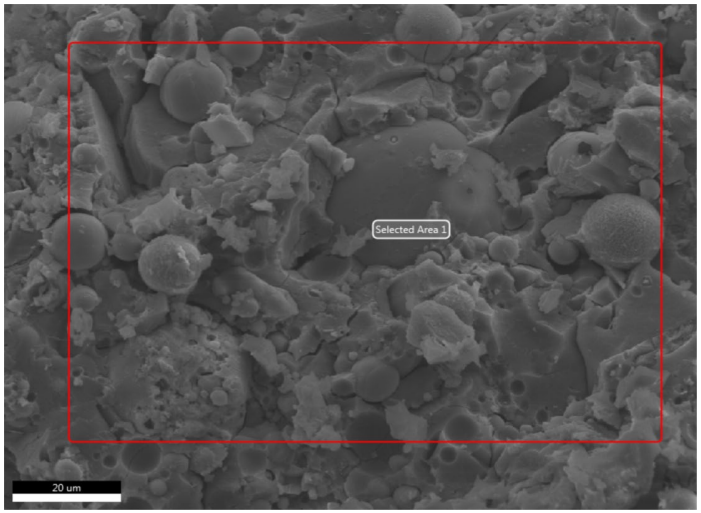
Selected Area 1
20 um

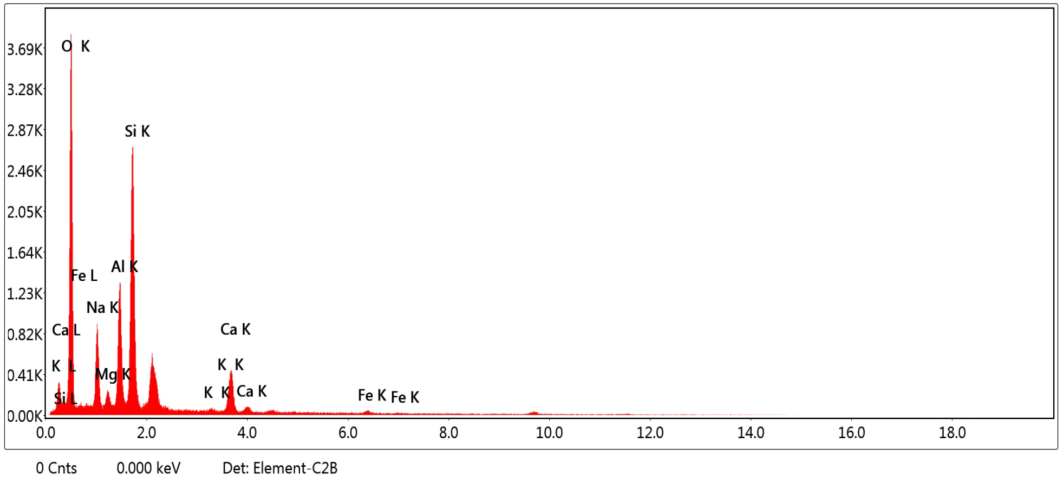
O K
Si K
Fe L
Al K
Na K
Ca L
Ca K
K L
Mg K
K K
K K Ca K
Fe K Fe K
3.69K
3.28K
2.87K
2.46K
2.05K
1.64K
1.23K
0.82K
0.41K
0.00K
0.0 2.0 4.0 6.0 8.0 10.0 12.0 14.0 16.0 18.0
0 Cnts 0.000 keV Det: Element-C2B

(c)

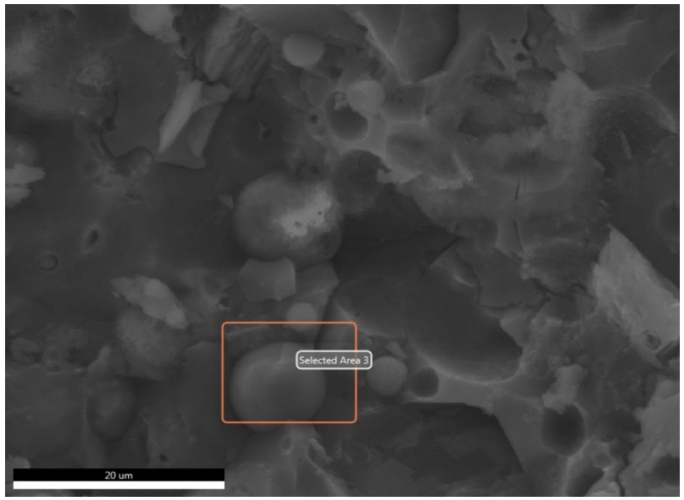
Selected Area 3
20 um

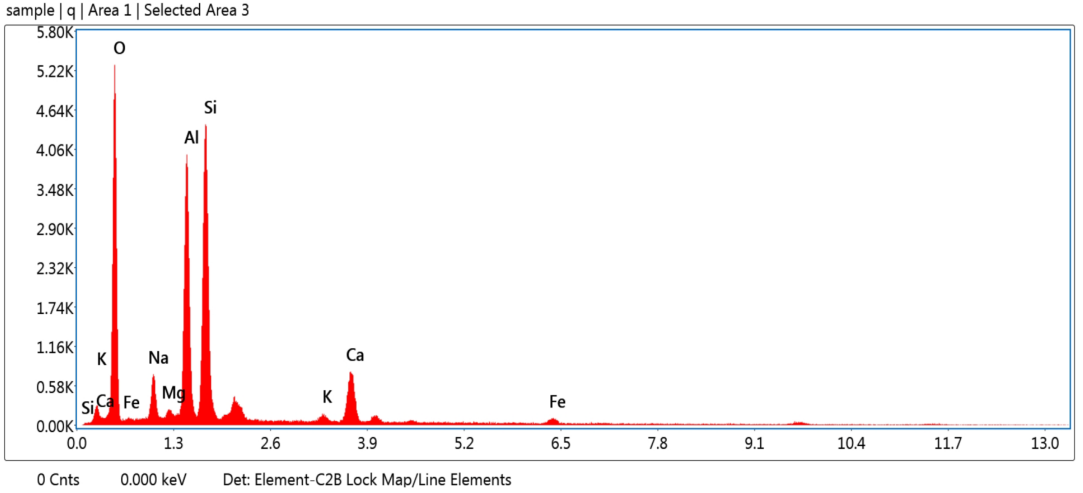
sample | q | Area 1 | Selected Area 3
O
Si
Al
K
Na
Ca
Si Ca Fe Mg K Fe
5.80K
5.22K
4.64K
4.06K
3.48K
2.90K
2.32K
1.74K
1.16K
0.58K
0.00K
0.0 1.3 2.6 3.9 5.2 6.5 7.8 9.1 10.4 11.7 13.0
0 Cnts 0.000 keV Det: Element-C2B Lock Map/Line Elements

(d)

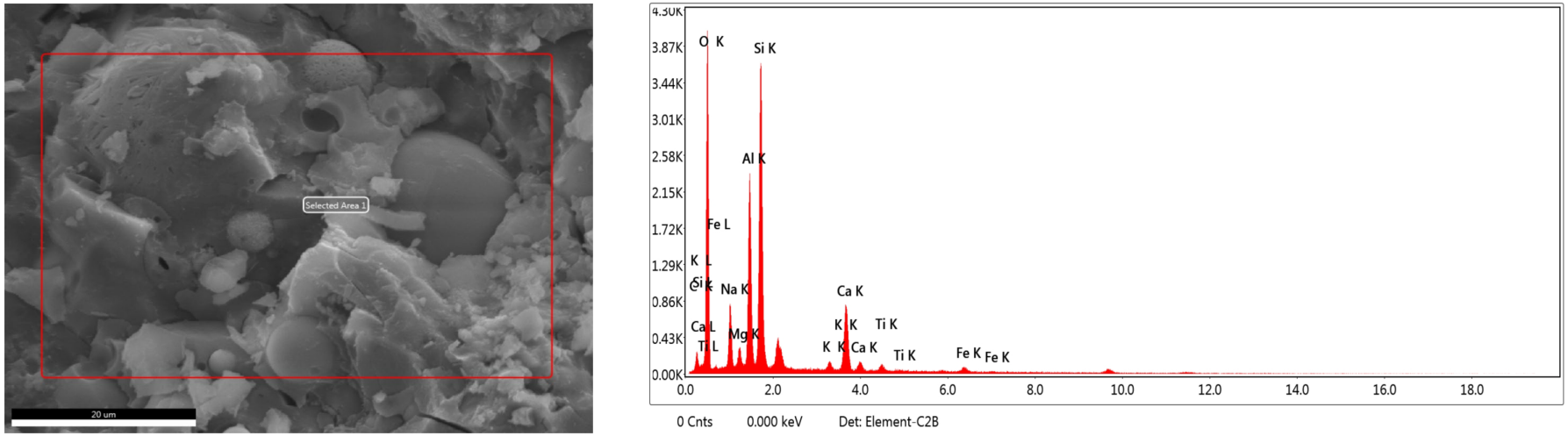

(e)

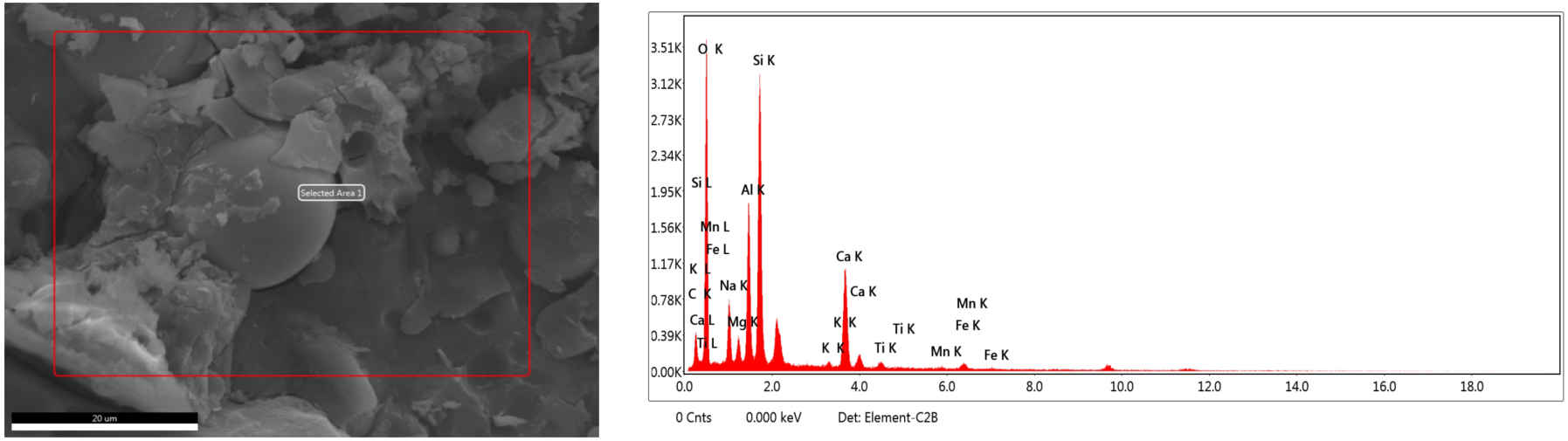

(f)

Figure 4.7: (a) SEM microphotograph and EDS of A0 (b) SEM microphotograph and EDS of A10 (c) SEM microphotograph and EDS of A20 (d) SEM microphotograph and EDS of A30 (e) SEM microphotograph and EDS of A40 (f) SEM microphotograph and EDS of A50

From SEM microphotograph of geopolymer mix sample mix A50 (Figure 4.7(f)), it can be observed that there is presence of amorphous and crystalline products in this particular mix. The important reaction product comprised C-A-S-H/N-A-S-H (sodium alumino-silicate hydrate) gel as calculated from major elements (Ca = 13.05%, Si = 14.44%, Al = 8.25%, Na = 6.31% and O = 43.13%) through EDS analysis. The elemental percentages obtained through EDS analysis are shown in Table 4.3.

Table 4.3: Details of EDS analysis of geopolymeric paste for an alkali binder ratio of 0.5

Mix Designation	GGBS %	Area	Elemental Composition (%wt.)					Ca/Si	Al/Si	Inference
			O	Al	Si	Ca	Na			
A0	0	1	42.58	11.86	20.91	3.98	6.85	0.19	0.56	N-A-S-H
		2	45.24	12.17	21.89	4.27	6.69	0.19	0.55	N-A-S-H
A10	10	1	40.87	12.91	21.65	7.79	7.94	0.36	0.60	C-(N)-A-S-H
		2	40.92	11.76	20.63	6.87	6.61	0.33	0.57	C-(N)-A-S-H
A20	20	1	43.45	10.60	22.30	9.43	9.62	0.42	0.47	C-(N)-A-S-H
		2	43.43	10.58	22.27	9.45	9.64	0.42	0.48	C-(N)-A-S-H
A30	30	1	39.77	10.68	17.96	13.77	4.90	0.76	0.59	C-(N)-A-S-H
		2	45.58	17.39	20.70	7.08	5.68	0.34	0.84	C-(N)-A-S-H
A40	40	1	44.80	11.70	18.75	7.87	7.05	0.42	0.62	C-(N)-A-S-H
		2	45.38	7.64	16.11	11.67	7.94	0.72	0.47	C-(N)-A-S-H
A50	50	1	43.99	9.23	15.82	10.73	6.47	0.67	0.58	C-(N)-A-S-H
		2	43.13	8.25	14.44	13.05	6.31	0.90	0.57	C-(N)-A-S-H

Higher Ca content in A50 paste sample aided in the breakdown of the precursor's silicate and aluminium ions. This dissolution of ions resulted in an enhanced alkali activation with the inclusion of extra binding phases (C-S-H (calcium silicate hydrate) and N-C-A-S-H/N-A-S-H) which are responsible for increased strength values (Figure 4.4(a)) in comparison with all other mixes. The existence of these extra binding stages were confirmed by determining Ca/Si and Al/Si ratios for the same six geopolymer mix samples (A0-A50) under group A, represented in figure 4.8.

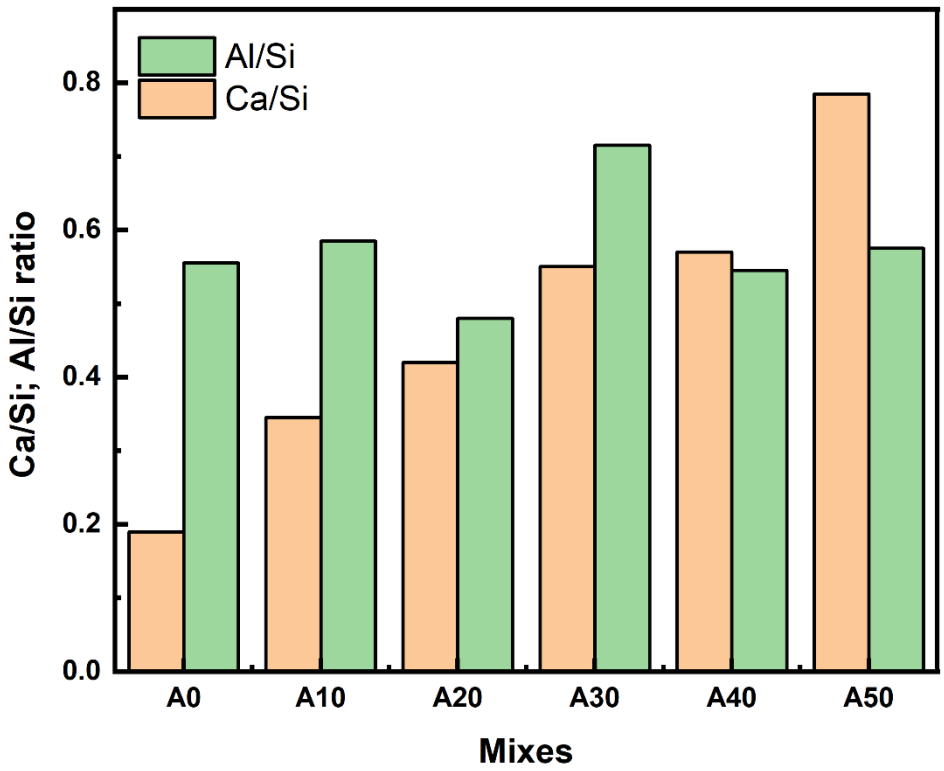

Figure 4.8: Representation of Ca/Si and Al/Si ratio in geopolymer mix samples

Figure 4.8 shows that greater Ca/Si values in the mixtures confirm the existence of some kind of C-S-H where Ca and Si predominates. Similarly, greater Al/Si values indicate the presence of some phase associated to A-S-H (Soutsos et al. 2016).

4.3.2 Relation between 28-days compressive strength and Ca/Si ratio

The compressive load carrying capacity results of geopolymer mix samples A0-A50 as a function of the Ca/Si ratio (derived from the obtained EDS data depicted in Figure 4.7) are shown in Figure 4.9.

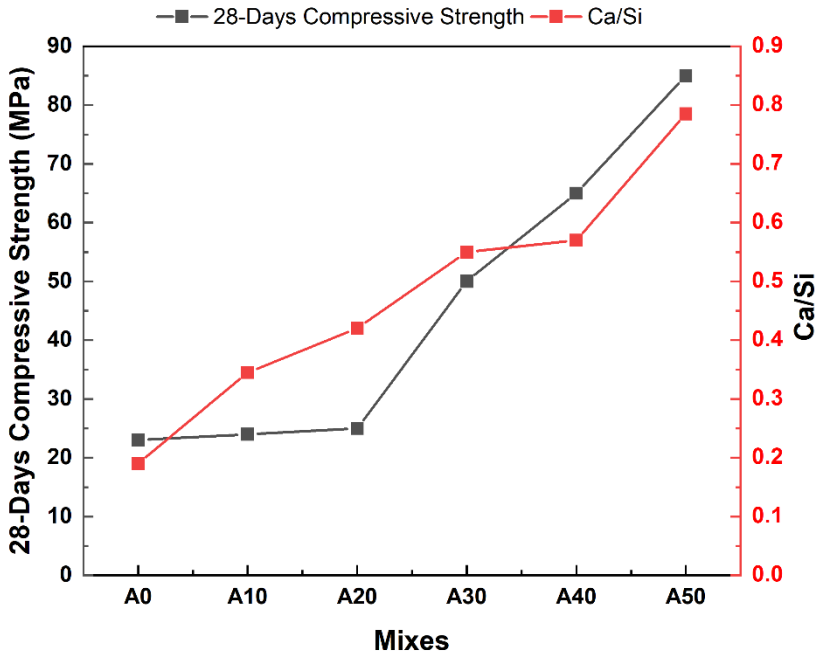

Figure 4.9: Relation between 28-days compressive strength and Ca/Si ratio

Figure 4.9 shows that sample A0 (100% FA and 0% GGBS) had a Ca/Si ratio of 0.19, indicating that FA predominated the polymerization reactions in the samples without the GGBS component, resulting in lower compressive strength values (Snehal et al. 2020). The existence of Ca increased significantly when the substitution level of GGBS in the samples (A10-A50) incremented, while the content of Si and Al in test samples declined. Ca/Si ratios incremented with incrementing GGBS levels (in samples A10-A40, they were 0.34, 0.42, 0.55, and 0.57, correspondingly) (i.e., from 10-40 % as a partial replacement to FA). The highest Ca/Si ratio (0.78) was attained for sample A50 (50% FA and 50 % GGBS) showed highest strength in compression value as 85 MPa. Attainment of higher strengths could be attributed to the better occurrence of geopolymerization reaction or may be due to the presence of structures that these binding gels possess (usually highly cross linked in nature,(Ismail et al. 2014). The polymerization reactions in the sample A50 appears to be associated with the hydration with respect to GGBS, tending to formation of C-A-S-H gel, i.e., rich in Ca content. However, as seen in Figure 4.7 (f), there is very less influence from FA in processes involved, as evidenced by unreacted FA particles.

Moreover, from SEM-EDS analysis presented in Figure 4.7, it can also be observed the emergence of binding gels due to increasing contents of GGBS that attributes to progression of various products formed within the geopolymer mix samples, as discussed in section 4.3.1. With a Ca/Si ratio of 0.19, reaction product in sample A0 was mostly N-A-S-H. Similarly, samples A10-A50 with increasing Ca/Si ratios as 0.34, 0.42, 0.55, 0.57 and 0.78, respectively,

specifies the presence of increasing Ca contents in the binder gels. This implies that a C-A-S-H type binding gel and an N-A-S-H gel are created concurrently (Rafeet et al. 2019). However, other investigations additionally state that reaction product N-A-S-H gel, which lacks of GGBS, predominates (Goudar et al. 2020; Ismail et al. 2014; Marjanović et al. 2015; Sahoo et al. 2017). Since composition of C-A-S-H gel in GGBS blended systems is comparable to geopolymer mix samples with increasing Ca/Si ratios (such as A10-A40), C-A-S-H was likely coexisting with N-A-S-H gel as primary product (Escalante García et al. 2006; Provis et al. 2012). Additionally, as GGBS content increased, the polymerization reaction evolved significantly, which could be ascribed to coexistence of N-A-S-H and C-A-S-H binding gels, resulting in higher strength in compression values (85 MPa for A50) and a shorter setting time (20-58 minutes) (Kumar et al. 2010).

4.3.3 FTIR analysis

Using FTIR technique, formation of chemical bonds in the reaction products produced through the activation of samples of a geopolymer mix that contained both FA and GGBS is depicted in Figure 4.10. The characteristic bands of raw materials i.e., FA and GGBS are also represented in figure 4.10. In FA sample, the spectra of mullite are depicted at band of 1093 cm^{-1} and in GGBS, the presence of Ca is represented at a small peak located at 1511 cm^{-1} (Samantasinghar and Singh 2019). Further, in GGBS, a broad peak from 785-1058 cm^{-1} represents the existence of silica in it. A very short peaks located at 3520 and 3514 cm^{-1} indicates existence of moisture in FA and GGBS respectively. In geopolymer mix samples A0-A50, the main peaks located at around 993, 983, 985, 968 and 958 cm^{-1} are assigned to symmetric stretching vibrational bond of Si-O-T (T can be either Si or Al), respectively. A shift in Si-O-T bonds observed for geopolymer mix samples cured for a longer duration indicates the formation of more amounts of aluminosilicate and silicate hydration products and a similar kind of observation with respect to the wavenumbers was reported by Samantasinghar & Singh, 2019. Wavenumbers 873 and 1470 cm^{-1} have smaller peaks that signify the O-C-O stretching vibration band, which indicates that carbon dioxide has been absorbed by the specimens and is also compatible with the presence of calcite (Ismail et al. 2013; Mozgawa and Deja 2009). Alkali hydroxides are shown by O-H bands at around 1700 and 2957 cm^{-1}. Table 4.4 gives information about the peak assignment of the identified functional groups for the geopolymer mix samples in this study.

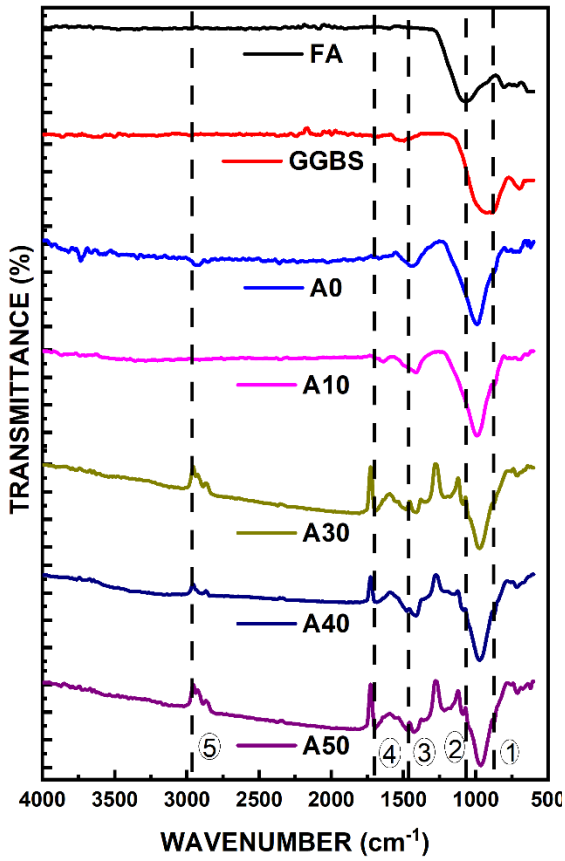

Table 4.4: Peak assignment with respect to the functional groups		
Sl No.	**Peaks (cm^{-1})**	**Assignment**
1	873	Carbonates (O-C-O)
Between 1-2	873-1072	Si-O-T (Si or Al)
3	1470	Carbonates (O-C-O)
4	1700	-O-H (Asymmetric bending)
5	2957	-O-H (Asymmetric bending)

Figure 4.10: FTIR spectrum of geopolymer paste samples

Figure 4.11 represents the comparison of FTIR spectra of few selected geopolymer mix samples from group A (A50), B(B50) and D(D50) for understanding the influence of alkaline to binder ratio (0.5, 0.6 and 0.8 respectively) on their respective spectra's. It can be observed that variation of alkaline to binder ratio is not having much of impact on the spectra's of A50, B50 and D50 geopolymer mix samples. But few bands at wavenumbers 1098, 1200, 1700 cm^{-1} are found to diminished or completely missing in spectra of alkali binder ratio of 0.8 sample (D50), as observed in Figure 4.10.

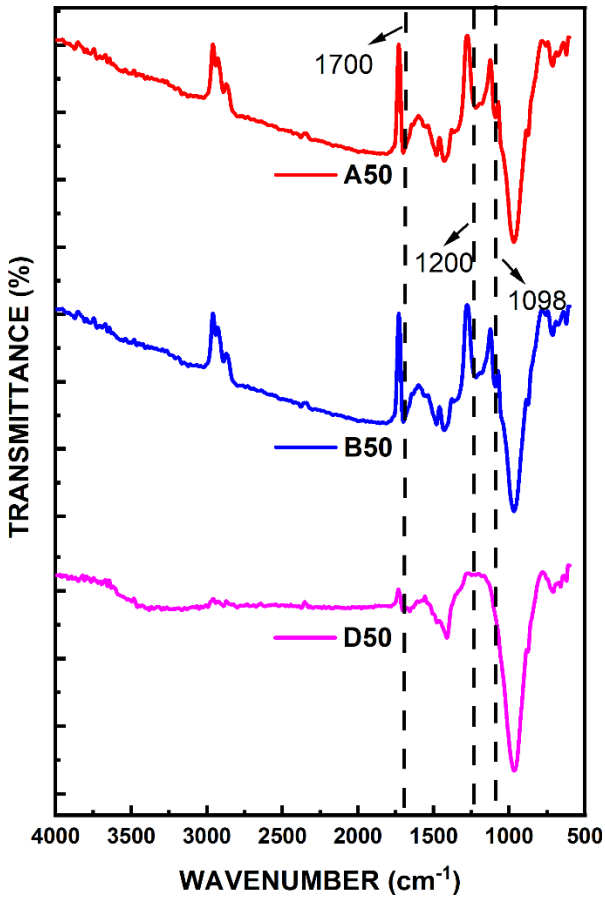

Figure 4.11: Comparison of FTIR spectra's of A50, B50 and D50 samples

CHAPTER – 5

RESULTS AND DISCUSSION ON GEOPOLYMERIC MORTAR

5.1 GENERAL

The relevant findings from the tests conducted on FA-based geopolymeric mortars that were cured at room temperature are presented in this chapter. Engineering properties of the geopolymeric mortars were evaluated in accordance with the testing specifications outlined by the BIS. Relevant discussions pertaining to these tests are presented. Advanced characterization techniques SEM-EDS were incorporated for characterizing the geopolymeric mortar samples.

5.2 ENGINEERING PROPERTIES OF FA BASED GEOPOLYMERIC MORTAR

5.2.1 Setting time and flow table test

Setting time and flow table test are the prominent benchmarks for measuring the performance of geopolymeric mortar samples. The obtained results for setting time for geopolymeric mortar samples with the variation in alkaline to binder ratio (0.5, 0.6, 0.7 and 0.8), partial replacement of FA with GGBS (0% to50% by weight of binder at an interval of 10%) while maintaining a constant binder to sand ratio 1:3 in all the trial mixes) is presented in subsequent sections.

5.2.1.1 Setting time and flowability results for geopolymeric mortar samples with the variation in alkaline to binder ratio and partial replacement of FA with GGBS

Figure 5.1 displays the IST and FST of geopolymeric mortar samples with varying alkaline to binder ratios and partial replacement of FA with GGBS. It is clear that F50G50 composition with an alkaline to binder ratio of 0.5 has the lowest IST and FST, which are 22 and 51 minutes, correspondingly. The highest IST and FST for F100G0 compositions with an alkaline to binder ratio of 0.8 are 316 and 668 minutes, correspondingly. The findings show that as alkaline to binder ratio increases from 0.5 to 0.8, setting time of geopolymer mixes for mortar samples also increases. In comparison to FA mixes, the IST was decreased by 40% with just 10% GGBS incorporation, as shown in Figure 5.1.

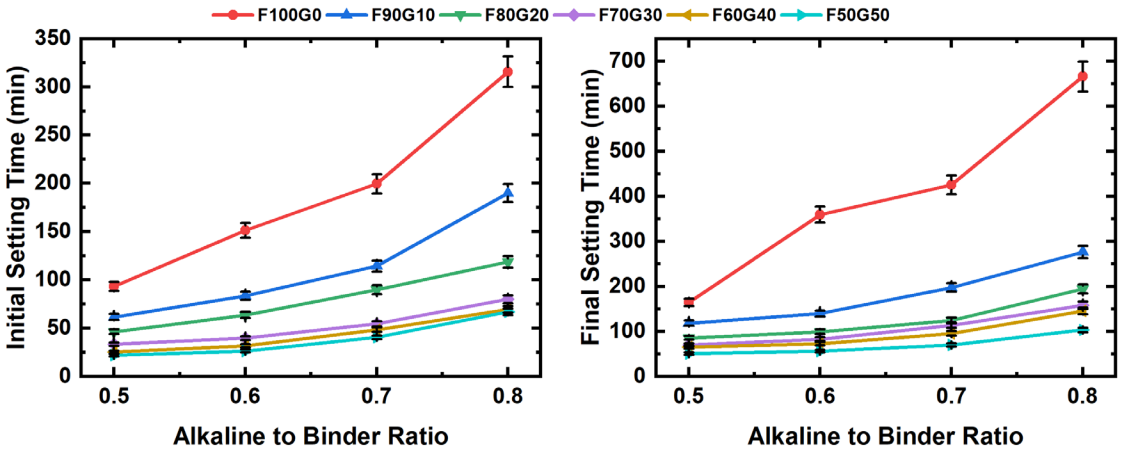

Figure 5.1: Impact of alkaline to binder ratio on initial and final setting time of geopolymeric mortars

Figure 5.1 show variation of IST and FST with alkaline to binder ratio for different GGBS percentages from 0 to 50%. There is a large variation in setting time values of 0% GGBS mixes for all alkaline to binder ratios, whereas the setting times of mixes containing GGBS have a relatively linear trend, thus suggesting the possibility of GGBS adding to the stability of the mixes. The setting time values for 30, 40 and 50% GGBS mixes do not vary much for all alkaline to binder ratios. It can be understood that development of geopolymeric mortar depends on growth of sodium aluminosilicate hydrate gel (N-A-S-H) by considering results for setting time of geopolymeric mortars (Poornima et al. 2022). However, GGBS is with high-Ca (CaO) content produces geopolymer mortar mixes containing C–S–H gel along with N–A–S–H gel at early duration (Poornima et al. 2022). Consequently, geopolymer mortar produced with GGBS shows an appreciably lesser time for IST and FST.

The flow table results are tabulated in Table 5.1, that demonstrates that samples of geopolymeric mortar (groups C and D), that corresponds to alkaline to binder ratios of 0.7 and 0.8, correspondingly, overflowed from base of the table, which may be related to higher alkaline to binder ratios in the specific geopolymeric mixes.

Table 5.1: Flow table test results of geopolymeric mortar

Alkali Binder Ratio	D1 (cm)	D2 (cm)	D3 (cm)	D4 (cm)	Flow (%)
0.5 (Trial 1)	19.5	20.2	19.0	18.8	61.45
0.5 (Trial 2)	19	19.3	18.8	20.4	
0.6 (Trial 1)	24	24.2	24	24.5	101.04
0.6 (Trial 2)	23.8	24.0	24.3	24.2	
0.7 (Trial 1 and 2)	Overflown				
0.8 (Trial 1 and 2)	Overflown				

5.2.2 Compressive load carrying capacity of geopolymeric mortar samples with variation in alkaline to binder ratio and partial replacement of FA with GGBS

Figure 5.2 (a), (b), and (c), respectively, show compressive load carrying capacity of geopolymeric mortar samples with different GGBS% and alkaline to binder ratio at curing ages 3, 7, and 28.

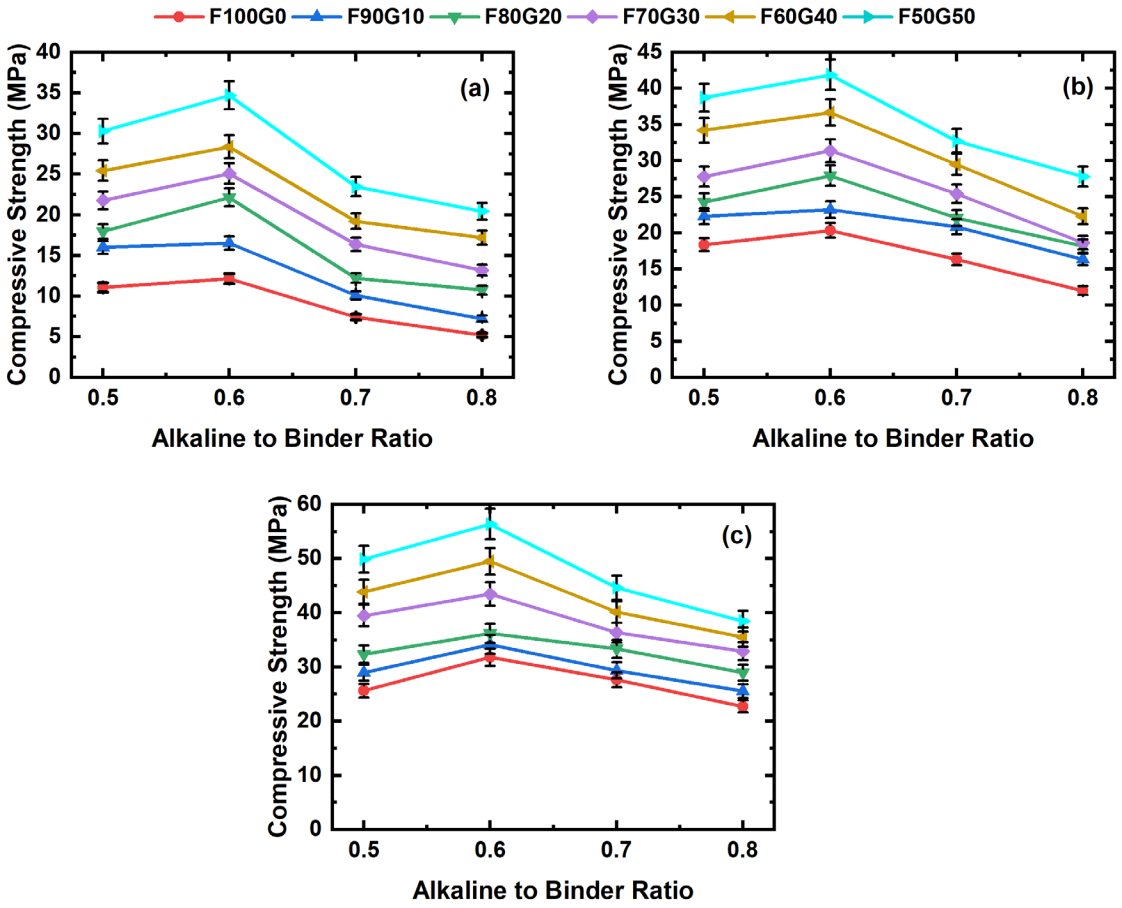

Figure 5.2: Compressive load carrying capacity of geopolymeric mortar samples at curing periods of (a) 3 days (b) 7 days and (c) 28 days

Figures 5.2 shows the variation of compressive strength with different alkaline to binder ratios and different GGBS percentages from 0 to 50%. The figures show that the alkaline to binder ratios of 0.6 and 0.8, correspondingly, produced highest and lowest strength in compression results for the curing ages 3, 7, and 28 days. The 50% mixes presented an increment in compressive load carrying capacity of 94, 77, 62 and 69% over the mixes containing no GGBS at 28 days. Similarly, the 3-day strength increase was more than 7- and 28-day strength for all mixes of all alkaline to binder ratios There are two possibilities that account for the likely causes of strength gain. The probable reasons for strength gain can be ascribed to the

occurrence of two probable mechanisms. One is either the occurrence of hydration reaction of GGBS as well as polymerization of FA is separate or simultaneous from one another. In the former case, it is assumed that the reaction of GGBS occurs first to form a matrix kind around the periphery of FA followed by the pores filling by FA, to provide an increasing strength. However, in the latter case, the occurrence of the two reactions takes place simultaneously along with GGBS reaction, hence activating the FA under ambient temperature conditions (Wardhono et al. 2015). Furthermore, the possibility of the decrement in strength of geopolymeric samples could be due to presence of excessive amounts of water in the mortar mixtures, leading to a higher permeability at incrementing alkaline to binder ratios (Naghizadeh and Ekolu 2019).

By comparing the obtained compressive load carrying capacities of geopolymeric pastes with that of mortar samples, it can be stated that the highest values that is 85 MPa at 28 days curing is attained for paste samples comprising an alkaline to binder ratio of 0.5 with 50% GGBS substitution against FA, whereas it is highest (that is 56 MPa at 28 days) with alkaline to binder ratio of 0.6 with 50% GGBS substitution in mortar samples. By generalizing the attained variably in the compressive strength carrying capacity of geopolymeric pastes as well as mortars, it can be said that the key rection product C-A-S-H/N-A-S-H has more dominance over the reaction product of mortar specimens which tended to impart superior strength characteristics in paste samples.

5.3 ADVANCED CHARACRTERIZATION STUDIES ON GEOPOLYMERIC MORTARS

5.3.1 SEM with EDS analysis

The geopolymeric mortar samples from group B (B0-B50) were chosen for SEM analysis because they showed higher compressive load carrying capacity values after 28 days curing age in comparison to other group mixes. Microphotographs of those specific samples are shown in Figure 5.3. Elemental compositions were calculated using EDS analysis which gives an inference about the presence of type of gel within the mortar samples.

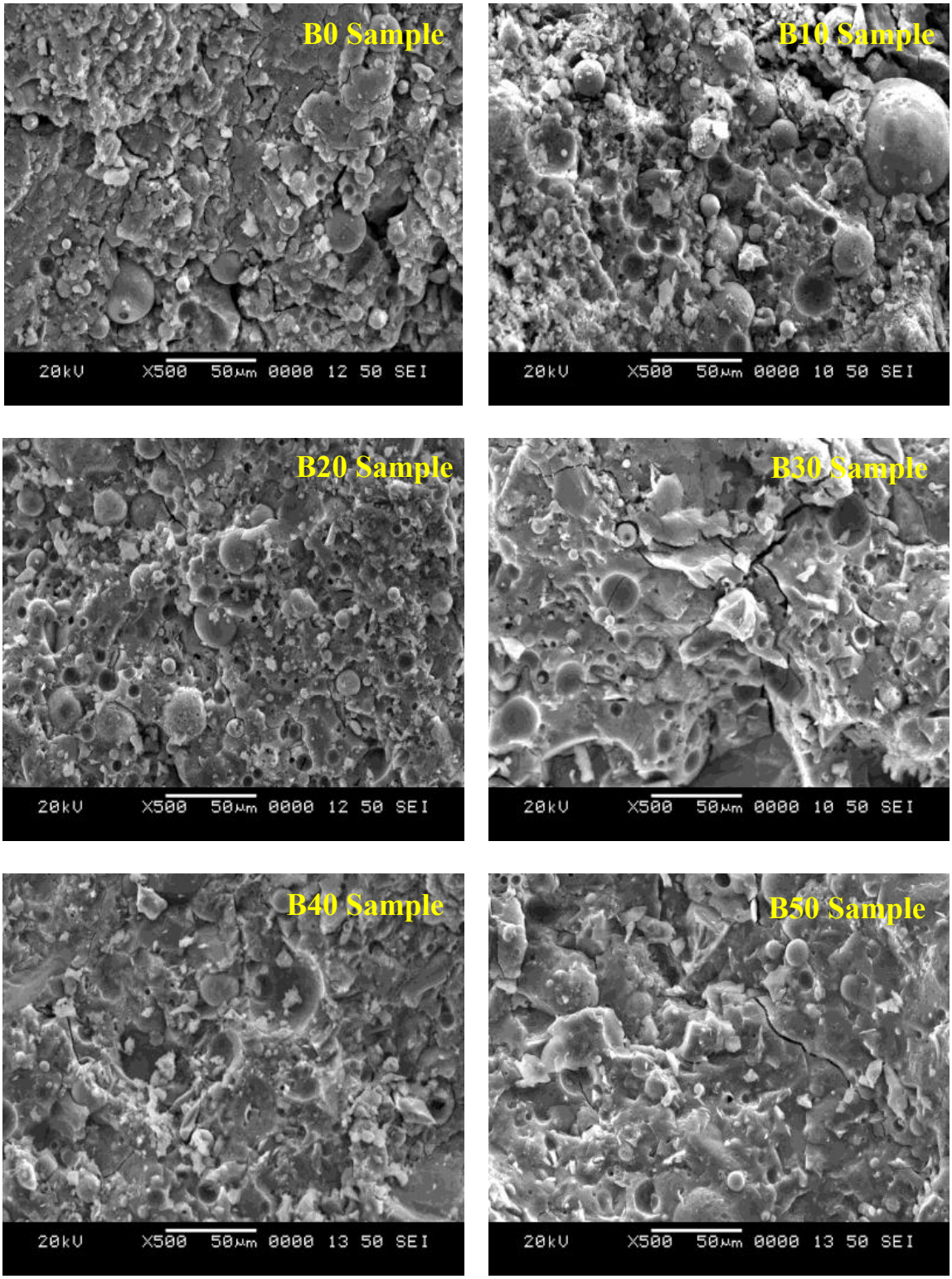

Figure 5.3: SEM microphotographs of group B mixes with alkaline to binder ratio of 0.6

From figures, it is clear that the mixture with zero percent GGBS included more unreacted spherical FA particles than the other mixtures. Lesser unreacted FA particles were seen in all mixes. Samples with 10% GGBS (sample B10) showed the gradual development of the geopolymer gel, which covers the crust of the FA particle, thereby proving the fact that

geopolymer reaction occurs at surface of the FA particle. A large number of pores can also be seen in the SEM image of the sample, with minor crack widths in the 20% GGBS samples (sample B20). The FA particles seem to be covered with the reaction products, and fewer unreacted FA particles are seen as compared with the 10% GGBS sample. The cracks are fewer because of the denser structure of the 20% GGBS sample, but the pores are still greater in number, although with a reduced size. The 30% GGBS sample has fewer pores and a compact structure, but the crack width has increased considerably over the sample with 20% GGBS. In the mixes with 40% GGBS (sample B40), the cracks have lessened and the structure looks homogenous, with a significant amount of unreacted GGBS particles. A compact glass-like structure can be seen for the 50% GGBS samples (sample B50), with a few unreacted FA and GGBS particles for which the number of cracks is observed.

According to available information in the literature, incorporating GGBS to the mixture may improve the synthesis of C-A-S-H (calcium alumino-silicate hydrate) gel through three mechanisms. First mechanism hypothesised is that surface Cain GGBS will contribute to increased C-A-S-H gel formation, that in turn increments strength in compression values (Kumar et al. 2010; Nath and Kumar 2013). Ca presence may cause water deficiency, which will increase the alkalinity of mixes through the higher dissolution of existing aluminosilicate (Khater 2012). A higher level of cross-linking and polymerization in the second mechanism reveals that GGBS predominates in synthesis of C-A-S-H gel throughout alkali activation process (Richardson et al. 1994). In third mechanism, N-A-S-H gel is a secondary product that reduces pore volume and improves gel compactness, increasing compressive strength (Ismail et al. 2013; Li and Liu 2007).

The principal elements identified in the samples included O, Si, Al, Ca, Mg, Fe, and Na. The energy spectra of the mortar samples at various GGBS percentages in the mix for the alkaline to binder ratio of 0.6 are depicted in Figure 5.4. It is noticed that as GGBS content incremented in the mixes, the intensity of Ca counts also increased and formed a gel more likely as C–A–S–H gel.

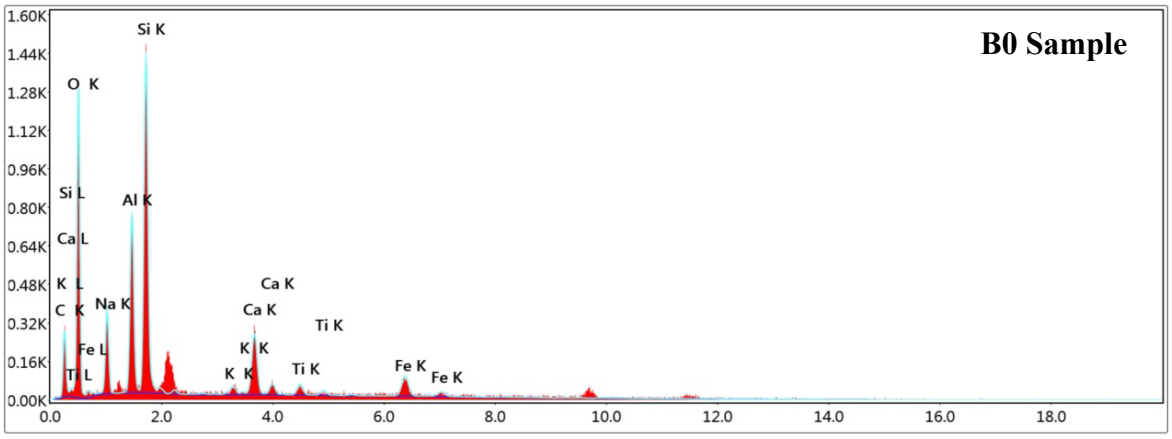
B0 Sample
Si K
O K
Si L
Al K
Ca L
K L
C K
Na K
Ca K
Ca K
Ti K
Fe L
K K
Ti L
Ti K
Fe K
Fe K
1.60K
1.44K
1.28K
1.12K
0.96K
0.80K
0.64K
0.48K
0.32K
0.16K
0.00K
0.0
2.0
4.0
6.0
8.0
10.0
12.0
14.0
16.0
18.0
0 Cnts
0.000 keV
Det: Element-C2B

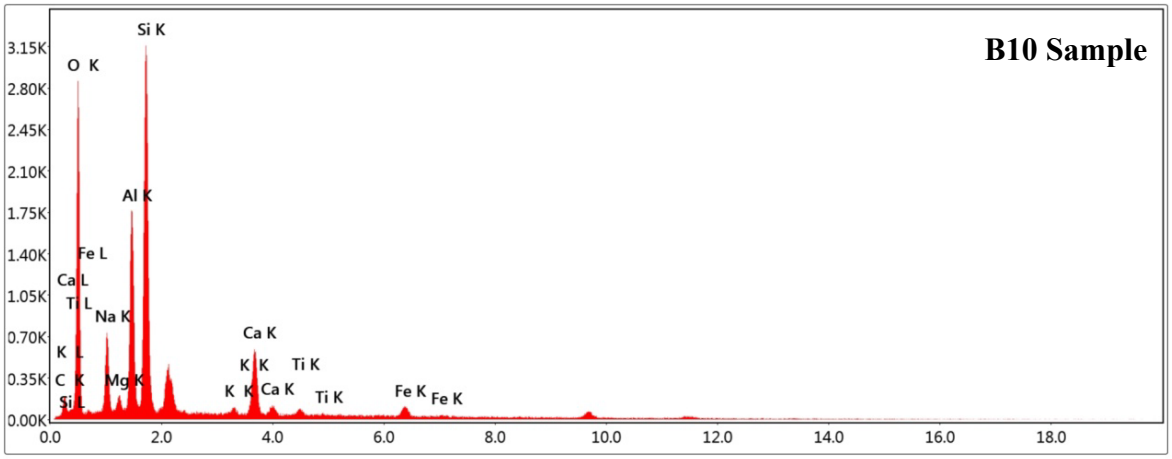
B10 Sample
Si K
O K
Al K
Fe L
Ca L
Ti L
Na K
Ca K
K L
K K
Ti K
C K
Mg K
K K
Ca K
Ti K
Fe K
Fe K
Si L
3.15K
2.80K
2.45K
2.10K
1.75K
1.40K
1.05K
0.70K
0.35K
0.00K
0.0
2.0
4.0
6.0
8.0
10.0
12.0
14.0
16.0
18.0
0 Cnts
0.000 keV
Det: Element-C2B

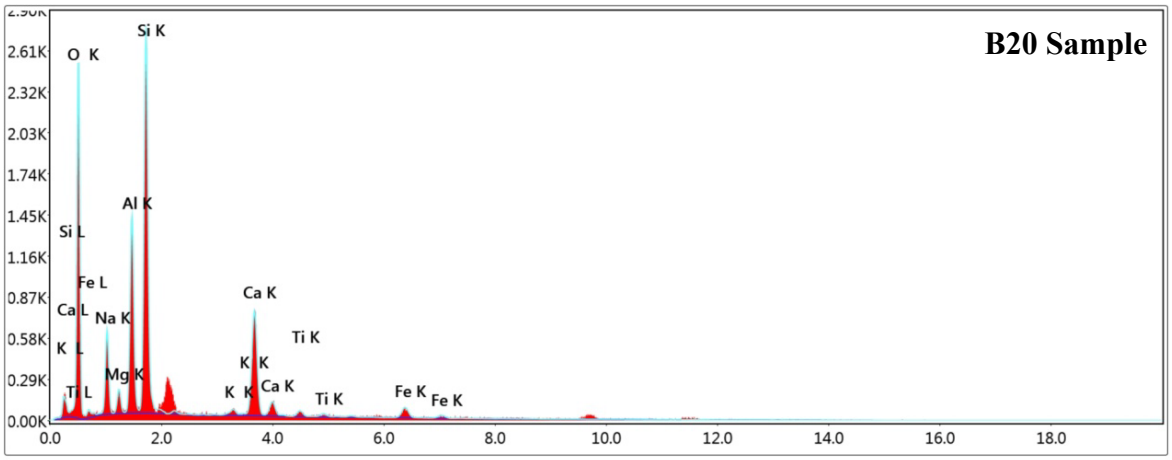
B20 Sample
Si K
O K
Al K
Si L
Fe L
Ca L
Na K
Ca K
Ti K
K L
K K
Mg K
K K
Ca K
Ti K
Fe K
Fe K
Ti L
2.61K
2.32K
2.03K
1.74K
1.45K
1.16K
0.87K
0.58K
0.29K
0.00K
0.0
2.0
4.0
6.0
8.0
10.0
12.0
14.0
16.0
18.0
0 Cnts
0.000 keV
Det: Element-C2B

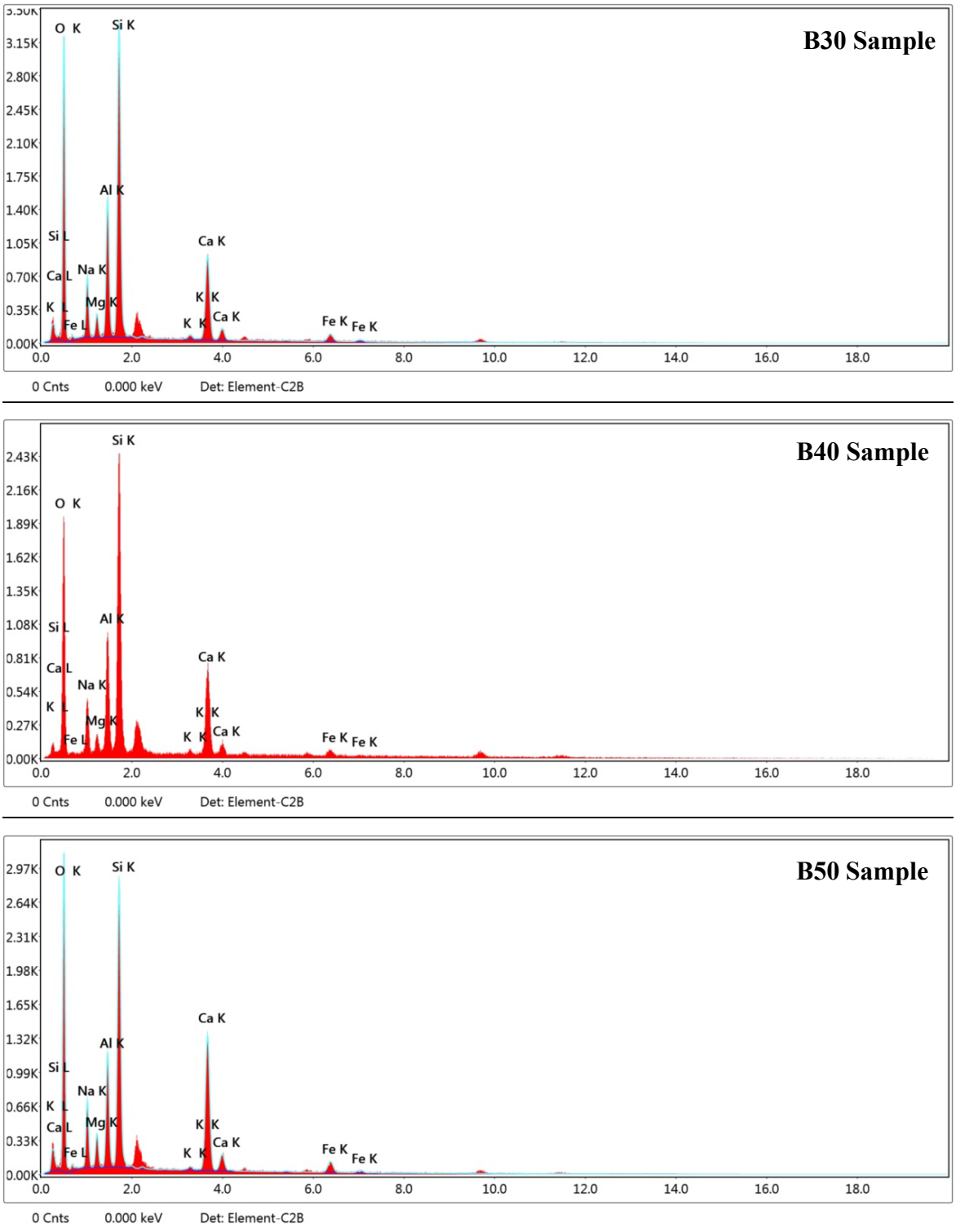

Figure 5.4: EDS spectrums of B mixes of geopolymeric mortar samples

Table 5.2: Elemental compositions obtained for B mixes of geopolymeric mortars from EDS

Designation	GGBS %	Point	Elemental Compositions (Weight %)				Si/Al	Ca/Si
			Na	Al	Si	Ca		
B0	0	1	7.3	9.18	18.83	6.4	1.83	0.38
		2	6.94	13.74	21.08	8.19	1.53	0.38
B10	10	1	7.76	11.84	21.08	7.18	1.78	0.33
		2	8.28	9.66	17.66	5.77	1.82	0.34
B20	20	1	7.95	11.06	20.92	11.9	1.89	0.47
		2	7.59	9.71	18.44	8.81	1.87	0.56
B30	30	1	6.4	10.34	18.64	11.33	1.8	0.6
		2	7.52	9.81	21.35	12.15	2.17	0.59
B40	40	1	7.97	9.88	21.7	14.59	2.19	0.67
		2	7.27	9.44	22.37	13.11	2.36	0.58
B50	50	1	9.54	8.09	18.32	12.85	2.26	0.7
		2	7.53	7.38	17.18	16.89	2.32	0.98

It is found from Table 5.2 that the elemental composition of the two randomly points in mixes B0 to B50 together with the Si/Al and Ca/Si ratios. The major elements in the mix B0 at both points are Si and Al; hence, based on Si/Al ratio, it is hypothesised that the phase present at both points may be alumino-silicate hydrate (A–S–H). Mix B10 exhibits a similar tendency, however the phase present in the B20 mix at point 1 (in Table 5.2) could be A-S-H, while that at point 2 could be calcium silicate hydrate (C–S–H) (Ismail et al. 2013). Phases present at points were obviously distinct in terms of their elemental composition even though they were in the same mix B20. The mixes B30, B40 and B50 showed calcium silicate hydrate phase as a major binding gel in the geopolymeric mortar mixes.

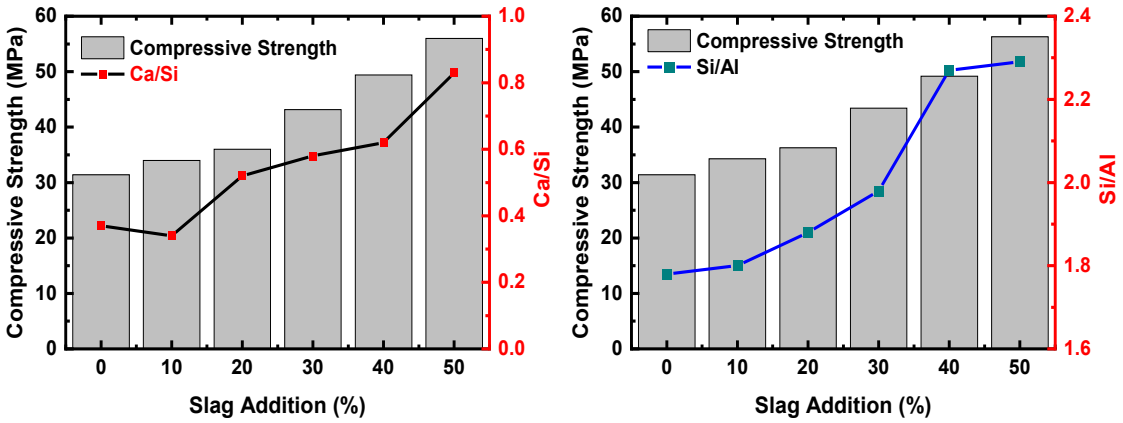

Figure 5.5: Trend of Ca/Si and Si/Al ratio with respect to compressive strength of geopolymeric mortar samples

The average Ca/Si and Si/Al ratios increased when more FA was substituted with GGBS, as seen in Figure 5.5, and it exhibited a positive relationship with the compressive load carrying capacity of the B-mixes for all percentages of GGBS. This may be because the geopolymerization reaction has occurred more frequently or because these binding gels have certain structural elements. (usually highly cross-linked in nature)(Ismail et al. 2014).

CHAPTER – 6

RESULTS AND DISCUSSION ON GEOPOLYMERIC MORTAR WITH STEEL FIBRES

6.1 GENERAL

In this chapter, the pertaining results obtained by conducting aforementioned tests on FA based geopolymeric mortars with steel fibres addition mortars cured in room temperature conditions are shown. Engineering characteristics of the geopolymeric mortars with inclusion of steel fibers were evaluated in accordance with the testing guidelines established by BIS. The ensuing discussions provide requisite analysis and findings. Advanced characterization techniques SEM-EDS were incorporated for characterizing the geopolymeric mortar samples with steel fibre additions.

6.2 ENGINEERING PROPERTIES OF FA BASED GEOPOLYMERIC MORTAR WITH STEEL FIBRES ADDITION

6.2.1 Setting time and flow table test

With varied alkaline to binder ratios and varying GGBS contents, the setting times of FA-based geopolymer mortar samples with steel fibre addition were measured for IST and FST using penetrometer. IST and FST with respect to alkaline to binder ratio are presented in Figure 6.1.

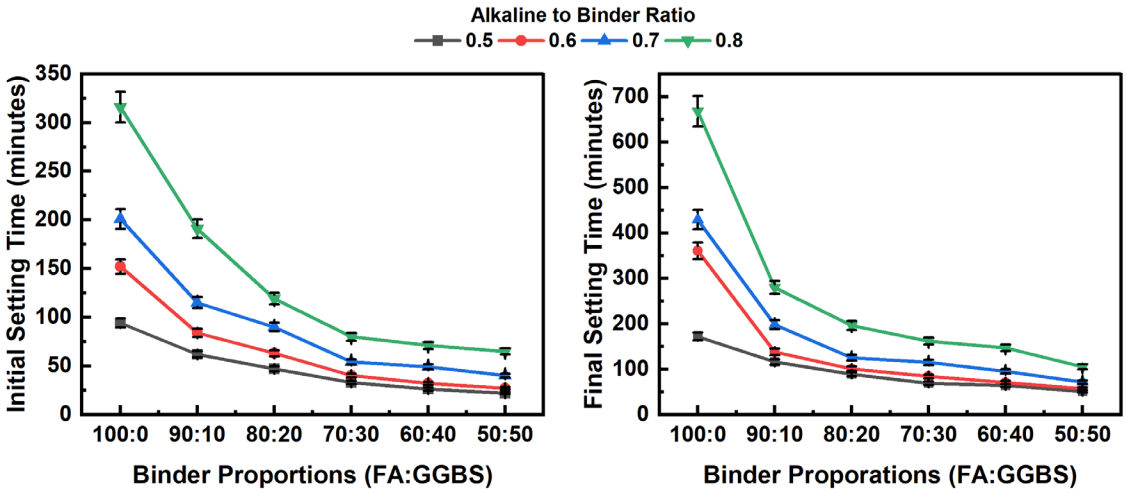

Figure 6.1: Evaluation of IST and FST for all alkaline to binder ratios with respect to variation of binder compositions

Figure 6.1 shows IST and FST in connection to alkaline to binder ratio. Comparison of IST of all alkaline to binder ratios in connection with GGBS content can be seen in the figure. The results indicate that the reduction in IST is around 142-236% based on the alteration of alkaline to binder ratio from 0.5 to 0.8. GGBS replacement in the mixture with FA significantly reduces the IST. The results show that the when GGBS variation from 0 to 50% by weight of binder the IST decreased about 76–82% depending on variation of alkaline to binder ratio. Furthermore, from Figure 6.1, it can also be noticed that additions of GGBS in the mixture significantly reduces the FST. The results show that the, when GGBS variation from 0 to 50% by weight of binder, the FST decreases about 70– 84% depending on the variation of alkaline to binder ratio. The figure illustrates an increase in FST of around 106-288% when alkaline to binder ratio increases from 0.5 to 0.8 with variation in GGBS content. Because of a slower rate of reaction at room temperature, it was found that geopolymeric combinations using 100% FA as the only binder typically take a long time to set. (Davidovits 2008). The geopolymeric mixes significantly reduced the setting time of mortar samples by adding GGBS. The variation IST and FST of geopolymeric mortar samples reduced with the increment in the GGBS content. It indicates that setting pace is influenced by the amount of GGBS in the geopolymeric mortar (Kumar et al. 2010; Sugama et al. 2005). The results show that adding GGBS and increasing the alkaline to binder ratio can speed up the setting time of geopolymeric mortar samples that are cured at room temperature (Nath and Sarker 2014).

Flowability test was conducted for evaluating the impact of incorporating steel fibres in plain geopolymer mortar on the flowing capacity. The average of four diameters measured for flow test for different trial runs are presented in Table 6.1.

Table 6.1: Flowability results of geopolymeric mortars with addition of steel fibres

Binder Proportion (FA: GGBS)	Alkali/Binder ratio	Steel Fibre Addition (%)	Average Diameter (cm)	Flow (%)
50%:50%	0.5	0	19.3	61.4
		0.5	13.1	31.0
		1	12.5	25.5
		1.5	12.1	21.0
50%:50%	0.6	0	24.1	101.0
		0.5	15.6	59.5
		1	14.9	49.0
		1.5	14.4	44.5
50%:50%	0.7	0	NA	NA
		0.5	18.8	88.3
		1	18.2	82.3
		1.5	18.0	80
50%:50%	0.8	0	NA	NA
		0.5	21.2	112.5
		1	20.5	105.8
		1.5	20.2	102.8

Variation of all average flow diameters are presented in Figure 6.2. From figure, it is noted that the increment in fibre content decreases the flow diameter in all alkaline to binder ratios. According to the percentage of steel fibres used in each mix, adding steel fibres to plain geopolymer mortar reduces the flow diameter by between 23.56 and 30.82% for an alkaline to binder ratio of 0.5, 24.77 and 33% for an alkaline to binder ratio of 0.6, and 24.7 and 32.82% for an alkaline to binder ratio of 0.7. Further, flow percentage of all alkaline to binder ratios with different variations of steel percentage are presented in Figure 6.3. From figure, it is noted that percentage of flow is incremented with the rise in alkaline to binder ratio. It is also clearly seen that incorporation and increase in steel fibres has a greater impact on flowing ability of geopolymer mortar in all mixes.

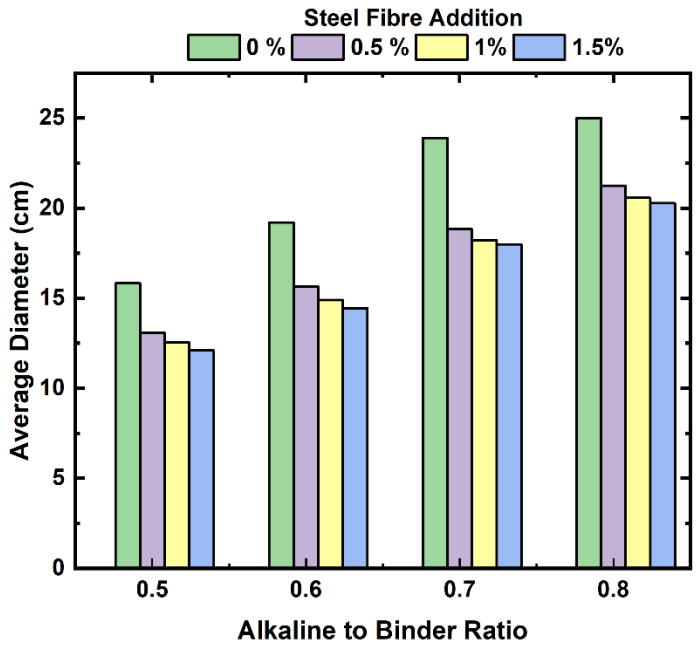

Figure 6.2: Average flow diameter with respect to variation of fibres content

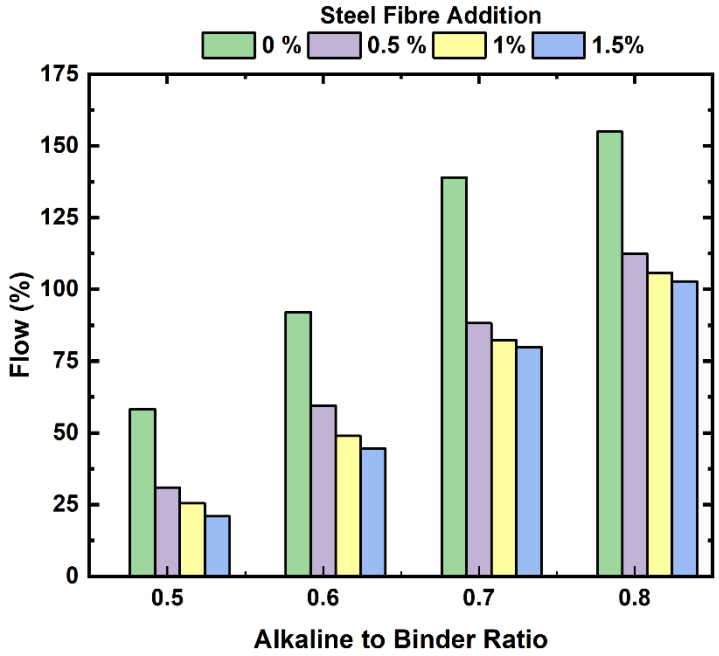

Figure 6.3: Flow in percentage with respect to variation of fibres content

6.2.2 Compressive strength results with respect to alkaline to binder ratio and varied binder proportions

Figures 6.4, 6.5, 6.6, and 6.7 show the variation in compressive strength of geopolymer composites with various fibre content percentages and various alkaline to binder ratios,

correspondingly. Figures show that compressive strengths increased as steel fibre content increased up to 1%; however, as fibre amount increased over 1%, strength in compression values decremented. Due to action of fibres on growth in their binding with mortar, the compressive strength up to 1% is increased, which boosts the compressive strength over 1%. The workability is reduced due to the higher percentage of fibre content and compaction of geopolymer mortar is severely affected, hence compressive strength decreased. Further, the addition and increase in steel fibres in plain geopolymer mortar increased its compressive strength values. The compressive strengths for 3, 7 and 28 days of 1% volume of fibres were found to be greater than those of 0.5 and 1.5% for all variations of alkaline to binder ratio and all variations of binder proportions (FA & GGBS).

Depending on the amount of steel fibre, the composition of the binder, and alkaline to binder ratio, increase in strength in compression values of geopolymer composites ranges from 5.1-22.6 MPa. The highest values for 28-day strength in compression values were 56.0, 69.5, 63.0 and 62.0 MPa for alkaline to ratios of 0.5, 0.6, 0.7 and 0.8, correspondingly, obtained at 1% of steel fibres content with 50:50 binder compositions.

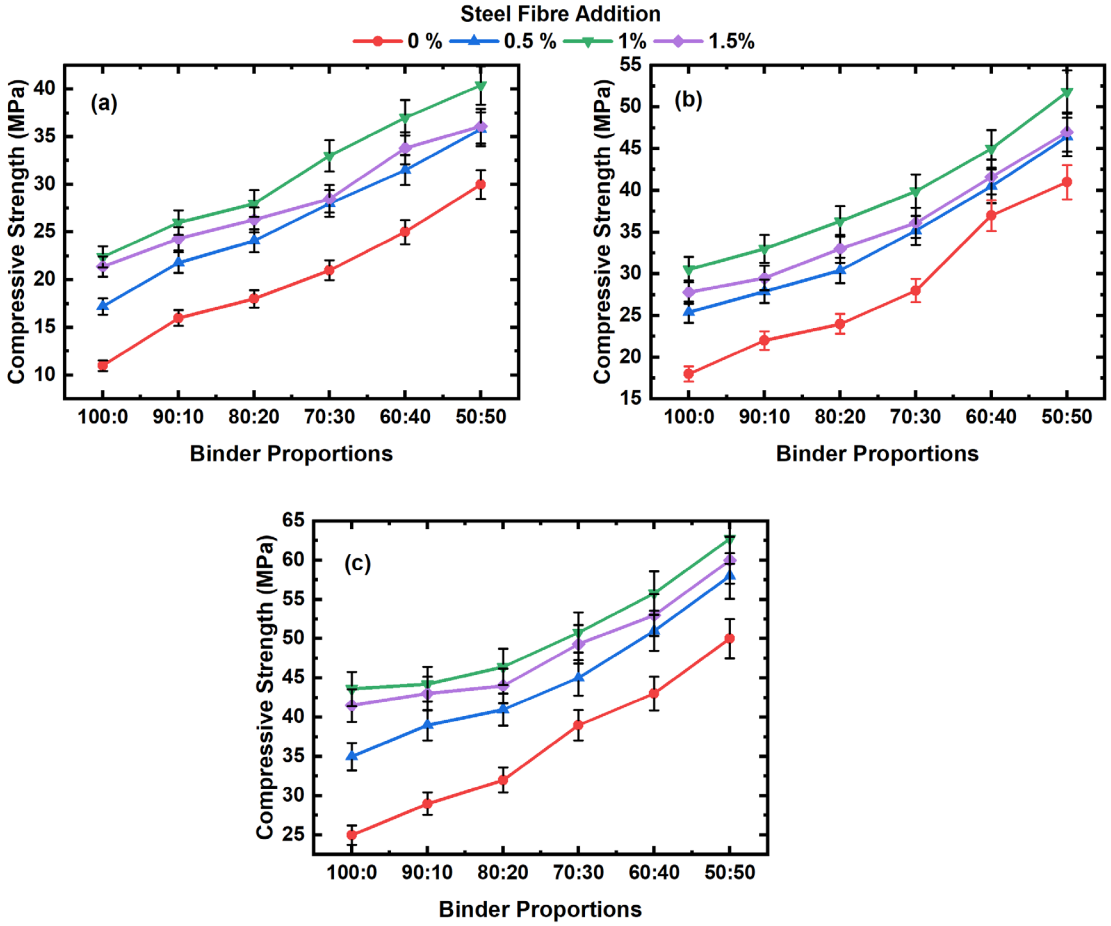

Figure 6.4: Compressive strength of geopolymeric mortar with steel fibres for an alkaline to binder ratio = 0.5 at (a) 3 days (b) 7 days and (c) 28 days

Variation of strength in compression values for an alkaline to binder ratio of 0.5 for curing period of 3, 7, and 28 days is shown in Figure 6.4. Figures demonstrate that adding and incorporating fibres with an alkaline to binder ratio of 0.5 in plain geopolymer mortar incremented the compressive load carrying capacity by 13.17-75%. The compressive strength increased by 19.33–75% more than that of plain mortar for 3-day curing, 13.17–69.44% more than that of plain mortar for 7-day curing and 15.38–74.44% more than that of plain mortar for 28-day curing depending on GGBS content and percentage of fibres.

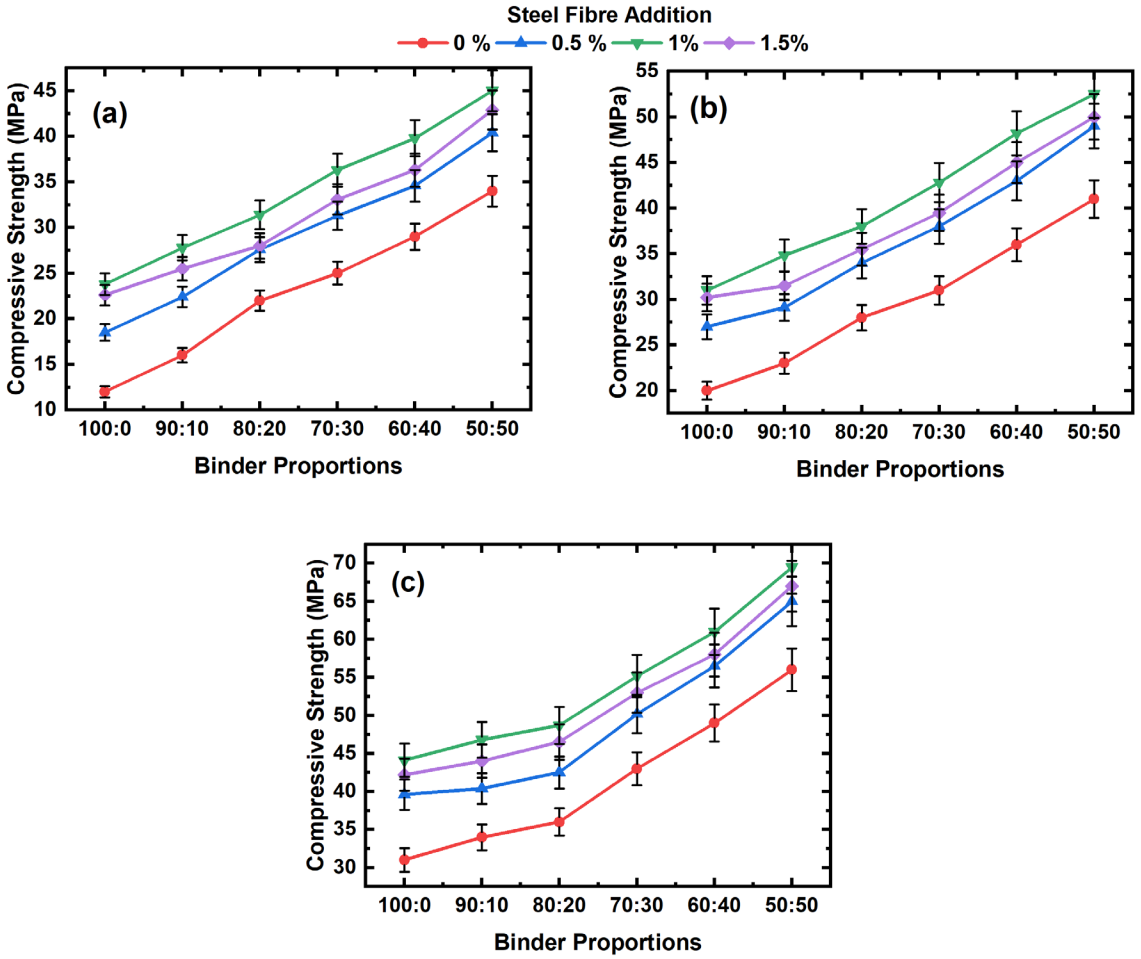

Figure 6.5: Compressive strength of geopolymeric mortar with steel fibres for an alkaline to binder ratio = 0.6 at (a) 3 days (b) 7 days and (c) 28 days

Variation of strength in compression values is depicted in Figure 6.5 for curing periods of 3, 7, and 28 days with an alkaline to binder ratio of 0.6. Figures demonstrate that adding and incorporating fibres increases strength in compression values of pure geopolymeric mortars by roughly 15.30–73.75% for an alkaline to binder ratio of 0.6. Compressive load carrying capacity increased by 19.82–73.75% more than that of plain mortar for 3-day curing, 19.44–55% more than that of plain mortar for 7-day curing and 15.3–42.25% more than that of plain mortar for 28-day curing depending on GGBS content and percentage of fibres.

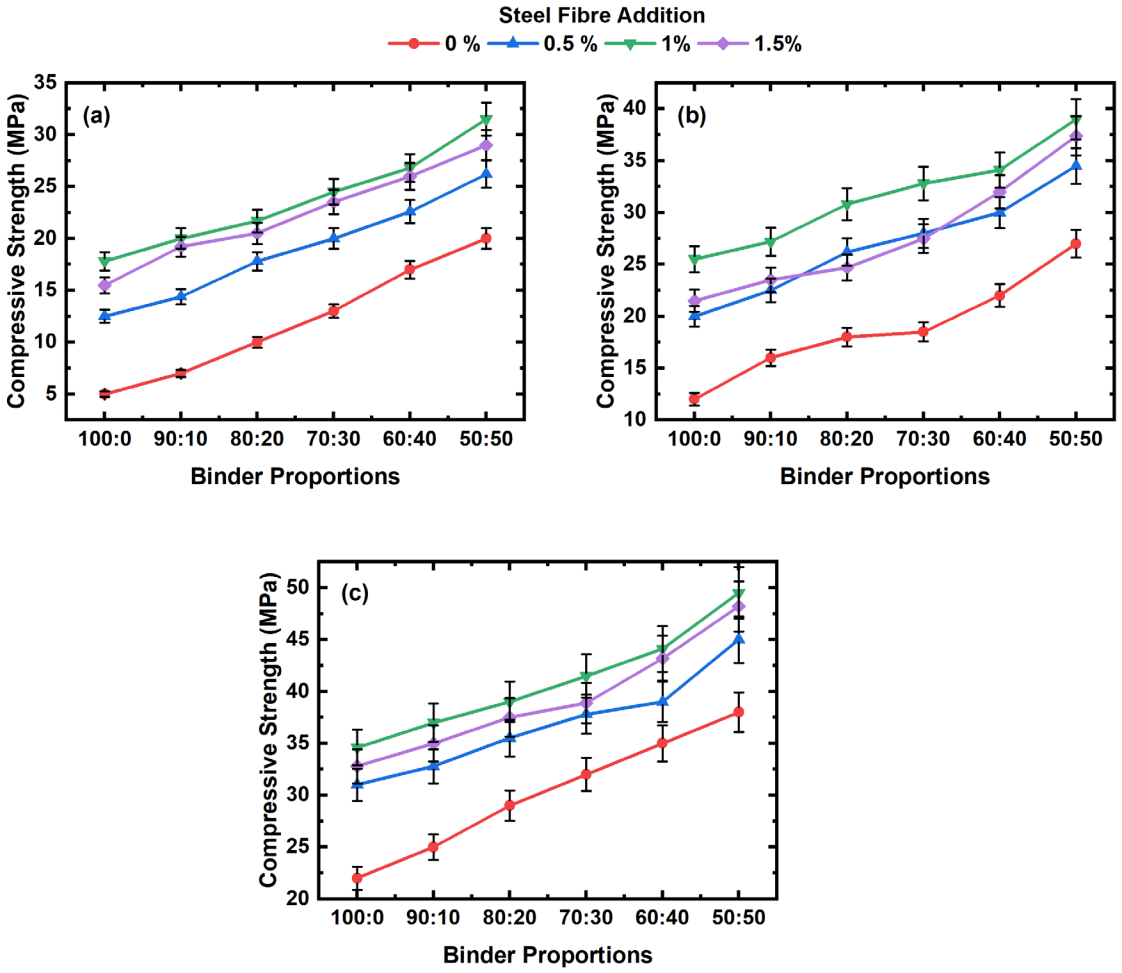

Figure 6.6: Compressive strength of geopolymeric mortar with steel fibres for an alkaline to binder ratio = 0.7 at (a) 3 days (b) 7 days and (c) 28 days

Variation of compressive strength for an alkaline to binder ratio of 0.7 for curing periods of 3, 7, and 28 days is shown in Figure 6.6. Figures demonstrate that adding and incorporating fibres increases the strength in compression values of pure geopolymeric mortars by roughly 17.58–75.75% for an alkaline to binder ratio of 0.7. Compressive load carrying capacity increased by 25–75.75% more than that of plain mortar for 3-day curing, 17.58–71.87% more than that of plain mortar for 7-day curing and 18.18–48.14% more than that of plain mortar for 28-day curing depending on GGBS content and percentage of fibres.

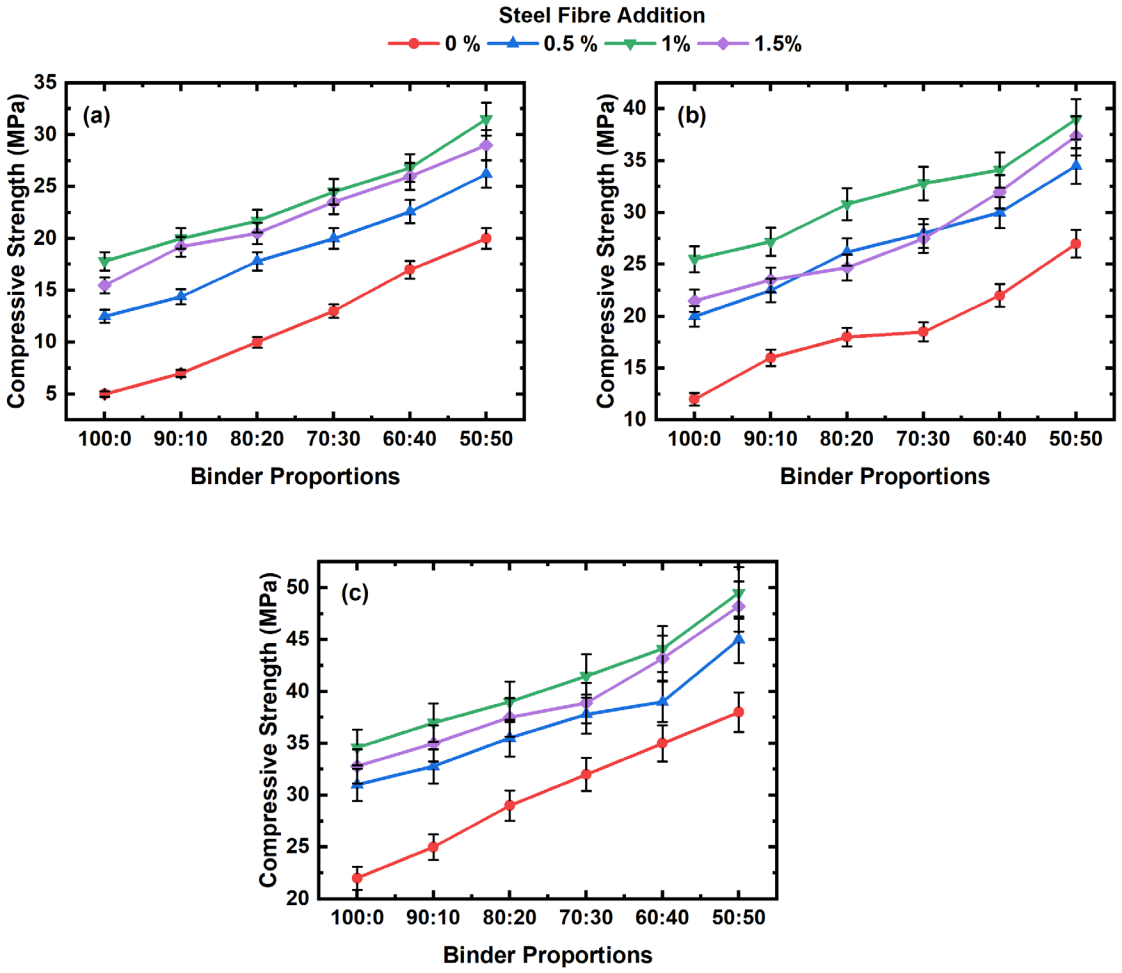

Figure 6.7: Compressive strength of geopolymeric mortar with steel fibres for an alkaline to binder ratio = 0.8 at (a) 3 days (b) 7 days and (c) 28 days

For alkaline to binder ratios of 0.8, Figure 6.7 shows variations in compressive load carrying capacity for curing periods of 3, 7, and 28 days, correspondingly. According to figures, adding more fibres and incorporating them into a plain geopolymer mortar with an alkaline to binder ratio of 0.8 incremented the compressive load carrying capacity by 18.42 to 88.46%. The compressive load carrying capacity incremented between 31 and 88.46% more than that of plain mortar for 3 days curing, between 52 and 83.33% more than that of plain mortar for 7 days curing and between 18.42 and 67.27% more than that of plain mortar for 28 days curing depending on GGBS content and percentage of fibres.

6.3 ADVANCED CHARACRTERIZATION STUDIES ON GEOPOLYMERIC MORTARS WITH STEEL FIBRES

6.3.1 SEM analysis

SEM microphotographs of geopolymer composites were analysed for assessing effect of steel fibre in geopolymer mortar for microstructural characteristics. The geopolymeric mortar samples with steel fibres under group B (B0-B50) which depicted higher compressive load carrying capacity/strength in compression values at 28 days curing in comparison with other group mixes were selected for SEM analysis and microphotographs of those respective samples is represented in Figure 6.8.

Sample B0 S_2

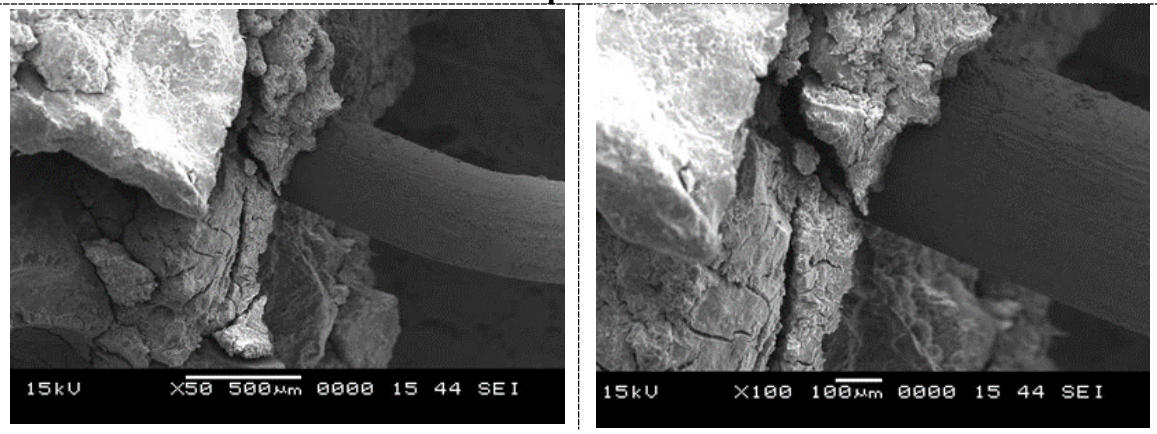

Sample B20 S_2

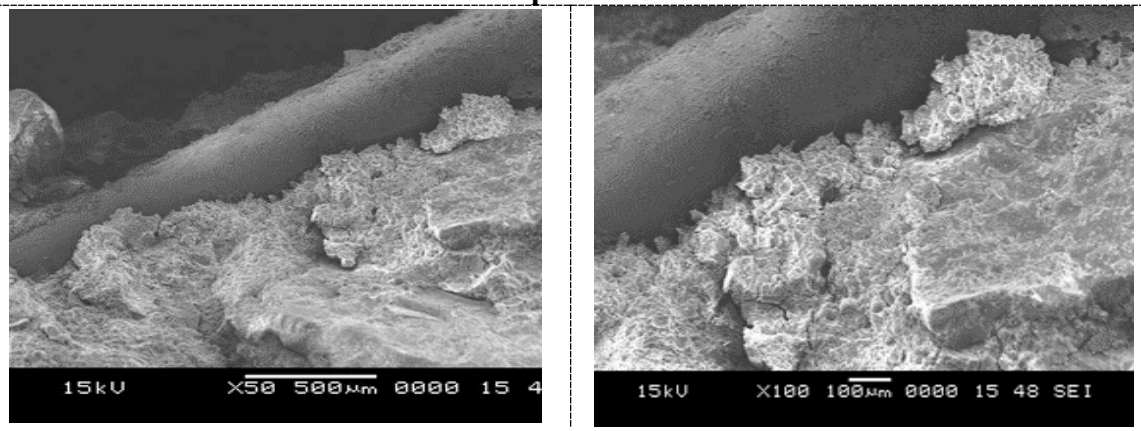

Sample B30 S_2

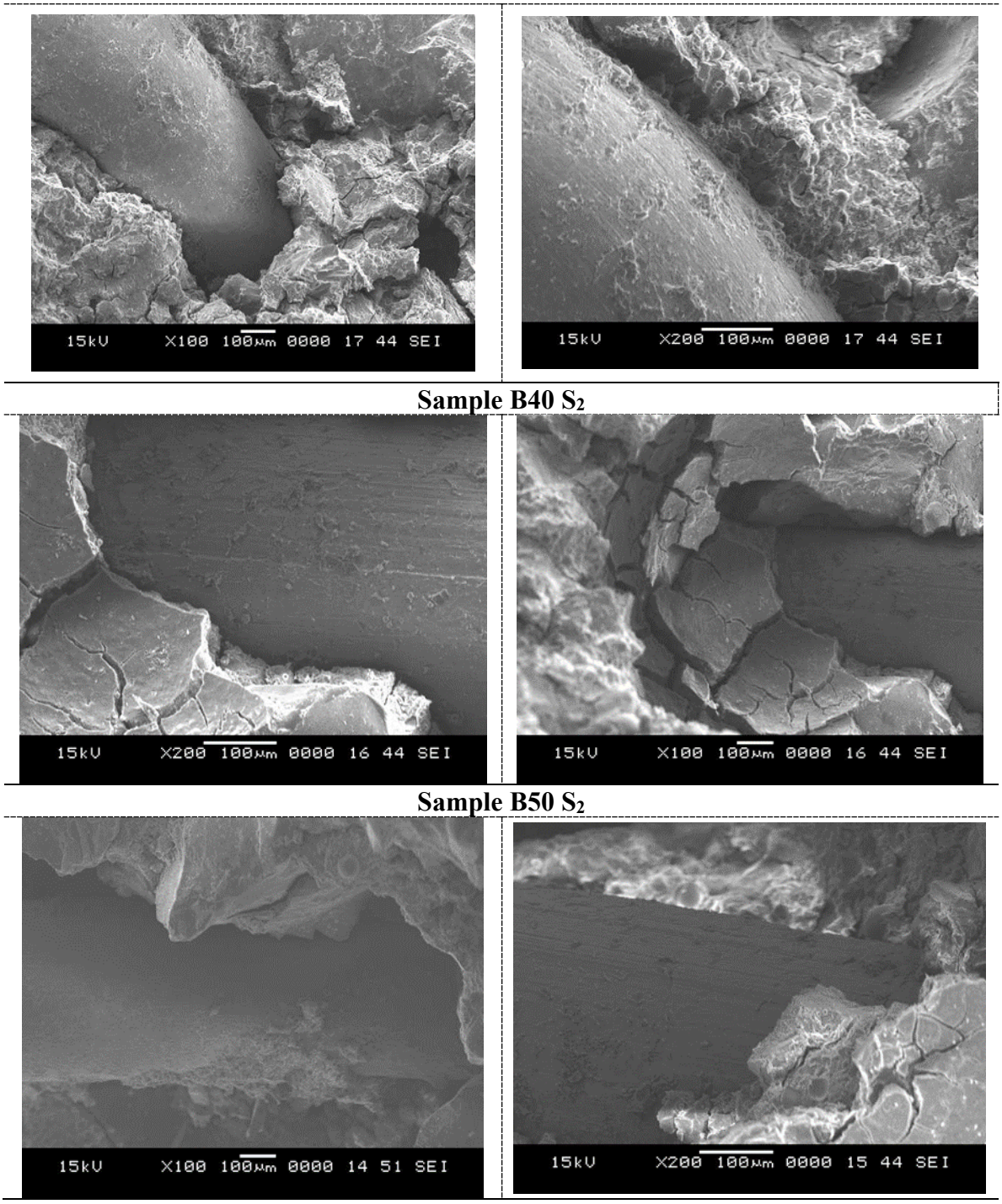

Figure 6.8: SEM microphotographs of group B geopolymeric mortar mixes with S_2 steel fibre additions (1% by weight of mortar)

Figure 6.8 demonstrates that surface of the steel fibre is significantly impacted by the geopolymer's interfacial characteristics. Increase in GGBS content leads to enhanced interfacial properties as shown in B20 S_2 and B30 S_2 in figure 6.8. According to section 6.2.2, these characteristics have a direct impact on the compressive strength of geopolymer composites. Figure 6.8 shows a geopolymer sample with 0% GGBS (B0 S2) that has a smooth

steel fibre surface, but samples with 50% GGBS (B50 S2) have a geopolymeric matrix that covers steel fibre surface.

Microphotographs of samples B40 S_2 and B50 S_2 depicted in Figure 6.8 also present SEM images of geopolymer samples containing 40 and 50% GGBS. It can be observed from the figure that a relative steel fibre surface is attached with geopolymer hydration products. This finding is supported by the relatively strong bond between the fibres and the geopolymer matrix. (Bhalchandra and Bhosle 2013). High compressive strength values, as stated in section 6.2.2, is a result of a stiff bond between geopolymer matrix and surface of the fibres.

CHAPTER – 7

CONCLUSIONS AND SCOPE FOR FURTHER STUDIES

7.1 GENERAL

This chapter presents the concluding points as well as findings of FA-based geopolymeric pastes, mortars, and mortars with steel fibres cured at ambient temperature conditions.

7.2 CONCLUSIONS

This experimental research focused on evaluating and understanding the substitution of GGBS against FA in designing the geopolymer mixtures for pastes, mortars and mortars with steel fibres, that clearly proved its beneficial usage in attaining the desired engineering and microstructural characteristics cured under ambient temperature conditions itself, hence making it as a sustainable and cost-reductive option for geopolymer mix. The subsequent sections present the conclusions from individual phases of this experimental research.

Production of geopolymeric pastes and its engineering properties

The ambient cured FA based geopolymeric paste admixed with GGBS can efficiently be produced by using alkaline solution as a binding media.

IST of paste gets effected by two factors which are, increase of Na_2O % and decrease of SiO_2 %. But FST of paste is majorly affected by an increase in Na_2O% as silica is involved in geopolymerization reaction. Na_2O/ SiO_2 ratio of 3.08 i.e., 1:2.5 ratio of NaOH to Na_2SiO_3 obtained fast setting results i.e., 140 and 240 minutes, respectively.

The IST and FST of the geopolymer mix samples decrements with an increment in GGBS incorporation. The samples with alkaline to binder ratio of 0.5 and 50 % of GGBS addition has IST and FST as 20 and 58 minutes, correspondingly.

Geopolymeric pastes with an alkaline to binder as 0.5 were found to depict optimum flowability, hence classifying it as a flowable mix.

The substitution of GGBS brings an increment in the strength in compression of geopolymeric mix samples. Samples with 50% of GGBS have shown maximum strength. Samples with more than 30% GGBS substitution resulted in a 28-day strength in compression of 50-85 MPa with an alkaline to binder ratio of 0.5, that is is almost equal to the compressive strength of a

conventional cement-based mix (56-69 MPa), satisfying the ASTM minimum compressive strength criteria.

The geopolymer mix samples possessing an alkaline to binder ratio of 0.8 showed occurrence of cracks in the early curing periods depicting the excessive presence of watery conditions within the paste samples.

The microstructural investigation of geopolymer mix samples using SEM-EDS and FTIR helped to confirm the information about setting time and strength. The presence of a dense microstructure, indication of co-existence of two binder gels and a shift in wavenumber of main absorption band in IR spectra collectively infers the beneficial substitution of GGBS in geopolymer mix samples that can be cured within the ambient temperature boundaries.

Production of geopolymeric mortars and its engineering properties

The ambient cured FA-based geopolymeric mortars admixed with GGBS can efficiently be produced by using alkaline solution as a binding media.

More than 10% GGBS replacement in mix reduces the setting time significantly in the geopolymeric mortar samples.

At all ages, increasing GGBS content as a replacement for FA increased the strength in compression regardless of alkaline to binder ratio. Additionally, when 50% FA was substituted with GGBS, strength in compression increased by up to 96% when compared to a mix with only FA for an alkaline to binder ratio of 0.5.

Adding up to 50% GGBS content of total binder achieved strength of mortar upto 56.2 MPa at 28 days of curing. Compressive load carrying capacity decremented with the increment of alkaline liquid content from 0.6 to 0.8.

The SEM and EDS results demonstrated that FA and GGBS-based geopolymeric mortars include a high quantity of Ca, which aids in crosslinking of C-S-H/N-A-S-H chains, resulting in denser and more compact amorphous gel structures with a high degree of polymerization.

Production of geopolymeric mortars with steel fibres addition and its engineering properties

In all mixes, the IST and FST of geopolymeric mortar reduced with incorporation and the increase in GGBS percentage. So, in order to produce a geopolymeric mortar with a rapid setting time, partial replacement of FA by GGBS can be a possible solution.

The amount of steel fibres incorporated into plain geopolymer and their percentage increase led to a reduction in flow capacity and diameter of mortar mixtures with all alkaline to binder ratios. Reduced flow diameter ranges from 23.56 to 32.94%

Alkaline to binder ratio of 0.6 shows the highest strength in compression values in all variation of steel fibre content and curing period.

Depending on the amount of steel fibre used, the composition of the binder, and the alkaline to binder ratio, adding more fibre and increasing the volume of fibre raises the compressive load carrying capacity of pure geopolymer mortar in the range of 5.1-22.6 MPa.

The strength in compression of geopolymer composites increments with the rise in GGBS content in mixes; so, to deliver a geopolymeric mortar with highest strength in compression and with a rapid setting under ambient temperature conditions, replacement of FA with GGBS can be a good possible solution.

The optimum fibre content in all combinations, which shows the highest strength value, is 1%. The highest compressive strength values at 28 days of curing are 69.5 MPa with 1% fibre content, a 0.6 alkaline to binder ratio, and 50:50 binder compositions.

According to the SEM images, the specimens' rough steel fibre surfaces and geopolymer hydration products provide proof of a rather strong bond between the geopolymer matrix and steel fibre, which increases strength in compression values.

7.3 SCOPE FOR FURTHER RESEARCH

The influence of additives used in geopolymeric pastes can be further studied to rectify the cracking phenomenon in higher alkaline to binder ratios samples as this will aid in minimizing the crack formation while maintaining the flowability of the geopolymeric paste.

Mechanical characterization of geopolymeric mortars and mortars with steel fibres can be studied with the inclusion of modulus of elasticity and possion’s ratio can be taken up by future researchers.

An experimental study with the inclusion of various types of fibres can be taken up to examine a betterment in the resultant engineering properties of geopolymeric mortars.

The economic and life cycle assessment of FA based geopolymeric pastes and mortars is very much essential.

An experimental can be taken by future researchers towards the possibility of using the ambient cured geopolymeric pastes for in-situ grouting applications.

REFERENCES

Abdul Rahim, R. H., Mohd Azizli, K. A., Rahmiati, T., and Nuruddin, F. (2014). "Effect of sodium hydroxide concentration on the mechanical property of non sodium silicate fly ash based geopolymer."

Abdulkareem, O. A., Kamarudin, H., and Nizar, K. (2012). "The Effect of Damp Sand Content on the Geopolymerization Reaction of Fly Ash-Based Geopolymer Mortars." *The 2nd International Malaysia-Ireland Joint Symposium on Engineering*, Science and Business (IMIEJS2012).

Aboulayt, A., Jaafri, R., Samouh, H., Idrissi, A. C. El, Roziere, E., Moussa, R., and Loukili, A. (2018). "Stability of a new geopolymer grout: Rheological and mechanical performances of metakaolin-fly ash binary mixtures." *Construction and Building Materials*, 181, 420–436.

Ahmed, M. M., El-Naggar, K. A. M., Tarek, D., Ragab, A., Sameh, H., Zeyad, A. M., Tayeh, B. A., Maafa, I. M., and Yousef, A. (2021). "Fabrication of thermal insulation geopolymer bricks using ferrosilicon slag and alumina waste." *Case Studies in Construction Materials*, 15, e00737.

Al-Majidi, M. H., Lampropoulos, A., and Cundy, A. B. (2017). "Steel fibre reinforced geopolymer concrete (SFRGC) with improved microstructure and enhanced fibre-matrix interfacial properties." *Construction and Building Materials*, 139, 286–307.

Al-Majidi, M. H., Lampropoulos, A., Cundy, A., and Meikle, S. (2016). "Development of geopolymer mortar under ambient temperature for in situ applications." *Construction and Building Materials*, 120, 198–211.

Allahverdi, A., Shaverdi, B., and Najafi, K. E. (2010). "Influence of sodium oxide on properties of fresh and hardened paste of alkali-activated blast-furnace slag."

Almutairi, A. L., Tayeh, B. A., Adesina, A., Isleem, H. F., and Zeyad, A. M. (2021). "Potential applications of geopolymer concrete in construction: A review." *Case Studies in Construction Materials*, 15, e00733.

Amor, N., Noman, M. T., and Petru, M. (2021). "Prediction of functional properties of nano TiO 2 coated cotton composites by artificial neural network." *Scientific Reports*, 11(1), 12235.

Arisoy, B., and Wu, H.-C. (2008). "Material characteristics of high performance lightweight concrete reinforced with PVA." *Construction and Building Materials*, 22(4), 635–645.

Bakharev, T. (2006). “Thermal behaviour of geopolymers prepared using class F fly ash and elevated temperature curing.” *cement and Concrete Research*, 36(6), 1134–1147.

Bakri Abdullah, M. M. Al, Kamarudin, H., Abdulkareem, O. A. K. A., Ghazali, C. M. R., Rafiza, A. R., and Norazian, M. N. (2012). “Optimization of alkaline activator/fly ash ratio on the compressive strength of manufacturing fly ash-based geopolymer.” *Applied Mechanics and Materials*, Trans Tech Publ, 734–739.

Barbosa, V. F. F., MacKenzie, K. J. D., and Thaumaturgo, C. (2000). “Synthesis and characterisation of materials based on inorganic polymers of alumina and silica: sodium polysialate polymers.” *International journal of inorganic materials*, 2(4), 309–317.

Bernal, S. A., San Nicolas, R., Myers, R. J., Gutiérrez, R. M. de, Puertas, F., Deventer, J. S. J. van, and Provis, J. L. (2014). “MgO content of slag controls phase evolution and structural changes induced by accelerated carbonation in alkali-activated binders.” *Cement and Concrete Research*, 57, 33–43.

Bhalchandra, S. A., and Bhosle, A. Y. (2013). “Properties of glass fibre reinforced geopolymer concrete.” *International Journal of Modern Engineering Research (IJMER)*, 3(4), 2007–2010.

Bilondi, M. P., Toufigh, M. M., and Toufigh, V. (2018). “Experimental investigation of using a recycled glass powder-based geopolymer to improve the mechanical behavior of clay soils.” *Construction and building Materials*, 170, 302–313.

Blash, A. M. A., and Lakshmi, T. V. S. V. (2016). “Properties of geopolymer concrete produced by silica fume and ground-granulated blast-furnace slag.” *Int. J. Sci. Res.*, 5(10), 319–323.

Brinkman, L., and Miller, S. A. (2021). “Environmental impacts and environmental justice implications of supplementary cementitious materials for use in concrete.” *Environmental Research: Infrastructure and Sustainability*, 1(2), 25003.

Bui, L. A., Hwang, C., Chen, C., Lin, K., and Hsieh, M. (2012). “Manufacture and performance of cold bonded lightweight aggregate using alkaline activators for high performance concrete.” *Construction and Building Materials*, 35, 1056–1062.

Çevik, A., Alzeebaree, R., Humur, G., Niş, A., and Gülşan, M. E. (2018). “Effect of nano-silica on the chemical durability and mechanical performance of fly ash based geopolymer concrete.” *Ceramics International*, 44(11), 12253–12264.

Cherki El Idrissi, A., Roziere, E., Loukili, A., and Darson, S. (2018). “Design of geopolymer

grouts: the effects of water content and mineral precursor." *European Journal of Environmental and Civil Engineering*, 22(5), 628–649.

Chindaprasirt, P., Chareerat, T., and Sirivivatnanon, V. (2007). "Workability and strength of coarse high calcium fly ash geopolymer." *Cement and concrete composites*, 29(3), 224–229.

Chindaprasirt, P., Silva, P. De, and Hanjitsuwan, S. (2014). "Effect of high-speed mixing on properties of high calcium fly ash geopolymer paste." *Arabian Journal for Science and Engineering*, 39(8), 6001–6007.

Chindaprasirt, P., Silva, P. De, Sagoe-Crentsil, K., and Hanjitsuwan, S. (2012). "Effect of SiO2 and Al2O3 on the setting and hardening of high calcium fly ash-based geopolymer systems." *Journal of Materials Science*, 47(12), 4876–4883.

Davidovits, J. (1999a). "Chemistry of geopolymeric systems, terminology." *Geopolymer*, sn, 9–39.

Davidovits, J. (1999b). "Chemistry of Geopolymeric Systems, Terminology In: Proceedings of 99 International Conference." *eds. Joseph Davidovits, R. Davidovits & C. James, France*.

Davidovits, J. (2008). "Geopolymer." *Chemistry and Applications. Institute Geopolymere, Saint-Quentin, France*.

Deb, P. S., and Sarker, P. K. (2017). "Effects of ultrafine fly ash on setting, strength, and porosity of geopolymers cured at room temperature." *Journal of Materials in Civil Engineering*, 29(2), 6016021.

Deventer, J. S. J. Van, Provis, J. L., and Duxson, P. (2012). "Technical and commercial progress in the adoption of geopolymer cement." *Minerals Engineering*, 29, 89–104.

Deventer, J. S. J. van, Provis, J. L., Duxson, P., and Brice, D. G. (2010). "Chemical research and climate change as drivers in the commercial adoption of alkali activated materials." *Waste and Biomass Valorization*, 1(1), 145–155.

Duxson, P., Fernández-Jiménez, A., Provis, J. L., Lukey, G. C., Palomo, A., and Deventer, J. S. J. van. (2007). "Geopolymer technology: the current state of the art." *Journal of materials science*, 42(9), 2917–2933.

Elyamany, H. E., Abd Elmoaty, M., and Elshaboury, A. M. (2018). "Magnesium sulfate resistance of geopolymer mortar." *Construction and Building Materials*, 184, 111–127.

Escalante García, J. I., Campos-Venegas, K., Gorokhovsky, A., and Fernández, A. (2006).

"Cementitious composites of pulverised fuel ash and blast furnace slag activated by sodium silicate: effect of Na2O concentration and modulus." *Advances in applied ceramics*, 105(4), 201–208.

Fang, Y., and Kayali, O. (2013). "The fate of water in fly ash-based geopolymers." *Construction and Building Materials*, 39, 89–94.

Fifinatasha, S. N., Bakri, A. M. M. Al, Kamarudin, H., Zarina, Y., Rafiza, A. R., and Liyana, J. (2013). "Reviews on the different sources materials to the geopolymer performance." *Advances in Environmental Biology*, 7(12 S2), 3835–3843.

Garcia-Lodeiro, I., Palomo, A., and Fernández-Jiménez, A. (2015). "An overview of the chemistry of alkali-activated cement-based binders." *Handbook of alkali-activated cements, mortars and concretes*, 19–47.

Ghosh, K., and Ghosh, P. (2018). "Effect of Alkali Concentration on Mechanical Properties, Microstructure, Zeta Potential and Electrical Conductivity of Thermally Cured Fly-Ash-Blast Furnace Slag Based Blended Geopolymer Composites." *Oriental Journal of Chemistry*, 34(2), 704.

Glukhovsky, V. D. (1965). "Soil silicates: Their properties, technology and manufacturing and fields of application." *Doct. Tech. Sc. Degree Thesis, Civil Engineering Institute, Kiev, Ukraine*.

Goudar, S. K., Das, B. B., Arya, S. B., and Shivaprasad, K. N. (2020). "Influence of sample preparation techniques on microstructure and nano-mechanical properties of steel-concrete interface." *Construction and Building Materials*, 256, 119242.

Güllü, H., and Agha, A. A. (2021). "The rheological, fresh and strength effects of cold-bonded geopolymer made with metakaolin and slag for grouting." *Construction and Building Materials*, 274, 122091.

Guo, X., and Pan, X. (2018). "Mechanical properties and mechanisms of fiber reinforced fly ash–steel slag based geopolymer mortar." *Construction and Building Materials*, 179, 633–641.

Hardjito, D., Cheak, C. C., and Ing, C. H. L. (2008). "Strength and setting times of low calcium fly ash-based geopolymer mortar." *Modern applied science*, 2(4), 3–11.

Hardjito, D., and Rangan, B. V. (2005). "Development and properties of low-calcium fly ash-based geopolymer concrete."

Hardjito, D., and Tsen, M. Z. (2008). “Strength and Thermal stability of fly ash based geopolymer mortar.” *The 3rd international conference-ACF/VCA*, 150.

Islam, A., Alengaram, U. J., Jumaat, M. Z., and Bashar, I. I. (2014). “The development of compressive strength of ground granulated blast furnace slag-palm oil fuel ash-fly ash based geopolymer mortar.” *Materials & Design (1980-2015)*, 56, 833–841.

Islam, A., Alengaram, U. J., Jumaat, M. Z., Bashar, I. I., and Kabir, S. M. A. (2015). “Engineering properties and carbon footprint of ground granulated blast-furnace slag-palm oil fuel ash-based structural geopolymer concrete.” *Construction and building materials*, 101, 503–521.

Ismail, I., Bernal, S. A., Provis, J. L., Hamdan, S., and Deventer, J. S. J. van. (2013). “Microstructural changes in alkali activated fly ash/slag geopolymers with sulfate exposure.” *Materials and structures*, 46(3), 361–373.

Ismail, I., Bernal, S. A., Provis, J. L., San Nicolas, R., Hamdan, S., and Deventer, J. S. J. van. (2014). “Modification of phase evolution in alkali-activated blast furnace slag by the incorporation of fly ash.” *Cement and Concrete Composites*, 45, 125–135.

Jamshaid, H., Mishra, R., Militký, J., and Noman, M. T. (2018). “Interfacial performance and durability of textile reinforced concrete.” *The Journal of The Textile Institute*, 109(7), 879–890.

Jamshaid, H., Mishra, R., Militky, J., Pechociakova, M., and Noman, M. T. (2016). “Mechanical, thermal and interfacial properties of green composites from basalt and hybrid woven fabrics.” *Fibers and Polymers*, 17, 1675–1686.

Jang, J. G., Lee, N. K., and Lee, H.-K. (2014). “Fresh and hardened properties of alkali-activated fly ash/slag pastes with superplasticizers.” *Construction and Building Materials*, 50, 169–176.

Khale, D., and Chaudhary, R. (2007). “Mechanism of geopolymerization and factors influencing its development: a review.” *Journal of materials science*, 42(3), 729–746.

Khater, H. M. (2012). “Effect of calcium on geopolymerization of aluminosilicate wastes.” *Journal of materials in civil engineering*, 24(1), 92–101.

Komljenović, M., Baščarević, Z., and Bradić, V. (2010). “Mechanical and microstructural properties of alkali-activated fly ash geopolymers.” *Journal of Hazardous Materials*, 181(1–3), 35–42.

Kong, D. L. Y., Sanjayan, J. G., and Sagoe-Crentsil, K. (2007). “Comparative performance of geopolymers made with metakaolin and fly ash after exposure to elevated temperatures.” *Cement and concrete research*, 37(12), 1583–1589.

Kumar, S., Kumar, R., and Mehrotra, S. P. (2010). “Influence of granulated blast furnace slag on the reaction, structure and properties of fly ash based geopolymer.” *Journal of materials science*, 45(3), 607–615.

Lee, N. K., and Lee, H.-K. (2013). “Setting and mechanical properties of alkali-activated fly ash/slag concrete manufactured at room temperature.” *Construction and Building Materials*, 47, 1201–1209.

Lee, W. K. W., and Deventer, J. S. J. Van. (2002). “Structural reorganisation of class F fly ash in alkaline silicate solutions.” *Colloids and Surfaces A: Physicochemical and Engineering Aspects*, 211(1), 49–66.

Leong, H. Y., Ong, D. E. L., Sanjayan, J. G., and Nazari, A. (2016). “The effect of different Na2O and K2O ratios of alkali activator on compressive strength of fly ash based-geopolymer.” *Construction and Building Materials*, 106, 500–511.

Li, X., Wang, Z., and Jiao, Z. (2013). “Influence of curing on the strength development of calcium-containing geopolymer mortar.” *Materials*, 6(11), 5069–5076.

Li, Z., and Liu, S. (2007). “Influence of slag as additive on compressive strength of fly ash-based geopolymer.” *Journal of Materials in civil engineering*, 19(6), 470–474.

Lyon, R. E., Balaguru, P. N., Foden, A., Sorathia, U., Davidovits, J., and Davidovics, M. (1997). “Fire-resistant aluminosilicate composites.” *Fire and materials*, 21(2), 67–73.

Mahmood, A., Noman, M. T., Pechočiaková, M., Amor, N., Petrů, M., Abdelkader, M., Militký, J., Sozcu, S., and Hassan, S. Z. U. (2021). “Geopolymers and fiber-reinforced concrete composites in civil engineering.” *Polymers*, 13(13), 2099.

Mallikarjuna Rao, G., and Gunneswara Rao, T. D. (2015). “Final setting time and compressive strength of fly ash and GGBS-based geopolymer paste and mortar.” *Arabian journal for science and engineering*, 40(11), 3067–3074.

Marjanović, N., Komljenović, M., Baščarević, Z., Nikolić, V., and Petrović, R. (2015). “Physical–mechanical and microstructural properties of alkali-activated fly ash–blast furnace slag blends.” *Ceramics International*, 41(1), 1421–1435.

Mohod, M. V. (2015). “Performance of polypropylene fibre reinforced concrete.” *IOSR Journal of Mechanical and Civil Engineering*, 12(1), 28–36.

Morsy, M. S., Alsayed, S. H., Al-Salloum, Y., and Almusallam, T. (2014). “Effect of sodium silicate to sodium hydroxide ratios on strength and microstructure of fly ash geopolymer binder.” *Arabian journal for science and engineering*, 39(6), 4333–4339.

Mozgawa, W., and Deja, J. (2009). “Spectroscopic studies of alkaline activated slag geopolymers.” *Journal of Molecular Structure*, 924, 434–441.

Mustafa, R., Ahmed, S., Gupta, A., and Venuto, R. C. (2012). “A comprehensive review of hypertension in pregnancy.” *Journal of pregnancy*, 2012.

Naghizadeh, A., and Ekolu, S. O. (2019). “Effect of mix parameters on strength of geopolymer mortars-experimental study.”

Natali, A., Manzi, S., and Bignozzi, M. C. (2011). “Novel fiber-reinforced composite materials based on sustainable geopolymer matrix.” *Procedia engineering*, 21, 1124–1131.

Nath, P., and Sarker, P. K. (2014). “Effect of GGBFS on setting, workability and early strength properties of fly ash geopolymer concrete cured in ambient condition.” *Construction and Building materials*, 66, 163–171.

Nath, S. K., and Kumar, S. (2013). “Influence of iron making slags on strength and microstructure of fly ash geopolymer.” *Construction and Building Materials*, 38, 924–930.

Nikolić, V., Komljenović, M., Baščarević, Z., Marjanović, N., Miladinović, Z., and Petrović, R. (2015). “The influence of fly ash characteristics and reaction conditions on strength and structure of geopolymers.” *Construction and Building materials*, 94, 361–370.

Noman, M. T., Petru, M., Louda, P., and Kejzlar, P. (2022). “Woven textiles coated with zinc oxide nanoparticles and their thermophysiological comfort properties.” *Journal of Natural Fibers*, 19(12), 4718–4730.

Pacheco-Torgal, F., Castro-Gomes, J., and Jalali, S. (2008). “Alkali-activated binders: A review. Part 2. About materials and binders manufacture.” *Construction and building materials*, 22(7), 1315–1322.

Palacios, M., Banfill, P. F. G., and Puertas, F. (2008). “Rheology and setting of alkali-activated slag pastes and mortars: Effect of organic admixture.” *ACI Materials Journal*, 105(2), 140.

Palomo, A., Grutzeck, M. W., and Blanco, M. T. (1999). “Alkali-activated fly ashes: A cement

for the future." *Cement and concrete research*, 29(8), 1323–1329.

Patankar, S. V, Ghugal, Y. M., and Jamkar, S. S. (2014). "Effect of concentration of sodium hydroxide and degree of heat curing on fly ash-based geopolymer mortar." *Indian Journal of Materials Science*, 2014.

Phoo-ngernkham, T., Maegawa, A., Mishima, N., Hatanaka, S., and Chindaprasirt, P. (2015). "Effects of sodium hydroxide and sodium silicate solutions on compressive and shear bond strengths of FA–GBFS geopolymer." *Construction and Building Materials*, 91, 1–8.

Plizzari, G. A. (2004). *Experimental study of fracture behavior of concrete reinforced with steel fibers*. Research Report.

Poornima, N., Sivasakthi, M., and Jeyalakshmi, R. (2022). "Microstructure investigation of the Na/Ca aluminosilicate hydrate gels and its thermal compatibility in fly ash–GGBS cementitious binder." *Journal of Building Engineering*, 50, 104168.

Porkodi, R., Dharmar, S., and Nagan, S. (2015). "Experimental Study on Fiber Reinforced Self-Compacting Geopolymer Mortar." 8354(4), 968–977.

Provis, J. L., Duxson, P., and Deventer, J. S. J. van. (2010). "The role of particle technology in developing sustainable construction materials." *Advanced Powder Technology*, 21(1), 2–7.

Provis, J. L., Myers, R. J., White, C. E., Rose, V., and Deventer, J. S. J. Van. (2012). "X-ray microtomography shows pore structure and tortuosity in alkali-activated binders." *Cement and concrete research*, 42(6), 855–864.

Rafeet, A., Vinai, R., Soutsos, M., and Sha, W. (2019). "Effects of slag substitution on physical and mechanical properties of fly ash-based alkali activated binders (AABs)." *Cement and Concrete Research*, 122, 118–135.

Rahmiati, T., Azizli, K. A., Man, Z., Ismail, L., and Nuruddin, M. F. (2015). "Effect of solid/liquid ratio during curing time fly ash based geopolymer on mechanical property." *Materials Science Forum*, Trans Tech Publ, 120–124.

Ramezanianpour, A., and Alapour, F. (2013). "Compressive strength of fly ash geopolymer paste designed by taguchi method." *Third International Conference On Sustainable Construction Materials And Technologies*.

Ramkumar, G., Sundarkumar, S., and Sivakumar, A. (2015). "Development of steel fibre reinforced geopolymer concrete." *International Journal of Advance Research in Science and*

Engineering, 4(1), 1717–1725.

Ranjbar, N., Talebian, S., Mehrali, M., Kuenzel, C., Metselaar, H. S. C., and Jumaat, M. Z. (2016). "Mechanisms of interfacial bond in steel and polypropylene fiber reinforced geopolymer composites." *Composites Science and Technology*, 122, 73–81.

Ranjbar, N., and Zhang, M. (2020). "Fiber-reinforced geopolymer composites: A review." *Cement and Concrete Composites*, 107, 103498.

Rashad, A. M. (2015). "Influence of different additives on the properties of sodium sulfate activated slag." *Construction and Building Materials*, 79, 379–389.

Rattanasak, U., and Chindaprasirt, P. (2009). "Influence of NaOH solution on the synthesis of fly ash geopolymer." *Minerals Engineering*, 22(12), 1073–1078.

Rattanasak, U., Pankhet, K., and Chindaprasirt, P. (2011). "Effect of chemical admixtures on properties of high-calcium fly ash geopolymer." *International Journal of Minerals, Metallurgy, and Materials*, 18(3), 364–369.

Richardson, I. G., Brough, A. R., Groves, G. W., and Dobson, C. M. (1994). "The characterization of hardened alkali-activated blast-furnace slag pastes and the nature of the calcium silicate hydrate (CSH) phase." *Cement and Concrete Research*, 24(5), 813–829.

Ridtirud, C., Chindaprasirt, P., and Pimraksa, K. (2011). "Factors affecting the shrinkage of fly ash geopolymers." *International Journal of Minerals, Metallurgy, and Materials*, 18(1), 100–104.

Saha, S., and Rajasekaran, C. (2017). "Enhancement of the properties of fly ash based geopolymer paste by incorporating ground granulated blast furnace slag." *Construction and Building Materials*, 146, 615–620.

Sahoo, S., Das, B. B., and Mustakim, S. (2017). "Acid, alkali, and chloride resistance of concrete composed of low-carbonated fly ash." *Journal of Materials in Civil Engineering*, 29(3), 4016242.

Saloma, S., Hanafiah, H., Saggaff, A., and Mawarni, A. (2016). "Geopolymer mortar with fly ash." *MATEC Web of Conferences*, EDP Sciences, 1–6.

Saludung, A., Ogawa, Y., and Kawai, K. (2018). "Microstructure and mechanical properties of FA/GGBS-based geopolymer." *MATEC Web of Conferences*, EDP Sciences, 1013.

Samantasinghar, S., and Singh, S. P. (2019). "Fresh and hardened properties of fly ash–slag

blended geopolymer paste and mortar." *International Journal of Concrete Structures and Materials*, 13(1), 1–12.

Sathonsaowaphak, A., Chindaprasirt, P., and Pimraksa, K. (2009). "Workability and strength of lignite bottom ash geopolymer mortar." *Journal of Hazardous Materials*, 168(1), 44–50.

Shaikh, F. U. A. (2013). "Review of mechanical properties of short fibre reinforced geopolymer composites." *Construction and building materials*, 43, 37–49.

Shuaibu, R. A. (2014). "Compressive strength of low calcium fly ash geopolymer concrete-A Review." *International Journal of Emerging Technology and Advanced Engineering*, 4(4).

Silva, G., Kim, S., Bertolotti, B., Nakamatsu, J., and Aguilar, R. (2020). "Optimization of a reinforced geopolymer composite using natural fibers and construction wastes." *Construction and Building Materials*, 258, 119697.

Singh, P. S., Trigg, M., Burgar, I., and Bastow, T. (2005). "Geopolymer formation processes at room temperature studied by 29Si and 27Al MAS-NMR." *Materials Science and Engineering: A*, 396(1–2), 392–402.

Snehal, K., Das, B. B., and Akanksha, M. (2020). "Early age, hydration, mechanical and microstructure properties of nano-silica blended cementitious composites." *Construction and Building Materials*, 233, 117212.

Soutsos, M., Boyle, A. P., Vinai, R., Hadjierakleous, A., and Barnett, S. J. (2016). "Factors influencing the compressive strength of fly ash based geopolymers." *Construction and Building Materials*, 110, 355–368.

Sugama, T., Brothers, L. E., and Putte, T. R. Van de. (2005). "Acid-resistant cements for geothermal wells: sodium silicate activated slag/fly ash blends." *Advances in cement research*, 17(2), 65–75.

Taher, S. M. S., Saadullah, S. T., Haido, J. H., and Tayeh, B. A. (2021). "Behavior of geopolymer concrete deep beams containing waste aggregate of glass and limestone as a partial replacement of natural sand." *Case Studies in Construction Materials*, 15, e00744.

Tayeh, B. A., Zeyad, A. M., Agwa, I. S., and Amin, M. (2021). "Effect of elevated temperatures on mechanical properties of lightweight geopolymer concrete." *Case Studies in Construction Materials*, 15, e00673.

Teixeira-Pinto, A., Fernandes, P., and Jalali, S. (2002). "Geopolymer manufacture and

application-Main problems when using concrete technology." *Geopolymers 2002 International Conference, Melbourne, Australia, Siloxo Pty. Ltd*.

Tennakoon, C., San Nicolas, R., Sanjayan, J. G., and Shayan, A. (2016). "Thermal effects of activators on the setting time and rate of workability loss of geopolymers." *Ceramics International*, 42(16), 19257–19268.

Thakur, R. N., and Ghosh, S. (2009). "Effect of mix composition on compressive strength and microstructure of fly ash based geopolymer composites." *ARPN Journal of Engineering and Applied Sciences*, 4(4), 68–74.

Vargas, A. S. de, Dal Molin, D. C. C., Masuero, Â. B., Vilela, A. C. F., Castro-Gomes, J., and Gutierrez, R. M. de. (2014). "Strength development of alkali-activated fly ash produced with combined NaOH and Ca (OH) 2 activators." *Cement and Concrete Composites*, 53, 341–349.

Wang, H., Li, H., and Yan, F. (2005). "Synthesis and mechanical properties of metakaolinite-based geopolymer." *Colloids and Surfaces A: Physicochemical and Engineering Aspects*, 268(1–3), 1–6.

Wardhono, A., Law, D. W., and Strano, A. (2015). "The strength of alkali-activated slag/fly ash mortar blends at ambient temperature." *Procedia Engineering*, 125, 650–656.

Wijaya, S. W., and Hardjito, D. (2016). "Factors affecting the setting time of fly ash-based geopolymer." *Materials Science Forum*, Trans Tech Publ, 90–97.

Xu, H., Gong, W., Syltebo, L., Izzo, K., Lutze, W., and Pegg, I. L. (2014). "Effect of blast furnace slag grades on fly ash based geopolymer waste forms." *Fuel*, 133, 332–340.

Xu, J., Kang, A. H., Wu, Z. G., Xiao, P., Li, B., and Lu, Y. M. (2021). "Research on the Formulation and Properties of a High-Performance Geopolymer Grouting Material Based on Slag and Fly Ash." *KSCE Journal of Civil Engineering*, 25(9), 3437–3447.

Yellaiah, P., Sharma, S. K., and Rao, T. D. G. (2014). "Tensile strength of fly ash based geopolymer mortar." *ARPN J. Eng. Appl. Sci*, 9(11), 2297–2301.

PUBLICATIONS BASED ON THE PRESENT RESEARCH WORK

INTERNATIONAL JOURNALS

Prasanna, K. M., B. P. Sharath, Himanshu Choukade, K. N. Shivaprasad, B. B. Das, and Gangadhar Mahesh. "Research on Setting Time, Compressive Strength and Microstructure of Fly Ash-Based Geopolymer Mixture Containing Slag." *Iranian Journal of Science and Technology, Transactions of Civil Engineering* (2022): 1-15. DOI: https://doi.org/10.1007/s40996-022-01010-9

(Impact Factor: 1.461)

CONFERENCE BOOK CHAPTERS

Prasanna, K. M., Irambona Theodose, K. N. Shivaprasad, and B. B. Das. "Fast setting steel fibre geopolymer mortar cured under ambient temperature." In *Recent Developments in Sustainable Infrastructure: Select Proceedings of ICRDSI 2019*, pp. 769-787. Springer Singapore, 2021. DOI: https://doi.org/10.1007/978-981-15-4577-1_65

Prasanna, K. M., Saif Tamboli, and B. B. Das. "Characterization of mechanical and microstructural properties of FA and GGBS-based geopolymer mortar cured in ambient condition." In *Recent Developments in Sustainable Infrastructure: Select Proceedings of ICRDSI 2019*, pp. 751-768. Springer Singapore, 2021. DOI: https://doi.org/10.1007/978-981-15-4577-1_64

ACHIEVEMENTS/AWARDS

Best Paper Award to "Fast setting steel fibre geopolymer mortar cured under ambient temperature." in the International Conference on Recent Developments in Sustainable Infrastructure (ICRDSI 2019) held during 11th – 13th July, 2019 at the School of Civil Engineering, KIIT DU (Kalinga Institute of Industrial Technology), Bhubaneswar, Orissa state, India.

CURRICULUM VITAE

PERSONAL DETAILS:

Name	:	**PRASANNA K M**
Father's Name	:	Malanna Gowda K P
Mother's Name	:	Suvarnalatha M G
Date of Birth	:	18-10-1967
E-Mail ID	:	prasannakm@lnteccc.com
Contact Number	:	Mobile: +91-9008911099

EDUCATIONCAL QUALIFICATION:

Course	Institution/University	Year of Passing	Class obtained	Percentage of Marks
B.E. (Civil Engineering)	SDM College of Engineering and Technology, Dharwad	1989	First Class	60%
M.Tech (Construction Technology and Management)	Nitte Mahalinga Adyantaya Memorial Institute of Technology (NMAMIT), Nitte	2015	First Class	

WORK EXPERIENCE:

SL NO.	NAME OF THE COMPANY	FROM - TO	WORK EXPERIENCE	YEARS	NATURE OF EMPLOYMENT
1	R N SHETTY GROUP OF COMPANY	DEC 1989 – SEPT. 1993	POWER PROJECT & INFRASTRUCTRE	3 YEARS 11 MONTHS	Site Engineer Konkan railway tunnels. Varahi and sharavathi Hydro Projects
2	LARSEN AND TOUBRO LTD	SEPT 1993 TO APRIL2006	HYDEL & NUCLEAR PROJECTS	12 YEARS 7 MONTHS	Manager HYDEL, NUCLEAR AND FOUNDATION ENGG.
3	AF-COLENCO LTD	APRIL 2006 -	HYDEL PROJECTS (Sikkim)	2 YEARS 9 MONTHS	Project Manager and Design Coordinator

		JAN 2009			DESIGN and CONSULTANCY
4	SK E&C KCT JV	JULY 2009 TO AUGUST 2014	Mangalore and Padur Crude oil Cavern works Indian Strategic Petroleum Reserves Ltd (ISPRL)	5 YEARS	Dy General Manager Very large underground Crude oil Cavern Works
5	YMSK JV	NOV 2014 TO DEC 2014	EURASIA TUNNEL (ISTANBUL TURKEY)	2 MONTHS	CIVIL ENGINEER MTech (Studies)
6	LARSEN AND TOUBRO LTD	JULY 2015 TILL AUGUST 2023	Mandovi Cable Stay Bridge, P1 Project, Bangalore Metro Project	8 YEARS	Deputy Project Manager
7	LARSEN AND TOUBRO LTD	AUGUST 2023 TILL DATE	Mumbai - Ahmedabad High Speed Rail Project	5 MONTHS	Construction Service Head
7	National Institute of Technology Karnataka, Surathkal, Mangalore	JULY 2016 TILL DATE		7 YEARS	RESEARCH SCHOLAR

RESEARCH PUBLICATIONS:

Type of Publication	Number of Publications
International Journal Papers	1
Book Chapters	2